Technical Report No. 32-223

Revision No. 1

Space Trajectories Program for the IBM 7090 Computer

D. B. Holdridge

JET PROPULSION LABORATORY
CALIFORNIA INSTITUTE OF TECHNOLOGY
PASADENA, CALIFORNIA

September 1, 1962

NATIONAL AERONAUTICS AND SPACE ADMINISTRATION
CONTRACT NO. NAS 7-100

Technical Report No. 32-223

Revision No. 1

Space Trajectories Program for the IBM 7090 Computer

D. B. Holdridge

W. R. Hoover

W. R. Hoover, *Chief*
Computer Applications and Data Systems

JET PROPULSION LABORATORY
CALIFORNIA INSTITUTE OF TECHNOLOGY
PASADENA, CALIFORNIA

September 1, 1962

CONTENTS

TABLES

ABSTRACT

The Space Trajectories Program for the IBM 7090 computer is described in comprehensive detail, with emphasis on the development of the equations. Equations of motion for both the Cowell and Encke methods are given. Numerical experience with the class of trajectories encountered in practice is included to compare the Cowell and Encke methods, and to obtain an estimate of the over-all accuracy of the program. Sources of error are pointed out, consistent with the precision of the numerical methods. Operating instructions and descriptions of input and output are provided for the successful running of trajectories. Flow charts presented serve as a guide to the understanding of the internal sequence of events and control methods. Major subroutines used in the program are contained in the Appendix. The program is written in the FORTRAN Assembly Program language.

I. INTRODUCTION

The Space Trajectories Program originated in the need to study trajectories of high precision formed by the transit of a space probe from the Earth to one of the three targets technologically feasible at present — the Moon, Venus, or Mars — under the influence of gravitational forces described by Newton's law alone. Although the major programming effort has gone into obtaining a solution for which the accuracy is consistent with the single precision arithmetic used, and which requires a reasonable amount of computer time (about 30 seconds), the program may be used for study of general interplanetary flight where it is sufficient to include the bodies Sun, Venus, Earth, Moon, Mars, and Jupiter for their gravitational influence.

Since the program solves the equations of motion for the probe only, and ignores the negligible perturbations of the probe on the bodies, it is sufficient to obtain the positions and velocities of the bodies in the form of planetary and lunar ephemerides in some convenient reference frame. Since the coordinates have been traditionally referred to the Cartesian system based on the mean equator and equinox of 1950.0, the ephemerides used by the program have been uniformly expressed in the same coordinate system. The collection of ephemerides was systematically done on magnetic tape.[1]

Having expressed the coordinates of the bodies in the 1950.0 reference, it was natural to write the equations of motion in the same coordinate system. But it was immediately necessary to obtain expressions for the precession

[1]A description of the standard source tape with origins is given in "Subtabulated Lunar and Planetary Ephemerides," by R. H. Hudson, Technical Release No. 34-239, Jet Propulsion Laboratory, Pasadena, Calif., November 2, 1960.

and nutation of the Earth's equator so that the oblateness perturbation of the Earth might be properly assessed in the 1950.0 frame and that injection conditions referenced to the Earth's true equator of date resulting from powered-flight arcs might be rotated to the fixed system. To assist in the latter transformation, the hour angle at Greenwich of the true vernal equinox was obtained by the synthesis of a calculated mean value and the nutation in right ascension formed from the nutations and the obliquity of the ecliptic.

As the planetary-position ephemerides are tabulated at four-day intervals and the lunar at one-day intervals on the ephemeris tape, it was necessary to use an interpolation scheme to obtain intermediate values of positions and velocities. An Everett's formula which utilizes second and fourth central differences was chosen for the positions; to obtain the velocities, the Everett's interpolating polynomials were differentiated to obtain polynomials to be applied to the tabulated positions. It was found convenient to tabulate the necessary differences on the ephemeris tape along with the positions, and to arrange the tape in 20-day records to permit efficient tape scanning in either the forward or the backward direction, and to avoid excessive tape reference; thus lunar trajectories require, at most, two records, and interplanetary on the order of ten, which keeps tape-handling time within reasonable limits. Additionally, for the Moon, the sixth and eighth central differences have been thrown back on the second and fourth, since the former are not negligible. To handle long flight times, the argument is carried in double precision; this technique also allows for smooth interpolation.

The equations of motion have been written to take advantage of the fact that usually a central body may be found, and the coordinates relative to that body expressed so that the dominant term in the acceleration arises from the chosen body, and the remaining terms are relatively small perturbations acting to displace the two-body orbit formed by the trajectory of the probe in the field of the central body alone. Thus the remaining gravitational bodies give rise to what is known as the n-body perturbation; the perturbation arising from the oblateness of the Earth and expressed by the second, third, and fourth harmonics is included when the probe is near the Earth; in a similar manner, the perturbation derived from the triaxial figure of the Moon and represented through a second harmonic term is included when the probe is in the vicinity of the Moon. The above method of representing the equations of motion is known as a Cowell scheme. If the central-body term is replaced by the acceleration arising from the deviation of a true orbit from a fixed reference two-body orbit and the equations of motion are referred to the deviation, then the method is called an Encke scheme. Either the Cowell or the Encke scheme may be used in the program, although the latter is generally preferred in practice because of a small advantage in speed and accuracy. But for the powered flight option, which simulates the burning of a constant-thrust motor, a Cowell scheme is generally advisable because the rapid deviation from the reference two-body orbit would force frequent recalculation of the reference if the Encke scheme were used. The motor is assumed to be of high thrust since the attitude is forced to remain fixed in space, a restriction which is unrealistic for a low-thrust motor.

The solution to the trajectory problem is obtained by a stepwise numerical integration of the equations of motion appropriate to either the Cowell or Encke scheme according to an Adams-Moulton predictor-corrector method which retains the sixth differences of the derivatives; a Runge-Kutta method accurate through fourth order is used to obtain starting values for the Adams-Moulton method. An additional refinement is the fact that the ordinates are accumulated in double precision to control the growth of roundoff error. To obtain the solution at desired points, the subroutine MARK is employed. (For details of subroutines, see Appendix.)

For purposes of control, the trajectory has been divided into segments which are referred to as "phases." Usually a phase is characterized by a dominant central body, and integration step size is determined by the distance of the probe from that body. Thus a normal Venus trajectory which injects near perigee and terminates with Venus impact would consist of three phases: phase one, integration to 2.5×10^6 km from the Earth, with the Earth as the central body; phase two, Sun-centered integration to 2.5×10^6 km from Venus; and phase three, Venus-centered integration to the surface of Venus at 6100 km. In addition, the phase may be used for the auxiliary function of controlling the density, type, and incidence of output.

The program operates internally in laboratory units, i.e., in kilometers and seconds, rather than the classical units utilized in celestial mechanics. Universal Time (U.T.) is used, although provisions have been made to augment U.T. by a constant to obtain Ephemeris Time (E.T.) for use as the argument of the ephemerides. For purposes of high resolution, time is carried in double-precision seconds past 0^h January 1, 1950. This choice also makes for consistent results, even though the phase-transfer points

may be changed somewhat for a particular trajectory; otherwise, the interpolated values of the coordinates might not be a smooth function of time, and hence give rise to systematic errors at the transfer point.

The motion of the Moon s true equator has been accurately represented by the program to provide for selenographic coordinates to be used for both input and output. The rotation necessary to transform from the 1950.0 reference to selenographic Cartesian coordinates is also needed to represent the perturbation arising from the nonspherical figure of the Moon. The description of the selenographic quantities may be found in the discussions of subroutines NUTATE, MNA, MNAMD, and XYZDD[2] given in the Appendix.

In summary, the Space Trajectories Program in its present form is the culmination of three years of work in the space trajectory field at the Jet Propulsion Laboratory, and is designed for the study of the motion of a space probe confined to the solar system and influenced by the nonspherical Earth and Moon, and the point masses defined by the Sun, Venus, Mars, and Jupiter. The program may also be employed in other applications, of which the following are some examples. A simplified powered-flight arc may be simulated which assumes a constant-thrust, constant-burning-rate motor with thrust direction fixed in space. Any of the above-mentioned bodies may serve as the reference body at the injection epoch, and stepwise numerical integration of the equations of motion appropriate to either a Cowell or an Encke scheme serves to step the probe along its flight path to one of the bodies, which then serves as a target. Standard-type trajectories injecting near the Earth, and having as target one of the bodies Earth, Moon, Venus, or Mars, have been given special treatment to reduce the volume of input necessary for execution. The injection conditions may be input in Cartesian or spherical coordinates based on one of four reference frames: mean equator and equinox of 1950.0, mean equinox and ecliptic of 1950.0, true equator and equinox of date, and the true equinox and ecliptic of date. For the Earth as injection body, the Earth-fixed spherical set, based on a rotating Earth, is available; for the Moon as injection body, the selenographic (Moon-fixed spherical) coordinate set, which takes into account the rotation of the Moon, may be used. For injection conditions taken with reference to the Earth, a quasi-orbital element set for escape hyperbolas, known as the energy-asymptote option, has been made available. For output, any of the above quantities may be obtained at will, along with ephemeris information expressed in any one of the four Cartesian or spherical coordinate systems; conic output may be called for which expresses the osculating two-body orbit in many sets of orbital elements referred to one of the standard Cartesian frames; all manner of the principal angles between the probe and the bodies may be displayed; up to a maximum of 15 tracking stations may be used to observe the probe in topocentric spherical coordinates; or view periods of the stations may be determined by the program and displayed in the form of rise, maximum elevation, and set prints.

[2]These subroutines were programmed with minor revisions from the equations described in "Selenographic Coordinates," by B. E. Kalensher, Technical Report No. 32-41, Jet Propulsion Laboratory, Pasadena, Calif., February 24, 1961.

II. EQUATIONS OF MOTION

A. Cowell Scheme

Let there be a small probe, body 0, in the gravitational field of n other bodies. Choosing an inertial frame of reference results, according to Newton, in

$$\ddot{\boldsymbol{\rho}}_i = -k^2 \sum_{\substack{j=0 \\ j\neq i}}^{n} m_j \frac{\boldsymbol{\rho}_{ji}}{\rho_{ji}^3} \qquad i = 0,\ldots,n \qquad (1)$$

where $\boldsymbol{\rho}_{ji} = \boldsymbol{\rho}_i - \boldsymbol{\rho}_j$; $\rho_{ji} = |\boldsymbol{\rho}_{ji}|$; $i, j = 0,\ldots,n$; and k is the gaussian gravitational constant (Sketch 1).

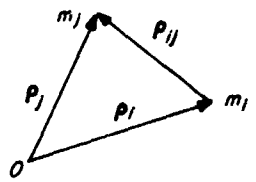

Sketch 1. Relationship of *i*th and *j*th body in an inertial frame centered at 0

Observe that

$$\mathbf{P} = \frac{1}{M} \sum_{j=0}^{n} m_j \boldsymbol{\rho}_j$$

the center of mass, has the interesting property that

$$\ddot{\mathbf{P}} = \frac{-k^2}{M} \sum_{j=0}^{n} m_j \sum_{\substack{i=0 \\ i\neq j}}^{n} m_i \frac{\boldsymbol{\rho}_{ij}}{\rho_{ij}^3} = \mathbf{0}$$

since

$$\boldsymbol{\rho}_{ij} = -\boldsymbol{\rho}_{ji}$$

and

$$\rho_{ij} = \rho_{ji} \quad \text{with } M = \sum_{j=0}^{n} m_j$$

Therefore $\dot{\mathbf{P}}$ is constant and the barycenter is an inertial frame.

Were it sufficient to express the motion of the probe, body 0, in an inertial coordinate system, the result would be

$$\ddot{\boldsymbol{\rho}}_0 = -k^2 \sum_{j=1}^{n} m_j \frac{\boldsymbol{\rho}_{j0}}{\rho_{j0}^3} \qquad (2)$$

where the coordinates are referred to the barycenter. Such a representation would naturally enough be called the barycentric form of the equations of motion. However, in practice it is convenient to rewrite Eq. (2) so that the coordinate system is referred to one of the n bodies, usually the dominant one.

Using Eq. (1) above with $l \geqq 1$ as the central body

$$\ddot{\mathbf{R}}_0 + \ddot{\boldsymbol{\rho}}_l = -k^2 \sum_{j=1}^{n} m_j \frac{\mathbf{R}_{j0}}{R_{j0}^3}$$

with

$$\mathbf{R}_i = \boldsymbol{\rho}_i - \boldsymbol{\rho}_l = \boldsymbol{\rho}_{li}$$
$$\mathbf{R}_{ij} = \mathbf{R}_j - \mathbf{R}_i = \boldsymbol{\rho}_j - \boldsymbol{\rho}_i = \boldsymbol{\rho}_{ij}, \quad i,j = 0,\ldots,n$$
$$R_{ij} = |\mathbf{R}_{ij}|$$

defined in the new coordinate system.

To obtain $\ddot{\mathbf{R}}_0$ from the above expression, calculate $\ddot{\boldsymbol{\rho}}_l$ with the aid of Eq. (1):

$$\ddot{\boldsymbol{\rho}}_l = -k^2 \sum_{\substack{j=0 \\ j\neq l}}^{n} m_j \frac{\boldsymbol{\rho}_{lj}}{\rho_{lj}^3} = k^2 \sum_{\substack{j=0 \\ j\neq l}}^{n} m_j \frac{\mathbf{R}_j}{R_j^3}$$

So

$$\ddot{\mathbf{R}}_0 = -k^2 (m_l + m_0) \frac{\mathbf{R}_{l0}}{R_{l0}^3} - k^2 \sum_{\substack{j=1 \\ j\neq l}}^{n} \left(m_j \frac{\mathbf{R}_{j0}}{R_{j0}^3} + m_j \frac{\mathbf{R}_j}{R_j^3} \right)$$

In practice, since $m_0/m_l \approx 0$, write in brief

$$\ddot{\mathbf{R}} = -\mu_l \frac{\mathbf{R}}{R^3} - \sum_{\substack{j=1 \\ j\neq l}}^{n} \mu_j \left(\frac{\mathbf{R}_{jp}}{R_{jp}^3} + \frac{\mathbf{R}_j}{R_j^3} \right) \qquad (3)$$

with $\mathbf{R} = \mathbf{R}_0 = \mathbf{R}_p$, $\mathbf{R}_{jp} = \mathbf{R}_{j0}$, p denoting the probe, and $\mu_j = k^2 m_j$; $j = 1,\ldots,n$.

In Eq. (3), the summation on the right will be known as the n-body perturbation which may be resolved into the direct terms, $-\sum \mu_j \mathbf{R}_{jp}/R_{jp}^3$, and the indirect terms, $-\sum \mu_j \mathbf{R}_j/R_j^3$; the latter sum represents the accelerating effect of the $n-1$ noncentral bodies on the central body and is what distinguishes Eq. (3) from Eq. (2). The effect of the central body has been deliberately isolated because normally it is the dominant term in the expression for the acceleration. In particular, in the case that all perturbations vanish, Eq. (3) may be solved completely for the geometric orbit, a conic. Even when the perturbations are small, the above conic solution may be used to

rewrite the equations of motion as in Encke's method described in Section IIB.

When the probe is in the vicinity of an oblate body, a perturbing term is added to the differential equations which may be described by the corresponding potential function.

For the Earth, use is made of the second, third, and fourth harmonics:

$$U_\oplus = \frac{\mu_\oplus}{R}\left\{\frac{Ja_\oplus^2}{3R^2}(1-3\sin^2\phi) + \frac{Ha_\oplus^3}{5R^3}(3-5\sin^2\phi)\sin\phi + \frac{Da_\oplus^4}{35R^4}(3-30\sin^2\phi+35\sin^4\phi)\right\}$$

where $\mu_\oplus$ is the gravitational coefficient of the Earth, $a_\oplus$ is the equatorial radius of the Earth, and ϕ is the geocentric latitude. The perturbing acceleration is then given by

$$\nabla U_\oplus = \left(\frac{\partial U_\oplus}{\partial X}, \frac{\partial U_\oplus}{\partial Y}, \frac{\partial U_\oplus}{\partial Z}\right)$$

where $\mathbf{R} = (X, Y, Z)$ and the coordinate system is oriented in the fixed 1950.0 system described in Section IVB. The precise form of $\nabla U_\oplus$ is given in the subroutine HARMN described in the Appendix.

The Moon may be regarded as a triaxial ellipsoid with the explicit expansion for the oblate potential being

$$U_\leftmoon = G\left(\frac{A+B+C-3I}{2R^3}\right)$$

where

$$G = \frac{\mu_\leftmoon}{m_\leftmoon} = k^2$$

$$I = A\left(\frac{x}{R}\right)^2 + B\left(\frac{y}{R}\right)^2 + C\left(\frac{z}{R}\right)^2$$

A, B, and C are moments of inertia about the three principal axes of the ellipsoid and $\mathbf{R} = (x, y, z)$ is the position of the probe expressed in the orthogonal right-handed coordinate system defined by the aforementioned principal axes. Specifically, the $x-y$ plane defines the Moon's true equator, the x axis emanates from the longest axis which is constrained to point in the general direction of the Earth, while the z axis lies in the direction of the Moon's spin vector; the figure may be likened to a distorted oblate spheroid, disfigured because of the Earth's proximity.

To obtain the acceleration, again form $\nabla U_\leftmoon$, with X, Y, Z given in the 1950.0 system. The explicit form of $\nabla U_\leftmoon$ may be found in subroutine XYZDD described in the Appendix; the body-fixed coordinate system for the Moon is given in the discussions of subroutines XYZDD, MNA, and MNAMD in the Appendix.

At times it may be necessary to simulate the performance of a small midcourse motor which burns with constant thrust with an attitude fixed in the 1950.0 reference system. Thrust duration is handled as a function of time alone:

$$\mathbf{a} = -\frac{F}{m_0 - \dot{m}(T-T_0)}\mathbf{C} \qquad T_0 \leqq T \leqq T_1 \qquad (4)$$

where $\mathbf{C}$ is the spin-axis vector of the probe fixed in space, F is the constant thrust, $\dot{m}$ is the constant mass flow rate, and m_0 is the initial mass.

During burning, Eq. (4) represents the largest contribution to the acceleration and Encke's method is not used. In general

$$\ddot{\mathbf{R}} = -\mu\frac{\mathbf{R}}{R^3} + \mathbf{P} \qquad (5)$$

where $\mu = \mu_I$ and $\mathbf{P}$ represents the contributions to the acceleration arising from the above-mentioned perturbations and any thrust which may be considered. The direct numerical integration of Eq. (5) is here defined as a Cowell integration, although the latter term is used differently by other authors.

B. Encke's Method

Let the probe be near a central body so that $\mathbf{P}$ becomes small compared to the central body term in Eq. (5). At the epoch T_0 the two-body problem may be solved with suitable initial conditions. The defining equations of motion for the unperturbed orbit are

$$\ddot{\mathbf{R}}_0 = -\mu\frac{\mathbf{R}_0}{R_0^3} \qquad (6)$$

Thus, $\mathbf{R}_0$ is available and, if necessary, $\dot{\mathbf{R}}_0 = \mathbf{V}_0$ as a function of time. Next, consider the differential equations for $\boldsymbol{\rho} = \mathbf{R} - \mathbf{R}_0$, the Encke displacement, where $\mathbf{R}$ is from the perturbed orbit defined in Eq. (5):

$$\ddot{\boldsymbol{\rho}} = -\mu\left(\frac{\mathbf{R}}{R^3} - \frac{\mathbf{R}_0}{R_0^3}\right) + \mathbf{P} \qquad (7)$$

At this point, the difference between the central-body terms must be expanded by means of the small parameter Q; otherwise, numerical differencing will result in significant errors introduced in the accelerations. So

$$\frac{\mathbf{R}}{R^3} - \frac{\mathbf{R}_0}{R_0^3} = \frac{1}{R_0^3}\left\{\left(\frac{R_0^3}{R^3} - 1\right)\mathbf{R} + \boldsymbol{\rho}\right\} \tag{8}$$

Define, as with Encke, Q by the relation $1 + 2Q = R^2/R_0^2$; in general, when the method is applicable, Q will be a small parameter. Now

$$1 - \frac{R_0^3}{R^3} = 1 - (1 + 2Q)^{-3/2}$$

and the difference may be expanded into the series

$$F(Q) = 1 - (1 + 2Q)^{-3/2} = Q\sum_{j=0}^{m} a_j Q^j \tag{9}$$

where m is chosen so that the remainder in the sum stays smaller than $a_0 \times 10^{-8}$ whenever $|Q| \leqq Q_0$.

An accurate numerical value for Q must be obtained in order to justify the expense of the series expansion in Eq. (9):

$$\begin{aligned} Q &= \frac{1}{2}\left(\frac{R^2}{R_0^2} - 1\right) \\ &= \frac{1}{2}\frac{(\mathbf{R}_0 + \boldsymbol{\rho})\cdot(\mathbf{R}_0 + \boldsymbol{\rho}) - R_0^2}{R_0^2} \\ &= \frac{1}{2}\frac{R_0^2 + 2\boldsymbol{\rho}\cdot\mathbf{R}_0 + \boldsymbol{\rho}\cdot\boldsymbol{\rho} - R_0^2}{R_0^2} \end{aligned}$$

$$Q = \frac{\boldsymbol{\rho}\cdot\left(\mathbf{R}_0 + \frac{\boldsymbol{\rho}}{2}\right)}{R_0^2} \tag{10}$$

It has been found that the above dot product is well defined numerically for most cases; further numerical safeguards which have been added to control the accuracy of Q are given in subroutine ENCKE, described in the Appendix.

If the difference appearing in Eq. (7) is evaluated, using Eq. (8) and Eq. (9), the final equations of motion for the Encke method become

$$\ddot{\boldsymbol{\rho}} = -\frac{\mu}{R_0^3}(\boldsymbol{\rho} - \mathbf{R}F(Q)) + \mathbf{P} \tag{11}$$

To start the integration at the epoch T_0, an arbitrary set of elements is chosen to describe the two-body motion; in all instances, judicious selection must be made so that the Encke term in Eq. (11) does not become large rapidly and so destroy the advantage over the Cowell method, which uses Eq. (5). In most cases the elements will be osculating, so that $\boldsymbol{\rho}(T_0) \sim 0$ and $\dot{\boldsymbol{\rho}}(T_0) \sim 0$ to the limitations of the numerical calculation. For the Encke initial conditions at the epoch T_0, use

$$\begin{aligned} \boldsymbol{\rho}(T_0) &= \mathbf{R}(T_0) - \mathbf{R}_0(T_0) \\ \dot{\boldsymbol{\rho}}(T_0) &= \dot{\mathbf{R}}(T_0) - \dot{\mathbf{R}}_0(T_0) \end{aligned}$$

If the perturbation $\mathbf{P}$ is large enough, both Q and ρ/R_0 will grow with time; Q may be small while ρ/R_0 is relatively large, since Q is defined by the dot product in Eq. (10). Under these circumstances it becomes necessary to rectify the reference orbit and restart the numerical integration. ρ/R_0 is used to assess the numerical accuracy of Eq. (10), and an empirical bound has been applied as indicated in the discussion of the control section of the program (see Section V).

The use of the Encke method is advantageous because the perturbation $\mathbf{P}$ enters the derivatives in Eq. (11) to more significant digits than in the corresponding ones in Eq. (5), and hence the effect of $\mathbf{P}$ is more accurately represented; step size may be increased by about a factor of two over Cowell if a dominant central body is chosen; and the differential equations are such that numerical stability of the Adams-Moulton predictor is not quite the problem that it is when Cowell derivatives are used, even though both methods use one application of Adams-Moulton corrector to insure ultimate stability. A comparison of the numerical results appears in Section III.

C. *Solutions to the Two-Body Problem*

As mentioned in the preceding section, for Encke's method it is necessary to obtain a solution to the two-body problem as a function of time. At epoch T_0, in general, a set of osculating elements is required, defined by $\mathbf{R}_0$, $\mathbf{V}_0$, and the equations of motion

$$\ddot{\mathbf{R}} = -\frac{\mu\mathbf{R}}{R^3} \tag{12}$$

Observe that $\mathbf{R} \times \mathbf{V}$ is a constant vector since

$$\begin{aligned} \frac{d(\mathbf{R}\times\mathbf{V})}{dt} &= \frac{d(\mathbf{R}\times\dot{\mathbf{R}})}{dt} = \dot{\mathbf{R}}\times\dot{\mathbf{R}} + \mathbf{R}\times\ddot{\mathbf{R}} \\ &= -\frac{\mu}{R^3}(\mathbf{R}\times\mathbf{R}) = \mathbf{0} \end{aligned}$$

$c_1 = |\mathbf{R}\times\mathbf{V}|$, the angular momentum, is defined as a constant of the motion. In the exposition below, $c_1 \neq 0$ is assumed; if the osculating elements give $c_1 \approx 0$, then a nonosculating set is used for the Encke program so that c_1 is clearly defined. Next

$$\mathbf{W} = \frac{\mathbf{R}\times\mathbf{V}}{c_1}$$

is defined so the motion is constrained to the plane defined by $\mathbf{W}$. The quantity $c_1 = V^2 - 2\mu/R$ is another constant of the motion

$$\frac{dc_3}{dt} = \frac{d}{dt}\left(\dot{\mathbf{R}}\cdot\dot{\mathbf{R}} - \frac{2\mu}{R}\right) = 2\left\{\ddot{\mathbf{R}}\cdot\dot{\mathbf{R}} + \frac{\mu\dot{R}}{R^2}\right\}$$

$$= 2\left\{-\frac{\mu\mathbf{R}}{R^3}\cdot\dot{\mathbf{R}} + \frac{\mu R\dot{R}}{R^3}\right\}$$

$$= 2\left\{-\frac{\mu\mathbf{R}}{R^3}\cdot\dot{\mathbf{R}} + \frac{\mu\mathbf{R}\cdot\dot{\mathbf{R}}}{R^3}\right\}$$

$$= 0$$

Thus, $c_3 = V^2 - 2\mu/R$ is defined as the "energy" constant.

It is possible now to solve the problem of the motion in the orbital plane defined by $\mathbf{W}$.

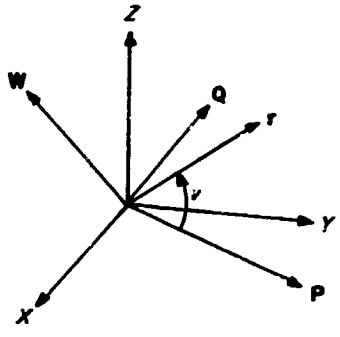

Sketch 2. Two-body orbit

Referring to Sketch 2, let the closest approach distance be q at the epoch T_p, and $\mathbf{P}$ defined as $\mathbf{R}_{min} = q\mathbf{P}$; define $\mathbf{Q} = \mathbf{W}\times\mathbf{P}$ so that a Cartesian coordinate system defined by $\mathbf{P}$ and $\mathbf{Q}$ may be set up in the orbital plane. If R = constant, then $T_p = T_0$. Polar coordinates may be used to write $\mathbf{r} = (x, y) = re^{iv}$, where v is the true anomaly. Note that since

$$\dot{\mathbf{r}} = \dot{r}e^{iv} + ie^{iv}r\dot{v} = \dot{r}e^{iv} + r\dot{v}e^{i(v+\pi/2)}$$

calculate $c_1 = r^2\dot{v}$, since the component $\dot{r}e^{iv}$ of the velocity lies along $\mathbf{r}$ and, hence, does not contribute to the cross product which defines c_1. Finally, by differentiating $\dot{\mathbf{r}}$ and comparing with Eq. (12),

$$\ddot{\mathbf{r}} = \left(\ddot{r} - \frac{c_1^2}{r^3}\right)e^{iv} = -\frac{\mu}{r^2}e^{iv}$$

or

$$\ddot{r} + \frac{\mu}{r^2} - \frac{c_1^2}{r^3} = 0$$

Making the classical change of variables, $1/u = r$, and solving for the geometric orbit with the true anomaly v,

$$\frac{d^2u}{dv^2} + \left(u - \frac{1}{p}\right) = 0$$

where $p = c_1^2/\mu$.

Measuring the initial conditions at epoch T_p, where $v = 0$, the solution has the form

$$u - \frac{1}{p} = \frac{\varepsilon}{p}\cos v$$

since $du/dv = 0$ at $v = 0$. In terms of r, the fundamental geometric solution becomes

$$r = \frac{p}{1 + \varepsilon\cos v} \tag{13}$$

while $q(1 + \varepsilon) = p$; $\varepsilon \geqq 0$ since $p \geqq q$.

An expression for ε is now obtained:

$$V^2 = \dot{r}^2 + \frac{c_1^2}{r^2};\ \dot{r} = \frac{\varepsilon c_1\sin v}{p}$$

$$c_3 = V^2 - \frac{2\mu}{r} = \frac{\mu}{p}(\varepsilon^2\sin^2 v + \varepsilon^2\cos^2 v - 1) \tag{14}$$

$$\varepsilon^2 - 1 = \frac{pc_3}{\mu}$$

$$\varepsilon = \sqrt{1 + \frac{pc_3}{\mu}}$$

The solution may then be expressed as

$$\mathbf{R} = \frac{p\cos v}{1 + \varepsilon\cos v}\mathbf{P} + \frac{p\sin v}{1 + \varepsilon\cos v}\mathbf{Q}$$

$$\mathbf{V} = \frac{-c_1\sin v}{p}\mathbf{P} + \frac{c_1(\varepsilon + \cos v)}{p}\mathbf{Q} \tag{15}$$

At the osculation epoch T_0, from Eq. (13)

$$\cos v_0 = \frac{1}{\varepsilon}\left(\frac{p}{R_0} - 1\right)$$

and by manipulation of Eq. (15)

$$\sin v_0 = \frac{1}{\varepsilon}\frac{p}{R_0 c_1}\mathbf{R}_0\cdot\mathbf{V}_0$$

Inverting Eq. (15) gives the vector expressions

$$\mathbf{P} = \cos v_0\frac{\mathbf{R}_0}{R_0} - \sin v_0\frac{\mathbf{W}\times\mathbf{R}_0}{R_0}$$

$$\mathbf{Q} = \sin v_0\frac{\mathbf{R}_0}{R_0} + \cos v_0\frac{\mathbf{W}\times\mathbf{R}_0}{R_0} \tag{16}$$

Equation (16) is satisfactory only for $\varepsilon \neq 0$; if $\varepsilon = 0$, it is customary to take

$$\mathbf{P} = \frac{\mathbf{R}_0}{R_0}$$

$$\mathbf{Q} = \mathbf{W} \times \mathbf{P}$$

To solve the dynamics, one approach is to work with v, the true anomaly, in the form $w = \tan v/2$.

$$R = \frac{q(1+w^2)}{1+\lambda w^2}$$

where $\lambda = (1-\varepsilon)/(1+\varepsilon)$, in terms of the new variable w.

From the relation $c_1 = R^2 \dot{v}$,

$$\frac{c_1}{2q^2}\, dT = \frac{1+w^2}{(1+\lambda w^2)^2}\, dw$$

or

$$g(T - T_p) = \int_0^w \frac{1+u^2}{(1+\lambda u^2)^2}\, du \qquad (17)$$

where $g = c_1/2q^2$.

In practice, the quadrature on the right side of Eq. (17) is obtained for small values of λ by expanding the integrand as a power series in λ and u^2 and integrating term by term. The resultant form appears in the discussion of subroutine PERI (see Appendix). Equation (15) may be rewritten in terms of w as

$$\begin{aligned} \mathbf{R} &= \frac{1-w^2}{1+\lambda w^2} q\,\mathbf{P} + \frac{2w}{1+\lambda w^2} q\,\mathbf{Q} \\ \mathbf{V} &= \frac{-c_1(1+\lambda)w}{q(1+w^2)}\mathbf{P} + \frac{c_1(1-\lambda w^2)}{q(1+w^2)}\mathbf{Q} \end{aligned} \qquad (18)$$

To complete the solution, it is necessary to obtain T_p. If $w_0 = \sin v_0/(1+\cos v_0)$ and λ are not too large, then λw_0^2 will be sufficiently small so that T_p may be calculated from Eq. (17) with the series expansion. It may turn out that λw_0^2 is not suitable, in which case T_p is computed using the eccentric anomaly which is described below. But once T_p is obtained, Eq. (17) may be solved at epoch T by iteration to give w, used to obtain the coordinates as in Eq. (18). Since λw^2 must be a small parameter for the method to work, the principal application comes when either λ is quite small or the motion is confined to a region near closest approach; the latter alternative gives rise to the name "pericenter" method applied to the above process involving w or v.

Another way to obtain the dynamics is through the introduction of the eccentric anomaly. A singularity appears at $c_3 = 0$ which is adequately handled by the pericenter method, as $c_3 = 0$ implies $\lambda = 0$. Otherwise, the elliptical case is distinguished with $c_3 < 0$ and its eccentric anomaly E, while for $c_3 > 0$ and the eccentric anomaly F, the hyperbolic case is considered.

If $c_3 < 0$, E is defined by

$$\begin{aligned} &R = a(1 - \varepsilon\cos E), 0 \leqq |E| \leqq 180^\circ \\ &a = -\frac{\mu}{c_3} \\ &\dot{E} > 0 \text{ so that } E \gtrless 0 \text{ if } T \gtrless T_p \end{aligned} \qquad (19)$$

By substitution into the equation $c_3 = V^2 - 2\mu/R$,

$$(1 - \varepsilon\cos E)\,\dot{E} = \sqrt{\frac{\mu}{a^3}} = n$$

or

$$E - \varepsilon\sin E = n(T - T_p) \qquad (20)$$

which is Kepler's equation for an ellipse.

Observing that

$$R = a(1 - \varepsilon\cos E) = \frac{p}{1+\varepsilon\cos v}$$

and

$$\dot{R} = a\varepsilon\sin E\,\dot{E} = \frac{\varepsilon c_1}{p}\sin v$$

leads to

$$\begin{aligned} \cos v &= \frac{\cos E - \varepsilon}{1 - \varepsilon\cos E} \\ \sin v &= \frac{\sqrt{1-\varepsilon^2}\sin E}{1 - \varepsilon\cos E} \end{aligned} \qquad (21)$$

Substitution of Eq. (21) into Eq. (15) yields

$$\begin{aligned} \mathbf{R} &= a(\cos E - \varepsilon)\,\mathbf{P} + a\sqrt{1-\varepsilon^2}\sin E\,\mathbf{Q} \\ \mathbf{V} &= \frac{-an\sin E}{1-\varepsilon\cos E}\mathbf{P} + \frac{an\sqrt{1-\varepsilon^2}\cos E}{1-\varepsilon\cos E}\mathbf{Q} \end{aligned} \qquad (22)$$

E_0 is determined at epoch T_0 by

$$\cos E_0 = \frac{1}{\varepsilon}\left(1 - \frac{R_0}{a}\right)$$

$$\sin E_0 = \frac{1}{\varepsilon}\frac{\mathbf{R}_0 \cdot \mathbf{V}_0}{a\sqrt{|c_3|}}$$

so that T_p may be determined using these equations along with Eq. (20).

To obtain the coordinates at epoch T for the elliptical orbits, Eq. (20) is solved by iteration given in the discussion of subroutine KEPLER (see Appendix).

The hyperbolic case defined by $c_3 > 0$ admits a similar solution. Start with the definition for F

$$R = a(\varepsilon \cosh F - 1)$$

$$a = \frac{\mu}{c_3} \qquad (23)$$

$$\dot{F} > 0 \text{ so that } F \gtrless 0 \text{ if } T \gtrless T_p$$

To obtain the form of Kepler's equation for the hyperbola, use c_3 as with the elliptical case, and obtain

$$(\varepsilon \cosh F - 1)\dot{F} = \sqrt{\frac{\mu}{a^3}} = n$$

and Kepler's equation

$$\varepsilon \sinh F - F = n(T - T_p) \qquad (24)$$

Comparing expressions for R and $\dot{R}$, v and F are related by

$$\cos v = \frac{\varepsilon - \cosh F}{\varepsilon \cosh F - 1}$$

$$\sin v = \frac{\sqrt{\varepsilon^2 - 1}\sinh F}{\varepsilon \cosh F - 1} \qquad (25)$$

Replacing the quantities in Eq. (15) by those in Eq (25), the expressions for the coordinates become

$$\mathbf{R} = a(\varepsilon - \cosh F)\mathbf{P} + a\sqrt{\varepsilon^2 - 1}\sinh F\,\mathbf{Q}$$

$$\mathbf{V} = \frac{-an\sinh F}{\varepsilon\cosh F - 1}\mathbf{P} + \frac{an\sqrt{\varepsilon^2 - 1}\cosh F}{\varepsilon\cosh F - 1}\mathbf{Q} \qquad (26)$$

At the epoch T_0, T_p may be determined from Eq. (24), when F_0 is obtained from

$$\cosh F_0 = \frac{1}{\varepsilon}\left(1 + \frac{R_0}{a}\right)$$

$$\sinh F_0 = \frac{1}{\varepsilon}\frac{\mathbf{R}_0 \cdot \mathbf{V}_0}{a\sqrt{c_3}}$$

The iterative solution of Kepler's equation at epoch T is used to obtain the coordinates; the discussion of subroutine QUADKP (see Appendix) describes the numerical technique used for the hyperbolic case.

III. NUMERICAL EXPERIENCE

Trajectories computed using single-precision derivatives calculated in the Encke manner should be slightly more accurate than those generated using the Cowell form of the equations of motion, provided that a proper choice of central body has been made. The difference between the two methods arises from the fact that the relatively small size of the perturbing acceleration, as compared with the central body acceleration, permits the Encke scheme to retain more significance in the total acceleration, as compared with the corresponding acceleration term in the Cowell scheme. It is assumed that the reference orbit for the Encke scheme lies sufficiently close to the true orbit so that the quantity $\rho/R_0 < 0.03$, where $\mathbf{R}_0$ is the position in the reference orbit while $\boldsymbol{\rho}$ is the difference between $\mathbf{R}$, the position in the true orbit, and $\mathbf{R}_0$. Under this assumption, the main term in the acceleration for the Encke method, viz., $-\mu/R_0^3\ (\boldsymbol{\rho} - F(Q)\mathbf{R})$, will in general be at least an order of magnitude smaller than the corresponding Cowell term, $-\mu\mathbf{R}/R^3$, for $F(Q) \approx 3Q = 3\boldsymbol{\rho}\cdot(\mathbf{R}_0 + \boldsymbol{\rho}/2)/R_0^2 \approx 3\rho/R_0$ at worst; thus $|\boldsymbol{\rho}/R_0 - F(Q)\mathbf{R}/R_0| \approx 4\rho/R_0$ and as $R_0^2/R^2 \approx 1 - 2Q$, the ratio of acceleration terms will never exceed 0.12. The ultimate accuracy of the Encke scheme is tied to the accurate solution of the two-body problem for obtaining the reference orbit; less accuracy in the reference orbit would be sufficient for computation of the main Encke acceleration term and a less accurate solution than this would suffice for the perturbations.

Rounding error in the computation of the main Cowell acceleration term propagates into the numerical solution in a strikingly simple fashion—T_p, the epoch of pericenter passage, alone of the orbital elements is significantly perturbed. To demonstrate the effect of roundoff, a high Earth-satellite trajectory was run with both Cowell and Encke schemes; additional information was obtained by successively chopping the last and the last two bits in each coordinate of the acceleration vector at each integration step. A comparison of the effect on the orbital elements at the first perigee point appears in Table 1.

As a measure of the over-all difference in the trajectories, comparison of the difference in range δR may be made near the perigee. Under the assumption that T_p is the only orbital element to be affected, then

$$\delta R = R_2 - R_1 = \delta R^* \frac{\sqrt{1-\varepsilon^2}\sin E^*}{1 - \varepsilon\cos E^*}$$

where

$$E^* = \frac{1}{2}(E_1 + E_2)$$

satisfies the equation

$$E^* - \varepsilon\sin E^* = n(T - T_p^*),$$

$$T_p^* = \frac{1}{2}(T_p^{(1)} + T_p^{(2)})$$

$$\delta R^* = \frac{an\varepsilon}{\sqrt{1-\varepsilon^2}}\delta T_p$$

$$\delta T_p = T_p^{(2)} - T_p^{(1)}$$

where the superscript 1 refers to a comparison trajectory while the superscript 2 refers to a perturbed trajectory. δR^* is the extreme value of δR occurring at $n(T - T_p^*) = \pm(\cos^{-1}\varepsilon - \varepsilon\sqrt{1-\varepsilon^2})$. A summary of results in Table 2 serves to demonstrate the adequateness of the conic approximation. The small perturbation in T_p contributes only a small difference in the coordinates, if a comparison is made at a greater time from perigee.

Table 1. Orbital elements at perigee

Case	q^a km	ε	T_p^b sec	I deg	ω deg	Ω deg
Normal Encke	8901.362	0.98534697	69.077	19.599986	200.94431	222.18236
Encke with last bit chopped	8901.362	0.98534687	69.074	19.599986	200.94431	222.18236
Encke with last two bits chopped	8901.362	0.98534697	69.088	19.599986	200.94431	222.18235
Normal Cowell	8901.425	0.98534641	22.029	19.600052	200.94427	222.18245
Cowell with last bit chopped	8901.420	0.98534644	27.063	19.600039	200.94428	222.18243
Cowell with last two bits chopped	8901.402	0.98534650	38.793	19.600027	200.94429	222.18241

[a]Closest approach distance.

[b]Time of pericenter passage, past 4[d] 12[h] 58[m] after the injection epoch.

As a further comparison of the Encke and Cowell methods, three lunar trajectories were selected which had flight times of 35 hr, 45 hr, and 66 hr, respectively. The trajectories were characterized by an injection altitude of about 200 km near perigee and a termination of 1738.09 km from the center of the Moon. Table 3 compares results obtained by the running of each trajectory four different ways: (1) Encke, Moon-centered second phase; (2) Encke, Earth-centered second phase; (3) Cowell, Moon-centered second phase; and (4) Cowell, Earth-centered second phase. In all instances the second phase was started at a distance of 30,000 km from the center of the Moon. It appears from the data that all four methods are consistent and yield results of satisfactory accuracy.

The 66-hr lunar trajectory was used to estimate the effect of integrating in a coordinate system based on the true equator and equinox of date. A precise comparison is impossible, since injection conditions expressed in the of-date system must be rotated to the mean equator and equinox of 1950.0 for integration in the normal case. Such an operation introduces a small variation in the injection coordinates which propagates under integration into the numerical solution, thus partially masking the difference between the two coordinate systems. However, an estimate of the variational effect was made which could account for about half of the observed difference in the Cartesian coordinates at lunar encounter. The perturbations in these coordinates, arising solely from the two different coordinate systems for integration, seem therefore to amount to about 1 km; in addition, the flight time received a perturbation amounting to about 0.6 sec. These differences appear to be significant when viewed in the light of the data in Table 3.

As interplanetary trajectories are usually run in three phases—phase one Earth-centered, phase two Sun-centered, and phase three target-centered—it is necessary

Table 2. Range differences near perigee

Case	δR at $45^d\ 12^h$ km		δR at $45^d\ 14^h$ km		Maximum δR km	
	Computed[a]	Observed[b]	Computed[a]	Observed[b]	Computed[a]	Observed[b]
Encke with last bit chopped minus normal Encke	−0.014	−0.014	0.014	0.010	0.014	0.014
Encke with two bits chopped minus normal Encke	0.050	0.052	−0.050	0.052	0.051	0.053
Normal Cowell minus normal Encke	−215.028	−214.943	213.824	213.705	220.168	220.064
Cowell with last bit chopped minus normal Cowell	23.025	23.017	−22.860	−22.850	23.557	23.548
Cowell with two bits chopped minus normal Cowell	76.661	76.631	−76.1[illegible]4	−76.103	78.450	78.413

[a]Values derived from the orbital elements.
[b]Values derived from the normal trajectory output.

Table 3. Comparison of lunar trajectories

Case	Lunar Impact Time	B · T[a] km	B · R[a] km	i[a] deg
35[h] Encke E-M	$1^d\ 10^h\ 53^m\ 08\overset{s}{.}619$	44.129	9.785	27.3[illegible]
35[h] Encke E-E	$1^d\ 10^h\ 53^m\ 08\overset{s}{.}624$	44.142	9.785	27.3384
35[h] Cowell E-M	$1^d\ 10^h\ 53^m\ 08\overset{s}{.}620$	44.139	9.787	27.3347
35[h] Cowell E-E	$1^d\ 10^h\ 53^m\ 08\overset{s}{.}625$	4[illegible].149	9.787	27.3341
45[h] Encke E-M	$1^d\ 20^h\ 51^m\ 32\overset{s}{.}279$	19.017	14.500	46.8673
45[h] Encke E-E	$1^d\ 20^h\ 51^m\ 32\overset{s}{.}284$	19.042	14.499	46.8322
45[h] Cowell E-M	$1^d\ 20^h\ 51^m\ 32\overset{s}{.}279$	19.031	14.499	46.8475
45[h] Cowell E-E	$1^d\ 20^h\ 51^m\ 32\overset{s}{.}287$	19.047	14.500	46.8408
66[h] Encke E-M	$2^d\ 17^h\ 49^m\ 03\overset{s}{.}028$	270.281	−88.532	37.1864
66[h] Encke E-E	$2^d\ 17^h\ 49^m\ 03\overset{s}{.}047$	270.324	−88.536	37.1848
66[h] Cowell E-M	$2^d\ 17^h\ 49^m\ 03\overset{s}{.}064$	270.300	−88.565	37.1906
66[h] Cowell E-E	$2^d\ 17^h\ 49^m\ 03\overset{s}{.}078$	270.339	−88.571	37.1894

[a]The orbital elements B · T and B · R are computed along with i, the inclination, at the time the distance 1738.09 km from the center of the Moon is reached.

at the change into phase two to compute the velocity of the Sun by numerical differentiation of position coordinates, which is inaccurate on two counts: first, the position ephemeris of the Sun displays noise in the seventh figure of the positions, which gives rise to inconsistencies in the velocities as obtained from neighboring segments of the ephemeris; second, even with eight-figure accuracy in the position data, calculation of the velocities entails differencing so that significant figures are lost.

To determine the magnitude of the error introduced in the velocity coordinates as used for normal cases, an 80-day arc of the Earth's orbit was smoothed by a least-squares fit which utilized a numerical integration of the equations of motion. Residuals on the order of two units in the seventh figure of the position coordinates were obtained by the fitting process. As a by-product of the fit, smooth velocity coordinates were obtained which were therefore consistent with the new position coordinates. Intermediate values of the velocities were then obtained by both a numerical differentiation of the new position ephemeris and a direct interpolation of the velocity ephemeris; a comparison of the results revealed maximum differences of about 0.02 m/sec, or discrepancies in the seventh figure. Next, the original noisy position coordinates were differentiated and compared with the interpolation in the velocity ephemeris. In this case, the maximum differences were observed to be about 0.15 m/sec, or a relative error of about 5×10^{-6}.

An actual Venus trajectory with a flight time of 108 days was studied for the effect of inaccuracies introduced by the velocity transformation in the transfer to phase two by the systematic variation of the epoch of the coordinate change, and also by running a trajectory which integrated geocentrically all the way to Venus encounter. The results are summarized in Table 4, which gives the deviation of the coordinates at the fixed epoch of transfer into phase three, and of the time of Venus encounter, all referred to a standard trajectory which used the ordinary phasing. The differences in the coordinates may be explained fairly well by the known magnitude of maximum error in the velocity of the Sun and the value of the appropriate variational coefficients. The trajectory, which was integrated all the way to Venus in phase one, does not suffer from the velocity problem, but because the noisy position coordinates used in the calculation of the now large perturbations in the acceleration undoubtedly contribute a significant amount of error in the solution, this technique does not solve the accuracy problem.

The Encke and Cowell methods for the interplanetary case were compared by running Venus and Mars trajectories in which the transfer point from phase one to phase two was kept fixed for the respective trajectories. Evidently, the difference between the two methods shows up more distinctly the longer the flight time, but is of acceptable magnitude, as Table 5 indicates.

In summary, the trajectory program gives consistent single-precision results for the Encke and Cowell meth-

Table 4. Differences at transfer to Venus-centered phase

Transfer time[a]	δX Mm[b]	δY Mm[b]	δZ Mm[b]	δTF sec
93.50	0.6	0.1	0.0	78
93.75	−0.1	0.0	0.0	−15
94.00	−0.7	−0.1	0.0	−87
94.25	−1.2	−0.1	0.0	−140
94.50	−1.2	−0.1	0.1	−132
94.75	−1.4	−0.2	0.1	−155
95.00	−1.6	−0.2	0.1	−181
95.25	−1.8	−0.3	0.1	−211
95.50	−1.9	−0.4	0.0	−234
95.75	−2.2	−0.5	0.0	−370
96.00	−2.3	−0.7	−0.1	−503
96.25	−2.4	−0.9	−0.2	−332
96.50	−2.7	−1.1	−0.2	−381
96.75	−2.7	−1.3	−0.3	−403
97.00	−2.7	−1.4	−0.4	−420
97.25	−2.7	−1.5	−0.4	−434
97.50	−2.9	−1.6	−0.5	−461
97.75	−2.8	−1.7	−0.6	−467
98.00	−2.7	−1.8	−0.7	−470
98.25	−2.6	−1.9	−0.7	−472
98.50	−2.0	−1.9	−0.7	−417
All geocentric	0.6	−1.0	−0.5	−37

[a]The transfer time represents the Julian date in E.T. at which entry was made into the heliocentric phase.
[b]Megameters.

Table 5. Comparison of interplanetary trajectories

Case	TF[a] sec	B · T[b] km	B · R[b] km	i, deg
108[d] Venus, Encke	51.279	−4120.9	1694.4	153.9196
108[d] Venus, Cowell	56.636	−4120.5	1693.2	153.9295
118[d] Venus, Encke	25.236	249632.8	−630020.9	76.8357
118[d] Venus, Cowell	26.827	249629.9	−630022.0	76.8359
231[d] Mars, Encke	9.743	−50153.6	−4537.4	173.4127
231[d] Mars, Cowell	34.938	−50205.4	−4541.3	173.4134

[a]The time of flight is measured from an arbitrary epoch.
[b]The orbital elements are calculated either at planetary encounter or at closest approach.

ods, but the ephemeris problem for interplanetary flight presents a source of systematic error. This problem will be largely eliminated by a study now in progress at the Jet Propulsion Laboratory to obtain smoothed position and velocity ephemerides which are gravitationally consistent.

IV. OPERATING INSTRUCTIONS AND DESCRIPTION OF INPUT

A. Operation of the Space Trajectories Program on the IBM 7090

The Space Trajectories Program is designed to accept offline card input in BCD on tape A2, to prepare an offline BCD output tape on A3, and to obtain ephemeris information from a tape mounted on A8 assumed to be written in high density. For operational convenience, the offline output may be monitored on the online printer by depressing sense switch 6, which permits simultaneous off- and online output. The other sense switches, the sense lights, the panel keys, and the sense indicator register are not used; additionally, the floating-point trapping mode of execution is not used.

A machine run usually consists of several cases which are defined by the appropriate case parameters punched on cards in a format accepted by the 7090 version of NYINP1, a SHARE input routine. The sets of cards which define individual cases are separated by TRA 3,4 cards, and each set may be trailed by its package of phase cards to complete the input for running the trajectory. A description of the available case parameters appears in Sections IVD-1 and D-2.

For the normal type of "minimum print" trajectory, a set of phase parameters suitable for the case may be selected from the parameters assembled in the program to be used for the standard targets Earth, Moon, Venus, and Mars. The values of the stored parameters appear in Section IVF. Complete control over the trajectory may be obtained by the appropriate choice of phase parameters for each sequential phase belonging to the case; the phase parameters read in are saved and may be used for subsequent cases so that one run might consist of several cases, all using a common set of phase cards which is read in but once. The functions of the specific parameters used in a phase are described in Sections IVE-2 and E-3.

B. Basic Coordinate Systems

The fundamental coordinate system used by the Space Trajectories Program for reference of the equations of motion is the Cartesian frame formed by the mean equator and equinox of 1950.0; the position of the mean equator of the Earth and the ascending node of the mean orbit of the Sun on that equator, taken at the beginning of the Besselian year 1950, serve as the definition. The X axis is directed along the node, the Z axis northward above the equator, and the Y axis in a direction to complete the usual right-handed coordinate system. The auxiliary reference frame based on the Earth's mean equator of date, and the mean equinox of date defined by the Sun's mean orbit about the Earth (ecliptic of date), may be obtained from the 1950.0 system by the application of the precession as described in the discussion of subroutine ROTEQ (see Appendix).

Reference to the Earth's true equator of date is obtained by the rotation of the mean equator of date about the mean equinox of date to the ecliptic of date via the mean obliquity of date, rotation in the ecliptic to form the true equinox of date via the nutation in longitude, and, finally, the rotation about the true equinox by means of the true obliquity of date formed by augmenting the mean obliquity by the nutation in obliquity. The three rotations described result in but a small change, hence the mean and true coordinates in general agree through the first four figures. The description of subroutine NUTATE (see Appendix) contains formulas for the rotation matrix which performs the necessary transformation from mean coordinates to true.

C. Coordinate Systems for Input

Provisions have been made to input directly into the Cartesian equatorial system of 1950.0 the basic coordinate frame for the numerical integration. A simple rotation about the mean vernal equinox of 1950.0, with magnitude the mean obliquity of 1950.0, permits input in the mean equinox and ecliptic of 1950.0. With the aid of the nutations in longitude and obliquity, along with the general precession, it becomes possible to input in either the true equator and equinox of date or the true equinox and ecliptic of date. The Cartesian coordinates expressed in any one of the above four systems may refer to one of the six available bodies Earth, Moon, Sun, Venus, Mars, and Jupiter.

It is convenient to input the injection conditions in a spherical set associated with one of the Cartesian coordinate systems which describes the position vector in terms of range and two angles, and the velocity vector corresponding as velocity (speed) and two angles. For this purpose, the Cartesian frame is regarded as being at rest in the case of the true of-date systems; the reference frame may be thought of as being "osculating" rather than

undergoing a slow rotation in inertial space and thus forming a rotating coordinate system. The set of equations necessary for the transformation from sphericals to Cartesian, along with the definitions of the angles, may be found in the description of subroutine RVIN (Appendix).

The Earth-fixed spherical set of injection conditions is based on a Cartesian coordinate system assumed to rotate with the Earth: the $x-y$ plane coincident with the Earth's true equator of date, the x axis lying in the Greenwich meridian, and the z axis along the Earth's spin axis. As described in subroutine GHA (Appendix), a formula is furnished which gives the Greenwich hour angle of the true vernal equinox of date so that the Earth-fixed Cartesian coordinates may be referred to the true equator and equinox of date via a simple rotation. Of course, the velocity vector in the Earth-fixed system is affected by the Earth's rotational rate; appropriate formulas for the velocity transformation to the nonrotating system are given in subroutine EARTH (Appendix).

A similar treatment of the Moon gives rise to injection conditions expressed in selenographic (Moon-fixed sphericals) coordinates; formulas for the position of the Moon's true equator, the prime meridian of selenographic longitude reference, and the rotation of the Moon are contained in the discussion of subroutines XYZDD, MNA, and MNAMD (Appendix).

A final input coordinate system, based on orbital elements of an escape hyperbola from the Earth, completes the number of options. The hyperbola has been characterized by its ascending asymptote given by right ascension and declination, by the energy, and by the constraint that the launch site lie in the orbital plane. The actual shape of the hyperbola and the injection point are given by the remaining two parameters, the path angle and the range at the injection time.

The equations for the energy-asymptote input option may be developed as illustrated in the following:

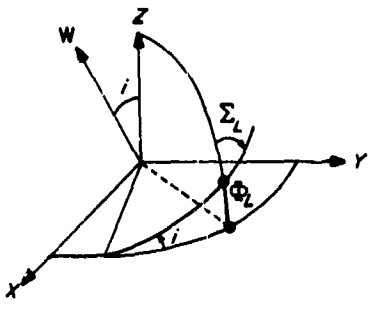

Sketch 3. Launch geometry

Given Σ_L, the azimuth at the launch site, as in Sketch 3,

$$W_z = \cos i = \sin \Sigma_L \cos \Phi_L$$

where $\Phi_L = 28.309$ deg, the latitude of the launch site, a program parameter.

$$\mathbf{S} = (\cos \Phi_S \cos \Theta_S, \cos \Phi_S \sin \Theta_S, \sin \Phi_S),$$
the ascending asymptote

$$W_y = \frac{-W_z \sin \Theta_S \sin \Phi_S - \cos \Theta_S \sqrt{\cos^2 \Phi_S - W_z^2}}{\cos \Phi_S}$$

If the radicand is negative, the error message

"DECLINATION OF ASCENDING ASYMPTOTE OUT OF RANGE"

is printed and the trajectory is aborted.

$$W_x = -\frac{S_y W_y + S_z W_z}{S_x},$$

completing the construction of W, the unit angular momentum vector.

$$V = \sqrt{c_3 + \frac{2\mu_\oplus}{R}}, \text{ the velocity}$$

$$c_1 = |\mathbf{R} \times \mathbf{V}| = RV \cos \Gamma, \text{ the angular momentum}$$

$$e^2 - 1 = \frac{c_3 c_1^2}{\mu_\oplus^2}, \text{ for the eccentricity}$$

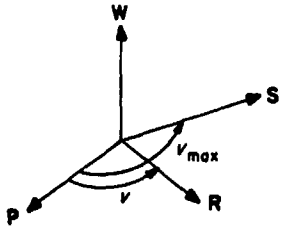

Sketch 4. Relationship of ascending asymptote and perigee

From $\sin \Gamma = e \sin (v - \Gamma)$, invert to obtain $-90° < v - \Gamma < 90°$ and v, the true anomaly. In particular, for $\Gamma = 90°$, an expression for v_{max}, the maximum true anomaly (Sketch 4) is

$$v_{max} = \cos^{-1}\left(-\frac{1}{e}\right), \quad 90° < v_{max} < 180°$$

$$\mathbf{R} = R\{\cos(v_{max} - v)\,\mathbf{S} + \sin(v_{max} - v)\,\mathbf{S} \times \mathbf{W}\}$$

The velocity vector (Sketch 5) is given by

$$\mathbf{V} = V\left\{\cos\Gamma\frac{\mathbf{W}\times\mathbf{R}}{R} + \sin\Gamma\frac{\mathbf{R}}{R}\right\}$$

completing the construction of the Cartesian coordinates.

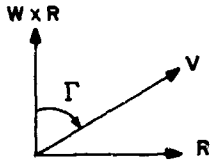

Sketch 5. Description of the velocity vector

D. Relationship Between Case Analysis and Phase Analysis

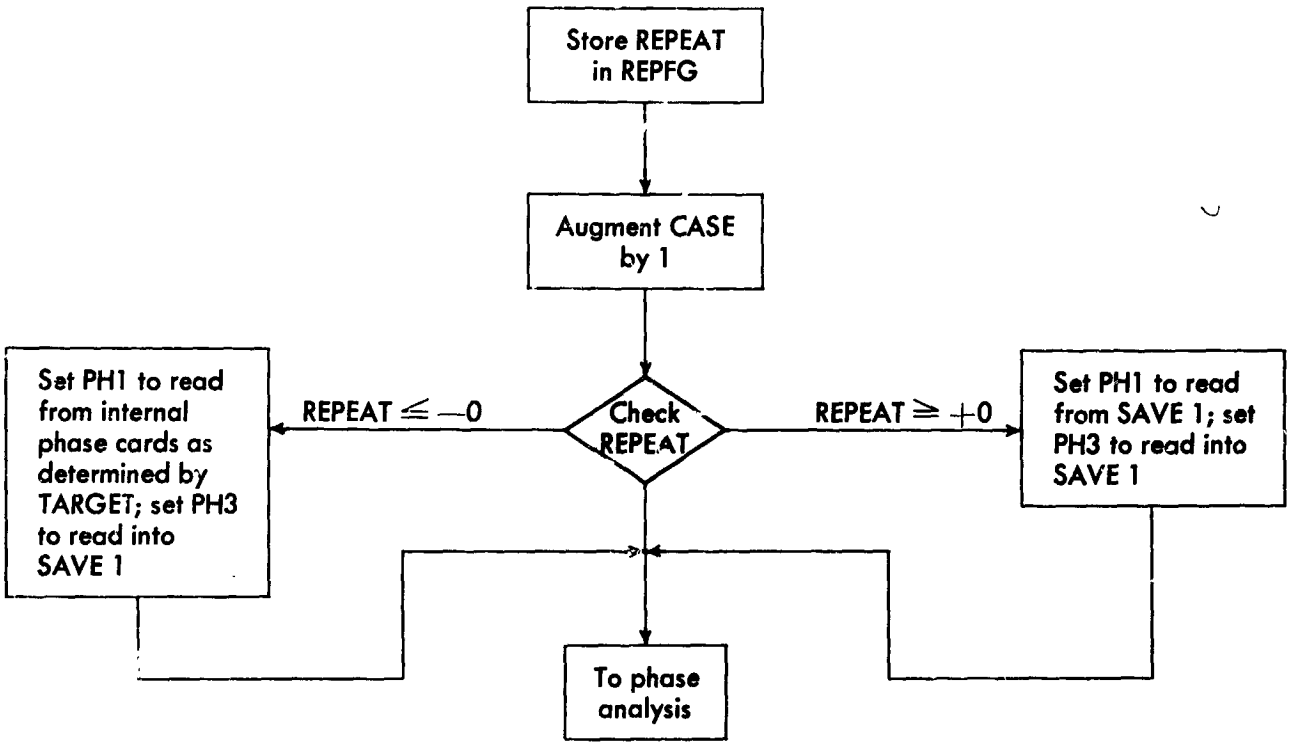

For CASE ANALYSIS, input desired value of CASE and REPEAT.

If REPEAT = ±0, all phase cards are read in and buffered at the same time.

Phase 1 cards
TRA 3,4
.
.
.
Last phase cards
TRA 3,4

} Stack of phase cards for all phases to be read in for the present case

Observe that the symbolic address card

CASE O −1

may be used to effect (CASE) = 0 at the phase-analysis point of the program.

D. (Cont'd)

1. Case Parameters

Input location (decimal)	*Class field*	*Program name*	*Identification*
100 109	BCD	60-character comment field printed at top of each page of output	
110	BCD	TARGET	BCD name of target body
111	BCD	KERN	BCD name of central body at injection
112	OCT	REPEAT	Phase input control word
113	OCT	INJECT	Injection input type
114–115	DEC	T1	Injection epoch in sexagesimal format
116–118	DEC	X1, Y1, Z1	Injection coordinates identified by INJECT
119–121	DEC	X1., Y1., Z1.	
122	DEC	GAMMAC	Thrust attitude angles giving fixed direction of thrust vector
123	DEC	SIGMAC	
124	DEC	ACC1	Thrust magnitude in lb force
125	DEC	MASS1	Initial mass in lb
126	DEC	MASS.1	Mass flow rate in lb/sec
127	DEC	TBO1	Duration of burning in sec
128–129	DEC	TGO1	Epoch for ignition of motor
136	DEC	RADP	Coefficient for radiation pressure
137	OCT	FLAGS	Bit 34 = integrate frequency equations Bit 35 = integrate variational equations
138	DEC	T(K)	Single-precision floating-point time
139	BCD	EQUNOX	Injection equator and equinox

2. Detailed Description of Case Parameters

Program name	*Explanation*
TARGET	May be Earth, Moon, Sun, Venus, Mars, or Jupiter. It is used to define the target quantities in the various print groups and to select the appropriate set of minimum phase cards when REPEAT ≤ -0 and the target is neither the Sun nor Jupiter.
KERN	May be any of the bodies as used with TARGET. KERN defines the central body of the coordinate system at injection and may be distinct from the central body of integration for phase one.
REPEAT	Determines whether or not phase input cards are to follow:

Value of REPEAT	Effect
−1	Does not input phase cards but uses one of the four internal sets as determined by TARGET.

D2. (Cont'd)

Program name		*Explanation*
	−0	Uses the internal sets of phase cards as with REPEAT = −1; modifications are read in on top of working buffer, and altered phase parameters are stored in a special buffer to be used later. After last cards for the last phase have been read in, REPEAT is set to +1.
	+0	Similar to REPEAT = −0 but does not make use of any internally stored phase cards.
	+1	Assumes all phases have been previously loaded and uses appropriate buffer for input.

INJECT — The seven available types are as follows:

Value of INJECT	Coordinate System
+0	Inertial Cartesian, equatorial
−0	Inertial Cartesian, ecliptic
+1	Inertial spherical, equatorial
−1	Inertial spherical, ecliptic
+2	Earth-fixed spherical
+3	Selenographic (spherical)
+4	Energy-asymptote Earth-centered equatorial

Note: For INJECT = ±0 or ±1, coordinate system may be modified by EQUNOX

T1 — Double precision epoch of injection in the two-word fixed-point decimal format which is denoted by "sexagesimal format."

Format of the two words is

yymmoddhh,nnssfff

where the fields are

yy = year, e.g., 61 for 1961

mm = month, e.g., 11 for November

odd = day, 3-digit field, where zero must appear before digits for day of month

hh = hours past start of day

nn = minutes

ss = seconds

fff = milliseconds

Note: This epoch is modified by T(K).

D2. (Cont'd)

Program name	*Explanation*	
X1, Y1, Z1, X1., Y1., Z1.	Value of INJECT	Interpretation
	+0	**R** and **V** in equatorial Cartesian coordinates
	−0	**R** and **V** in ecliptic Cartesian coordinates
	+1	R, Φ, Θ; V, Γ, Σ inertial equatorial spherical coordinates
	−1	R, β, λ; V, Γ, Σ inertial ecliptic spherical coordinates
	+2	r, ϕ, θ; v, γ, σ Earth-fixed spherical
	+3	$r_{\mathbb{C}}$, $\phi_{\mathbb{C}}$, $\theta_{\mathbb{C}}$; $v_{\mathbb{C}}$, $\gamma_{\mathbb{C}}$, $\sigma_{\mathbb{C}}$ selenographic (spherical) coordinates
	+4	Σ_L, R, Γ; c_3, Φ_S, Θ_S energy-asymptote in Earth-centered equatorial system

Interpretation is modified by EQUNOX below. Position units are km, velocity units are km/sec, and angles are in deg.

GAMMAC, SIGMAC — At injection the position vector **R** is formed. A fixed-thrust attitude vector **C** is characterized by the path angle γ_c and the azimuth angle σ_c with respect to a plane perpendicular to **R** and the Z axis as a reference direction. **R** may be a body-fixed vector so that γ_c and σ_c would have a different interpretation if the selenographic input option were used rather than Moon-centered Cartesian for instance.

For powered-flight computation the following formula is used for the acceleration with the parameters described below:

$$\mathbf{a} = \frac{-F}{m_0 - \dot{m}(T - T_{0j})}\mathbf{C} \text{ for } T_0 \leqq T \leqq T_0 + t_b$$

ACC1 — F, thrust in lb force; internally multiplied by $g = 0.0098$ to obtain a in km/sec²

MASS1 — m_0, initial mass in lb

MASS.1 — $\dot{m}$, mass flow rate in lb/sec

TBO1 — t_b, duration of burning in floating-point sec

TGO1 — T_0, epoch of motor ignition in sexagesimal format as with T1, or the modified sexagesimal format as with PRTENT in Section IVE-3.

Further phase control must be provided for the powered flight as indicated in the flow diagrams of the phase logic (Section V) and the description of the phase parameters; i.e., there must be a phase to start the motor.

For radiation pressure calculation the following equation is used:

$$\mathbf{a} = \frac{Ag}{W} K\alpha^2 \frac{\mathbf{R}_{sp}}{R^3_{sp}}$$

where

α = number of km/A.U., included to make $\alpha^2\mathbf{R}_{sp}/R^3_{sp}$ dimensionless

D2. (Cont'd)

Program name	*Explanation*
	$\mathbf{R}_{sp}$ = the Sun-probe vector
	$K = 1.03034 \times 10^{-6}$ lb force/m², the solar-flux constant
	A = effective area in m²
	W = mass of spacecraft in lb
	$g = 0.0098$, conversion factor to express acceleration in km/sec² internally
RADP	Ag/W with units as above, m²-km/sec² lb force
FLAGS	The two low-order bits are used to control the introduction of the 10 frequency equations ($b_{34} = 1$) and the 36 variational equations ($b_{35} = 1$) for numerical integration in the Jet Propulsion Laboratory tracking program.
T(K)	After T1 is converted internally to double-precision floating-point sec past 0^h January 1, 1950, T(K) is added on to give the effective injection time.
EQUNOX	If the BCD field is all blanks, then the input is regarded as being expressed in the true equator and equinox of date or the true ecliptic and equinox of date. Otherwise the reference is the mean system of 1950.0. As EQUNOX is displayed along with the injection conditions, it is customary to use the six characters "1950.0" for the latter case.

The data for case parameters describing the injection conditions and powered-flight parameters and the associated control is terminated by the card TF \ 3,4.

Further cases may follow unless the phase-card input is triggered via REPEAT = ±0. In that event, of course, all the necessary cards for the various phases must follow, then the subsequent cases.

E. Phase-Card Reading and Buffering

1. Storage Layout of Internal Buffers

Input locations
140 to 179

USE buffer

USE buffer
mapped onto SAVE
buffers ↔ REPEAT = ±0

$SAVE_1$
$SAVE_{10}$

10 buffers

Nominal phase cards stored in core:

☾

⊕	phase 1
☾	phase 2

☿

⊕	phase 1
⊙	phase 2
☿	phase 3

♂

⊕	phase 1
⊙	phase 2
♂	phase 3

⊕

⊕	phase 1
⊙	phase 2
⊕	phase 3

☾ Moon
⊙ Sun
☿ Venus
♂ Mars
⊕ Earth

2. Phase Parameters

Location	*Type field*	*Program name*	*Description*
140	OCT	LAST	Controls last phase and some of the print
141	BCD	REND	Body used to form R_{np}
142	DEC		Value of R_{np} used to terminate phase
143	BCD	REND.	Body used to form $\dot{R}_{np}$
144	DEC		Suppression distance from central body

E2. (Cont'd)

Location	*Type field*	*Program name*	*Description*
145	OCT	MODE	Integrate Encke or Cowell
146	BCD	CENTER	Central body for integration
147–148	DEC	H	Initial step size, modified sexagesimal format
149	OCT	DOUBLE	Number of initial doubles
150	BCD	HKERN	Body from which to compute step sizes
151–162	DEC	PRTEND, DELPRT	3 print end times and intervals
163–166	DEC	ODDPRT	2 odd-print epochs
167	OCT	GROP	12-octal-character field to control print groups
168–169	OCT	CODE1	24-octal-character field for station prints
170–171	OCT	VIEW	24-octal-character field for stations for view periods
178	OCT	ORBETT	Reference for **B** · **T** and **B** · **R** in conic output
179	BCD	EQUNX1	Output equator and equinox

3. Detailed Description of Phase Parameters

Program name	*Explanation*
LAST	sgn { − = call PRINTD at $T\phi$; + = don't call PRINTD at $T\phi$
	bit 33 { 0 = reset T_{PRT} to $T\phi$ at start of phase ; 1 = use old T_{PRT} from previous phase
	bit 34 { 0 = call PRINTD at end of phase ; 1 = don't call PRINTD at end of phase
	bit 35 { 0 = last phase ; 1 = more phases to follow

PRINTD is the subroutine which prints the selected groups.

T_{PRT} is the print epoch constructed in the previous phase which would have been reached for printing had the previous phase extended in time to T_{PR1}.

When new phase cards are being read, bit 35 = 0 also flags the end of the reading process.

$T\phi$ is the epoch at change of phase.

E3. (Cont'd)

Program name	*Explanation*
REND REND.	End-of-phase devices: A phase may be terminated by one of the following three conditions: 1. R_{END} 2. $\dot{R}_{END}$ 3. T_{END}
	1. R_{END}: The BCD name of the body to which R_{END} refers is input in 141; the desired value $R_{np} = R_{END}$ is input in 142. R_{END} is used as a dependent variable stop.
	2. $\dot{R}_{END}$: The BCD name of the body from which $\dot{R}_{NP}$ is measured is input in 143; 144 is interpreted as: (1) (REND. + 1) = 0: suppress $\dot{R}$ test (2) (REND. + 1) $\neq$ 0: test effective in the following ways: a. If CENTER = TARGET, stop at $\dot{R} = 0$ via a dependent variable stop b. If CENTER $\neq$ TARGET, suppress test until: *1.* $R >$ (REND. + 1) if (REND. + 1) > 0; or *2.* $R <$ |(REND. + 1)| if (REND. + 1) < 0 R refers to the central body.
	3. T_{END}: $T_{END} = \max(T\phi, T_{END_1}, T_{END_2}, T_{END_3})$ where the T_{END_i}'s are the end of print times input in 151, 155, and 159 and $T\phi$ is the epoch of phase change.
MODE	0 = integrate the equations of motion as developed for a Cowell scheme 1 = integrate Encke's modification of the equations of motion
CENTER	Any of the six bodies may be used as the central body; but for R_{END} and $\dot{R}_{END}$ the following bodies are available:

Central Body	Perturbing Bodies
Earth	Moon, Sun; Jupiter if $R > 10^6$ km
Moon	Earth, Sun
Sun, Venus, Mars, Jupiter	All remaining bodies

H	Adams-Moulton step size in modified sexagesimal format: yy = 0 and mm = 0, so that the remainder is converted to sec. If (H), (H + 1), and (DOUBLE) = 0, the step size is selected automatically as a function of HKERN and is halved or doubled under program control as the need arises.

E3. (Cont'd)

Program name	*Explanation*
DOUBLE	If (H) or (H + 1) $\neq 0$, a fixed-point number in this field gives the number of times the step is to be doubled consecutively.
HKERN	Selects the body from which the step size is to be computed; resultant calculated step size is used for other purposes so that HKERN is effective even though (H) or (H + 1) $\neq 0$.
PRTEND, DELPRT	The 12 input locations are divided into three 4-word fields giving control over print intervals: T_{END_1}, ΔT_{PRT_1}; T_{END_2}, ΔT_{PRT_2}; T_{END_3}, ΔT_{PRT_3} The T_{END_i} may be input as epochs in the usual sexagesimal format or as intervals past injection expressed in the modified sexagesimal format in which yy = mm = 0. In the latter event, the epoch T_{END_i} is formed by augmenting the injection epoch by the interval. The ΔT_{PRT_i} are intervals as represented in the modified sexagesimal format. If T_{END_i} is input as zero, it is replaced by a large number but is ignored in the calculation of T_{END}. Finally the T_{END_i} are internally sorted and consequently need not be input in ascending sequence. The location for T_{END_2} is PRTEND + 4 or DELPRT + 2, since PRTEND and DELPRT define the first of the two words in T_{END_1} and ΔT_{PRT_1} respectively.
ODDPRT	T_{ODD_1} and T_{ODD_2} are input to provide execution of PRINTD without interrupting the main printing sequence. The format is the same as for T_{END_i} and the two resultant epochs are sorted as before. $T_{ODD_i} = 0$ is replaced by a large number.

Treatment of print times:

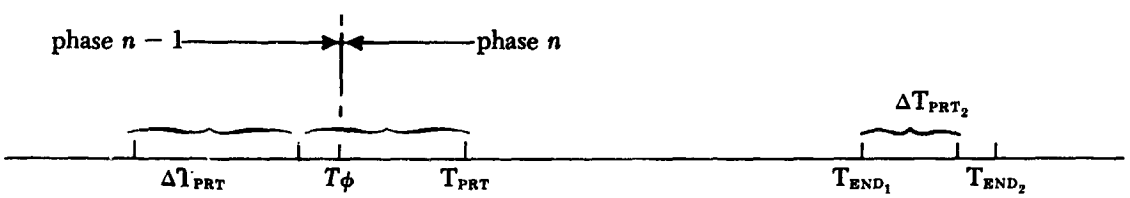

At time of entry to the new phase, T_{PRT} is the next print time as determined by phase $n - 1$. If the print reset option is chosen, $T_{PRT_0} = T\phi$ will be the first print time. Otherwise,

$$T_{PRT_0} = \min \{T_{PRT}, T_{END_1}\}$$

No matter how T_{PRT_0} is chosen,

$$T_{PRT_1} = \begin{cases} \min \{T_{PRT_0} + \Delta T_{PRT_1}, T_{END_1}\}, \text{ if } T_{END_1} > T_{PRT_0}; \\ \min \{T_{END_1} + \Delta T_{PRT_2}, T_{END_2}\} \text{ otherwise} \end{cases}$$

Thus the T_{END_i}'s function is to reset the printing interval and print epoch. $T\phi$ is the time at which the nth phase starts.

E3. (Cont'd)

Program name	*Explanation*
GROP	The 12 octal characters of GROP are mapped onto the 12 words GROPS + 0, · · · , GROPS + 11:

GROPS	+0	geocentric
	+1	geocentric conic
	+2	heliocentric
	+3	heliocentric conic
	+4	spacecraft and powered flight
	+5	target
	+6	target conic
	+7	print at $\dot{R} = 0$ (central body only)
	+8, +9, +10, +11	not used

The 3 bits of the octal digits have the following use:

bit 1 { 0 = print effective whenever called
1 = print effective as a function of the status of phase

bit 2 { 0 = print only when the start-of-phase condition holds } holds for bit 1 = 1; ignore if bit 1 = 0
1 = print only when the end-of-phase condition holds }

bit 3 { 0 = ecliptic output
1 = equatorial output

Special cases are:

1. All bits zero → don't print group
2. Configuration = $3)_8$, same as (1) above

At $\dot{R} = 0$ print, the value in GROPS + 7 is mapped onto the cell for the central body conic and PRINTD is executed.

Start of phase means the first time that PRINTD is called in the phase unless the end-of-phase condition has been met at that time.

End of phase means that phase has been terminated by one of the following conditions:

1. R_{END} attained
2. $\dot{R}$ test fulfilled
3. T_{END} attained

E3. (Cont'd)

Program name	*Explanation*
CODE1	Only the leftmost 15 octal characters of the two input words are used. 0 = suppress station, 1 = include station. At print time, station print is suppressed if $\gamma_i < -10°$

The 15 stations are, in order:

1. Antigua
2. Ascension
3. Millstone Hill
4. Mobile Tracker
5. A.M.R. G.E. Tracker
6. Bermuda
7. Goldstone Receiver
8. Goldstone Transmitter
9. Grand bahama Island
10. Johannesburg
11. Hawaii
12. Jodrell Bank
13. Puerto Rico
14. San Salvador
15. Woomera

VIEW

Printouts of the station occur at $\dot{\gamma}_i = 0$, provided $\gamma_i \geqq \gamma_0$, and at $\gamma_i = \gamma_0$, where γ_0 may be input by the symbolic card

STACRDD-001 γ_0

Enough triggers have been provided to take care of a maximum of five stations.

Provisions have been made for symbolic card input of station coordinates and names if necessary.

STABCD	STACRD	
0-3} Station 1 name	0 ϕ_1	
4-7} Station 2 name	1 θ_1	
•	2 r_1	Station 1
•	3 f_{B_1}	
•	4 f_{C_1}	
	•	
	•	
	•	

ORBETT

If 0, uses T lying in the orbital plane of body concerned. If 1, uses T lying either in the equatorial or ecliptic, as called for by the conic GROPS location.

The orbital planes are defined as follows:

Body:	Orbital Plane With Respect to:
Earth	Sun
Moon	Earth
Sun	Earth
Venus	Sun
Mars	Sun
Jupiter	Sun

E3. (Cont'd)

Program name	*Explanation*
EQUNX1	If blank, output is referred to true equator or ecliptic and equinox of date; otherwise, the reference is to the mean equator or ecliptic and equinox of 1950.0. Normally the BCD "1950.0" is used here when mean equator or ecliptic and equinox of 1950.0 is desired.
	The cards representing input for the phase parameters for a given phase are terminated by a TRA 3,4 card. The last phase cards read in are indicated by a zero in the low-order bit of the parameter LAST.

F. Standard Phases

Standard phases are available for the Moon, Earth, Venus, and Mars as the target. The words TARGET and REPEAT in the case parameters control the use of the stored parameters.

If REPEAT = −1, the standard phases are used.

If REPEAT = −0, the standard phases are used but modifications may be read in to replace the stored parameters.

The stored values of the standard phases are listed in the following:

1. Stored Phase Cards for Moon as Target

Location	*Type field*	*Phase 1*	*Phase 2*
140	OCT	−1	0
141	BCD	MOON	MOON
142	DEC	30E3	1738.09
143	BCD	MOON	MOON
144	DEC	330E3	1E3
145	OCT	1	1
146	BCD	EARTH	MOON
147	DEC	0,0,0	0,0,0
150	BCD	EARTH	MOON
151	DEC	15 00,0	20 00,0
153	DEC	15 00,0	20 00,0
155	DEC	0,0,0,0	0,0,0,0
159	DEC	0,0,0,0	0,0,0,0
163	DEC	0,0,0,0	0,0,0,0
167	OCT	55 00 0 00 00 000	11 20 1 11 00 000
168	OCT	0,0	0,0
170	OCT	0,0	0,0
178	OCT	0	0
179	BCD	blank	blank

F. (Cont'd)

2. Stored Phase Cards for Earth as Target

Location	*Type field*	*Phase 1*	*Phase 2*	*Phase 3*
140	OCT	−1	−1	0
141	BCD	EARTH	EARTH	EARTH
142	DEC	2.5E6	2.4E6	6378.
143	BCD	EARTH	EARTH	EARTH
144	DEC	0	152E6	1E3
145	OCT	1	1	1
146	BCD	EARTH	SUN	EARTH
147	DEC	0,0,0	0,0,0	0,0,0
150	BCD	EARTH	SUN	EARTH
151	DEC	140 00,0	190 00,0	200 00,0
153	DEC	140 00,0	190 00,0	200 00,0
155	DEC	0,0,0,0	0,0,0,0	0,0,0,0
159	DEC	0,0,0,0	0,0,0,0	0,0,0,0
163	DEC	0,0,0,0	0,0,0,0	0,0,0,0
167	OCT	55 00 0 00 00 000	00 22 0 00 00 000	10 20 0 01 00 000
168	OCT	0,0	0,0	0,0
170	OCT	0,0	0,0	0,0
178	OCT	0	0	0
179	BCD	blank	blank	blank

3. Stored Phase Cards for Venus as Target

Location	*Type field*	*Phase 1*	*Phase 2*	*Phase 3*
140	OCT	−1	−1	0
141	BCD	EARTH	VENUS	VENUS
142	DEC	2.5E6	2.5E6	6100.
143	BCD	VENUS	VENUS	VENUS
144	DEC	0	−110E6	1E3
145	OCT	1	1	1
146	BCD	EARTH	SUN	VENUS
147	DEC	0,0,0	0,0,0	0,0,0
150	BCD	EARTH	SUN	VENUS
151	DEC	20 00,0	190 00,0	200 00,0
153	DEC	20 00,0	190 00,0	200 00,0
155	DEC	0,0,0,0	0,0,0,0	0,0,0,0
159	DEC	0,0,0,0	0,0,0,0	0,0,0,0
163	DEC	0,0,0,0	0,0,0,0	0,0,0,0
167	OCT	55 00 0 00 00 000	00 22 0 00 00 000	10 20 0 22 00 000
168	OCT	0,0	0,0	0,0

F3. (Cont'd)

Location	*Type field*	*Phase 1*	*Phase 2*	*Phase 3*
170	OCT	0,0	0,0	0,0
178	OCT	0	0	1
179	BCD	blank	blank	blank

4. Stored Phase Cards for Mars as Target

Location	*Type field*	*Phase 1*	*Phase 2*	*Phase 3*
140	OCT	−1	−1	0
141	BCD	EARTH	MARS	MARS
142	DEC	2.5E6	2E6	3415.
143	BCD	MARS	MARS	MARS
144	DEC	0	240E6	1E3
145	OCT	1	1	1
146	BCD	EARTH	SUN	MARS
147	DEC	0,0,0	0,0,0	0,0,0
150	BCD	EARTH	SUN	MARS
151	DEC	20 00,0	250 00,0	270 00,0
153	DEC	20 00,0	250 00,0	270 00,0
155	DEC	0,0,0,0	0,0,0,0	0,0,0,0
159	DEC	0,0,0,0	0,0,0,0	0,0,0,0
163	DEC	0,0,0,0	0,0,0,0	0,0,0,0
167	OCT	55 00 0 00 00 000	00 22 0 00 00 000	10 20 0 22 00 000
168	OCT	0,0	0,0	0,0
170	OCT	0,0	0,0	0,0
178	OCT	0	0	1
179	BCD	blank	blank	blank

V. FLOW CHARTS AND METHOD OF CONTROL

A. Control in the Space Trajectories Program

After the necessary transformation of the injection conditions to the Cartesian coordinates based on the mean equator and equinox of 1950.0, the Space Trajectories Program is controlled primarily by the subroutine MARK (see Appendix) which performs the stepwise numerical integration of the equations of motion to obtain the solution at desired points along the trajectory. The trajectory is divided into phases to permit control of output format and print frequency and of the numerical integration process itself. Each phase is characterized by a set of phase parameters which are interpreted before the numerical integration proceeds.

During numerical integration in a phase, the derivatives are requested by MARK; the derivative routine provides the necessary information and also performs the calculation of the auxiliary dependent variables which MARK might need as requested by the associated dependent variable triggers. The end-of-step routine monitors the numerical process by computing the step size and communicating this information to MARK, by control of rectification, and by determination of closest approach to a noncentral body.

At the print times, as determined by the triggers to MARK, the requested output groups are printed as described in Section VI.

B. General Flow in Space Trajectories Program

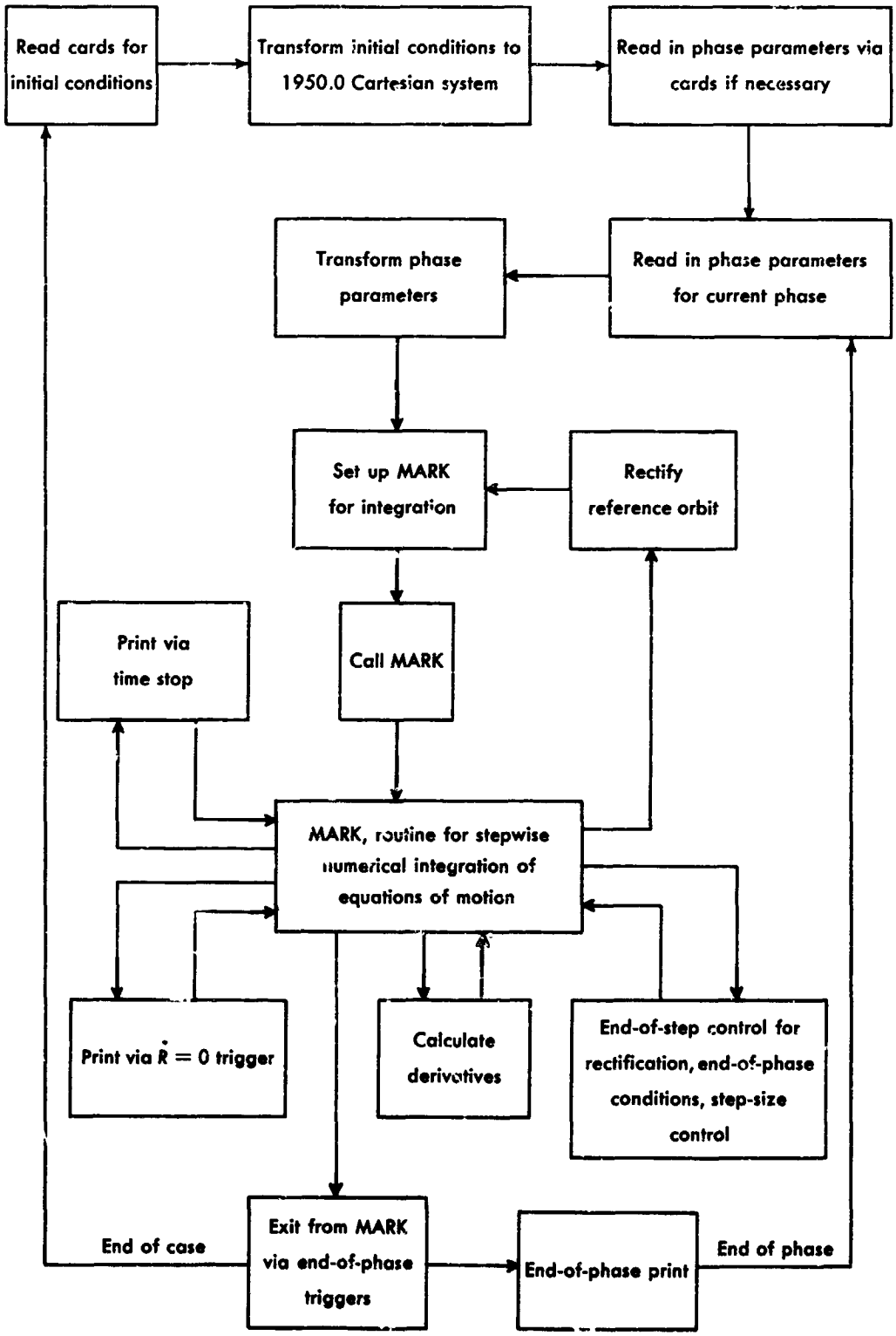

C. Flow During Transformation of Injection Conditions

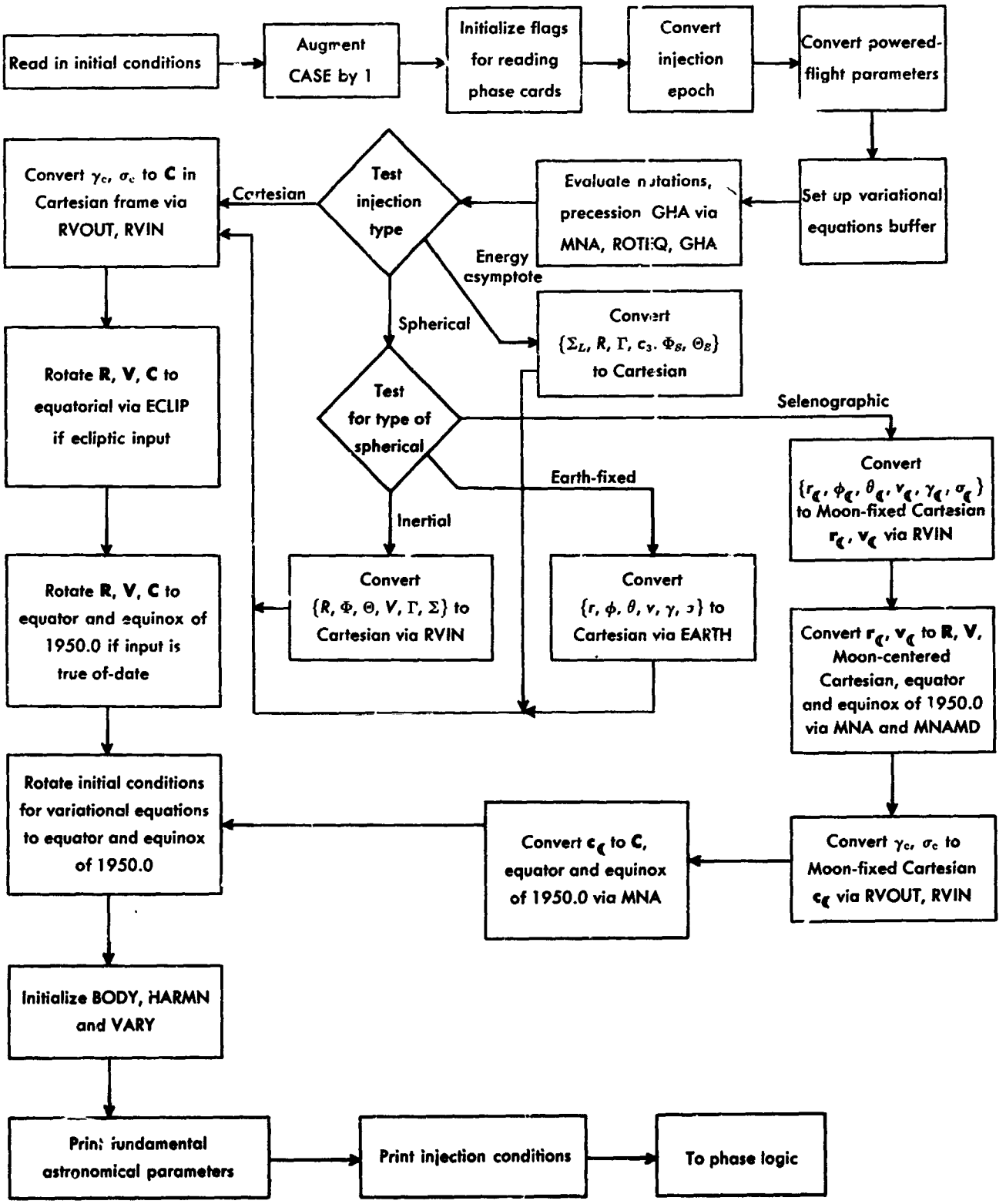

D. Flow During Transfer of Phase Parameters

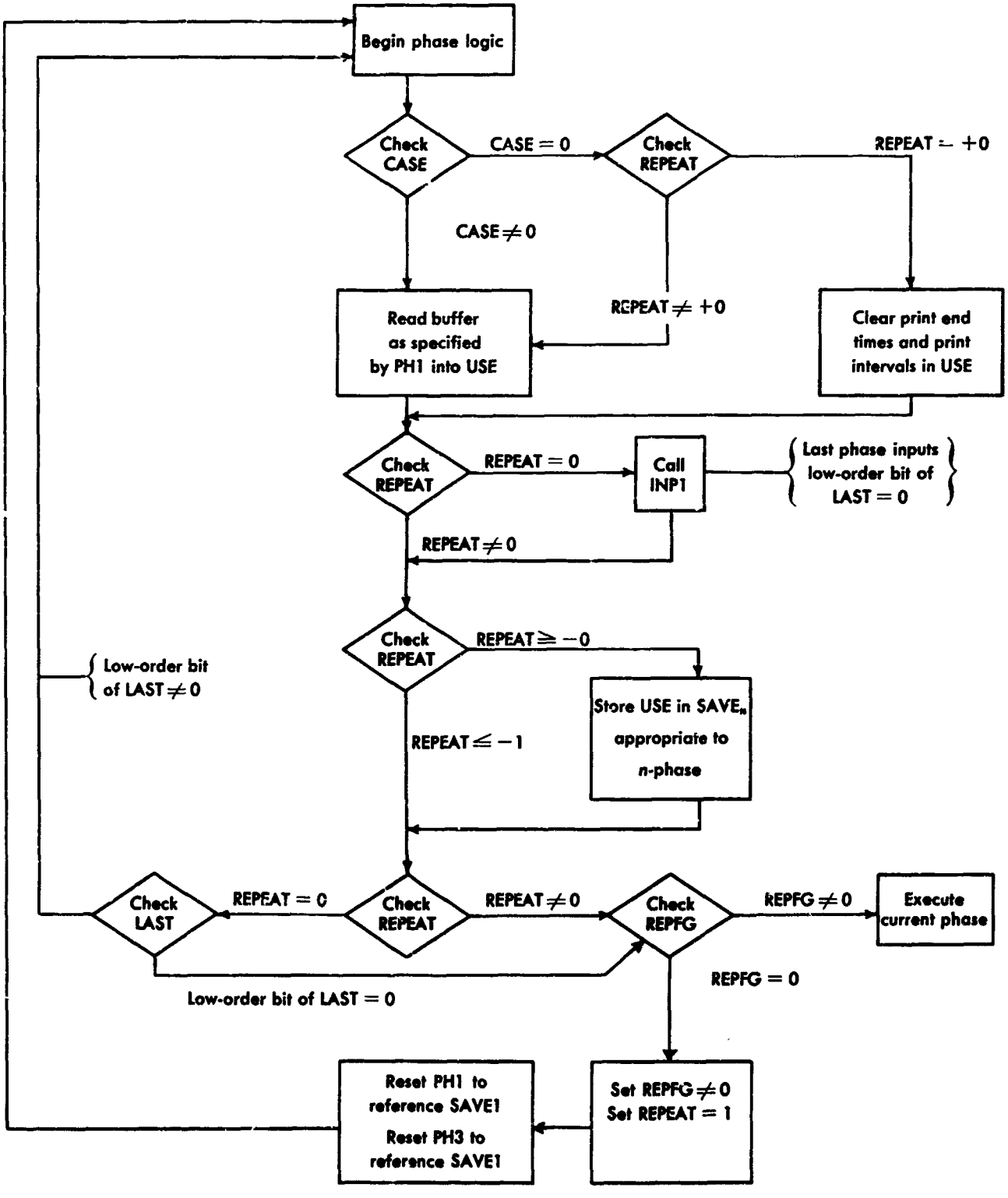

E. Flow in Phase Setup

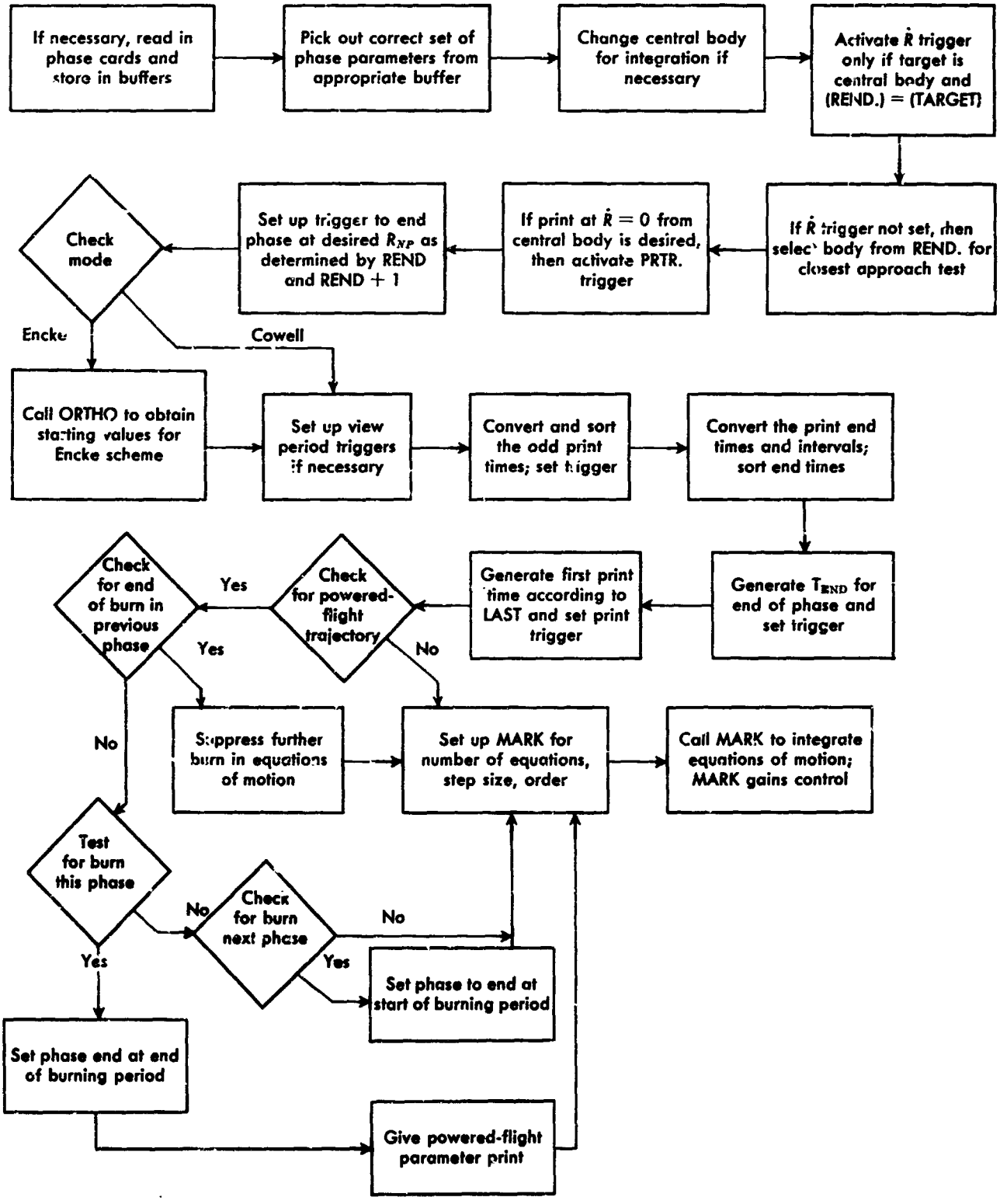

F. End-of-Step Logic

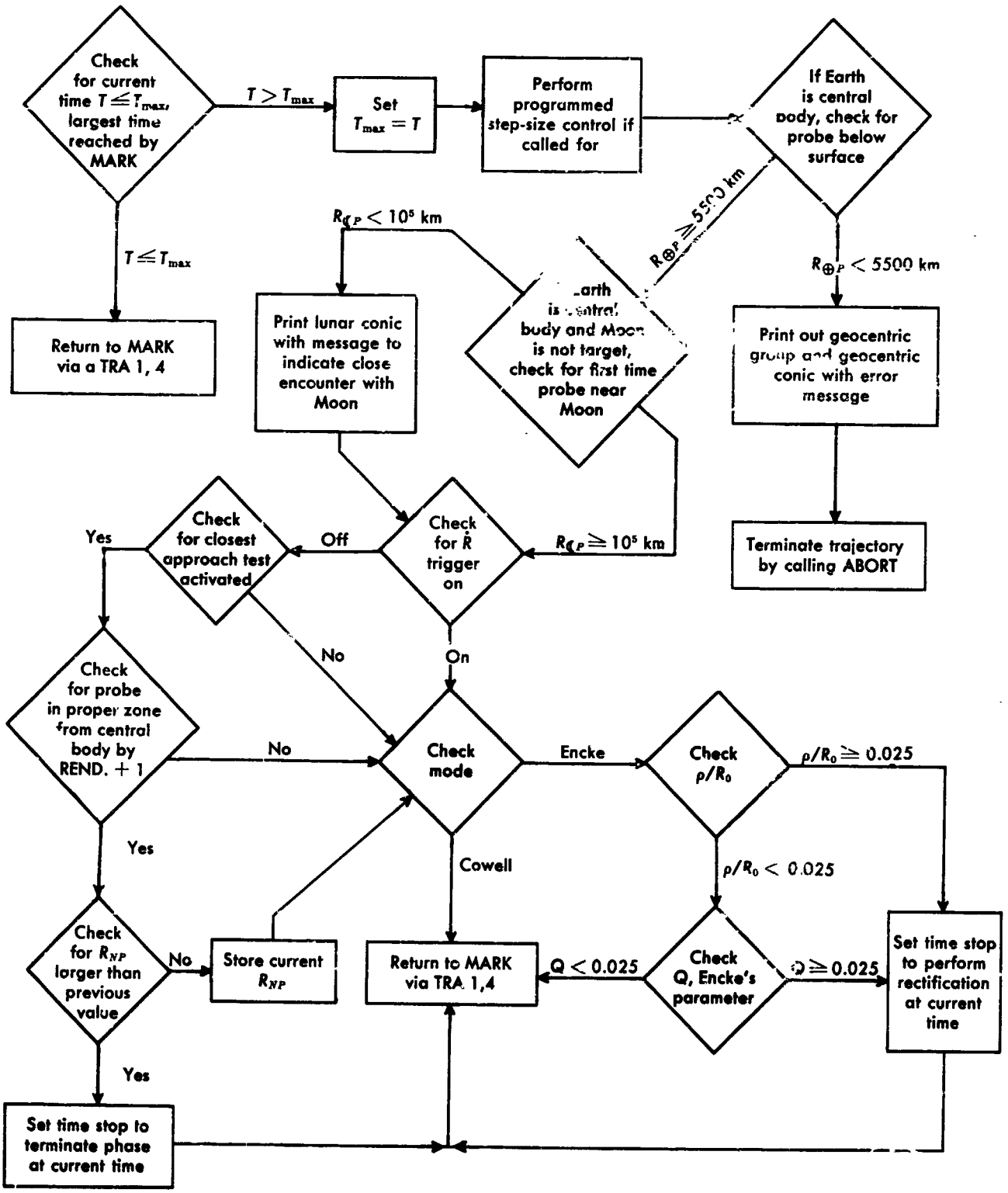

G. Function of the Derivative Routine

The derivative routine DOT assumes the COMMON storage layout for the following quantities; coordinates are in the mean equator and equinox of 1950.0.

Symbol	*Storage*	*Explanation*
T	BSS 2	Double-precision time in sec past 0^h January 1, 1950, U.T.
CX CY CZ		**R** if Cowell, **ρ** if Encke
CX. CY. CZ.		**V** if Cowell, $\dot{\boldsymbol{\rho}}$ if Encke
VAR	BSS 36	Solution of the variational equations $\frac{\partial \mathbf{R}}{\partial X_0}, \frac{\partial \dot{\mathbf{R}}}{\partial X_0}, \frac{\partial \mathbf{R}}{\partial Y_0}, \cdots, \frac{\partial \mathbf{R}}{\partial \dot{Z}_0}, \frac{\partial \dot{\mathbf{R}}}{\partial \dot{Z}_0}$
	BSS 3	Derivative of **R** if Cowell, of **ρ** if Encke; placed in buffer by DOT from CX., CY., CZ.
CX.. CY.. CZ..		$\ddot{\mathbf{R}}$ if Cowell, $\ddot{\boldsymbol{\rho}}$ if Encke; computed by DOT and placed in buffer
VAR.	BSS 36	Derivatives of quantities appearing in the VAR buffer; $\partial\ddot{\mathbf{R}}/\partial X_0, \cdots, \partial\ddot{\mathbf{R}}/\partial \dot{Z}_0$ computed by DOT and placed in buffer; remaining quantities are selected from the VAR buffer; final order is $\frac{\partial \dot{\mathbf{R}}}{\partial X_0}, \frac{\partial \ddot{\mathbf{R}}}{\partial X_0}, \frac{\partial \dot{\mathbf{R}}}{\partial Y_0}, \cdots, \frac{\partial \ddot{\mathbf{R}}}{\partial \dot{Y}_0}, \frac{\partial \dot{\mathbf{R}}}{\partial \dot{Z}_0}, \frac{\partial \ddot{\mathbf{R}}}{\partial \dot{Z}_0}$
QX QY QZ		$\mathbf{R} = \mathbf{R}_0 + \boldsymbol{\rho}$ if Encke, same as contents of CX, CY, CZ if Cowell; placed in buffer by DOT
QX. QY. QZ.		$\mathbf{V} = \mathbf{V}_0 + \dot{\boldsymbol{\rho}}$ if Encke, same as the contents of CX., CY., CZ. if Cowell; placed in buffer by DOT only if velocity needed
QX0 QY0 QZ0		$\mathbf{R}_0$, position solution to the two-body orbit; calculated by ENCKE only when in Encke mode
QX0. QY0. QZ0.		$\mathbf{V}_0$, velocity solution to the two-body orbit; calculated by SPEED only when velocity is necessary in the Encke mode

H. Flow in the Derivative Routine

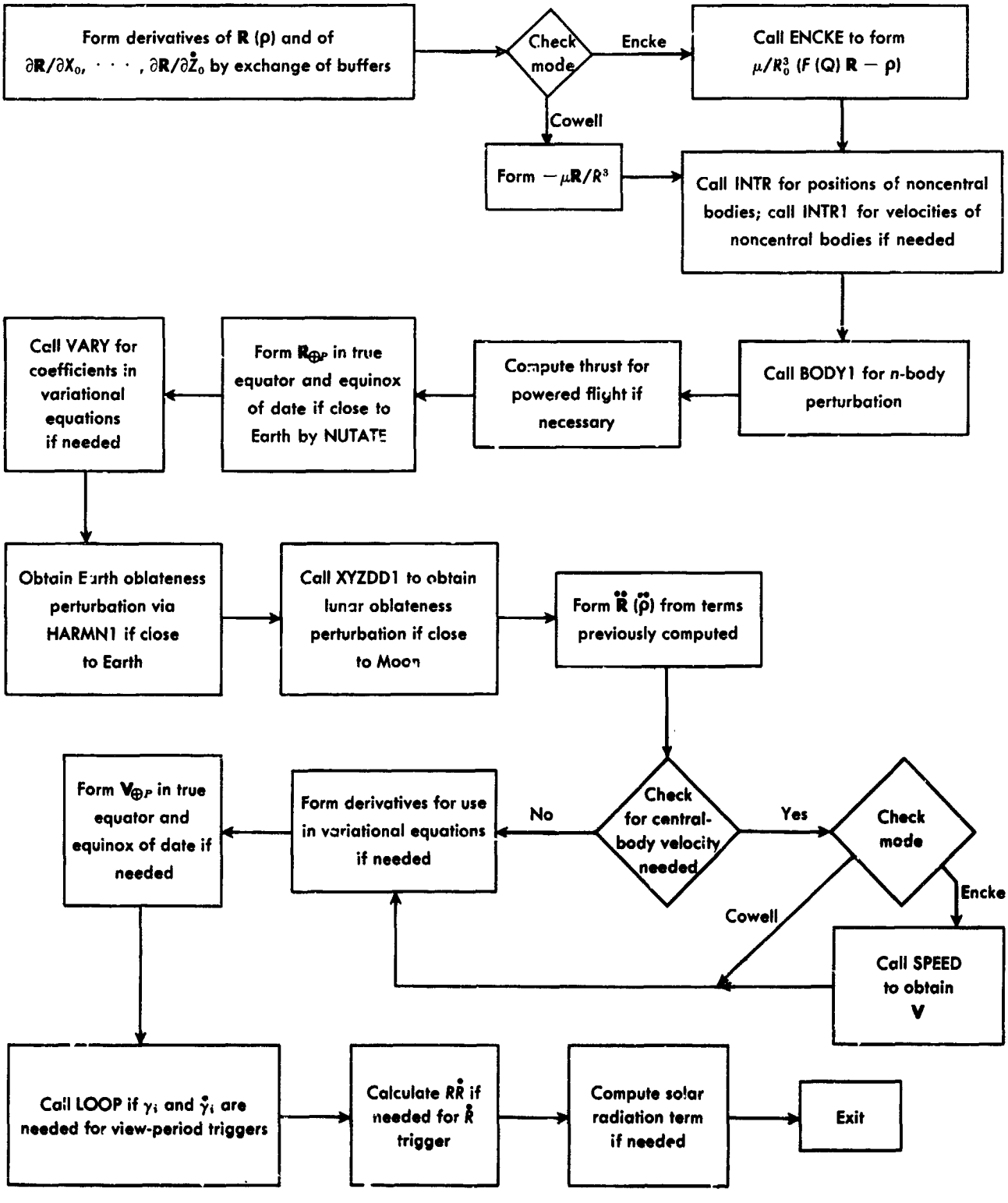

I. Automatic Step-Size Control

Step-size control is provided as a function of the range from a selected body during a particular phase. For this purpose each body has associated with it a list of range intervals; the step size remains constant during a particular interval and is doubled for the next higher interval. For the lowest interval there is defined an h_{min}; all other step sizes chosen will therefore be of the form $h = 2^n h_{min}$.

At the start of the integration MARK uses Runge-Kutta for the first m steps. Therefore, at the onset, $h_0 = \frac{1}{4}h_c$ is set in HBANK while HBANK1 is set to 2; after m Runge-Kutta steps and $2m$ Adams-Moulton steps, MARK would be using $h = 4h_0$ for its next step. The control section permits the Runge-Kutta steps to be carried out before attempting to modify the step size to new h_c.

Assuming MARK is using Adams-Moulton for the integration, h_c is computed at the end of each step and compared with h, the value MARK is using. If $h_1 = 2^k h$, where k is the number of uncompleted doubles, then the following tests are made:

1. $h_c = h_1$: No action to be taken
2. $h_c > h_1$: Augment HBANK1 by the number of additional doubles necessary to make $h = h_c$ and call ABTB to let MARK pick up the additional doubles. Record the change.
3. $h_c < h = h_1$: Augment HBANK2 by number of halves necessary to make $h = h_c$ and call ABTB to let MARK pick up the additional halves. Record the change. $h = h_1$ was indicated by the fact that HD = 0.
4. $h_c \leq h < h_1$: Set ND = HBANK1 = 0 and wait until HD = 0 at a later integration step. Save number of necessary halves and execute (3) when $h = h_1$, i.e., when HD = 0.
5. $h < h_c < h_1$: Let MARK double up to h_c by altering both HBANK1 and ND. Record change and continue, but do not call ABTB.

It is to be noted that controlling step size in the above manner does not produce instantaneous changes in the current MARK step h. Therefore, a conservative choice of values has been made in the range lists to insure stability of the numerical solution in all the practical cases which have arisen. Each h_{min} for the planets has been chosen to give good results for a low-altitude satellite whose orbit is to be calculated using an Encke scheme.

If a Cowell scheme is to be used, the program sets $h'_{min} = h_{min}/2$; thus the step-size regimen consists of a precise and uniform halving of all step sizes in the range intervals; automatic halving and doubling are consequently executed in general in a shorter time span in the Cowell mode.

The base step-size and range lists are accessible via the symbolic input location H((0)). The exact internal structure follows:

Location	*Value, sec*	*Explanation*
− 6	120	♃
− 5		not used
− 4	60	♂
− 3	60	♀
− 2	43,200	☉
− 1	60	☾
H((0)) − 0	60	⊕

Range list for Earth and Venus

Location	*Value, km*
H((0)) + 1	10^{20}
+ 2	2.8×10^{6}
+ 3	1.8×10^{6}
+ 4	10^{6}
+ 5	600,000
+ 6	400,000
+ 7	120,000
+ 10	80,000
+ 11	30,000
+ 12	16,000
LST00 = H((0)) + 13	8,000

Range list for Mars

Location	*Value, km*
H((0)) + 14	10^{20}
+ 15	2×10^6
+ 16	1.2×10^6
+ 17	800,000
+ 20	500,000
+ 21	300,000
+ 22	100,000
+ 23	60,000
+ 24	25,000
+ 25	12,000
LST04 = H((0)) + 26	6,000

Range list for Moon

Location	*Value, km*
H((0)) + 27	10^{20}
+ 30	70,000
+ 31	45,000
+ 32	30,000
+ 33	20,000
+ 34	12,000
LST01 = H((0)) + 35	5,000

Range list for Jupiter

Location	*Value, km*
H((0)) + 36	10^{20}
+ 37	5×10^6
+ 40	3×10^6
+ 41	2×10^6
+ 42	1.2×10^6
+ 43	10^6
+ 44	800,000
+ 45	600,000
+ 46	400,000

Range list for Jupiter (cont'd)

Location	*Value, km*
+ 47	300,000
+ 50	200,000
LST06 = H((0)) + 51	100,000

Range list for Sun

Location	*Value, km*
H((0)) + 52	10^9
+ 53	600×10^6
+ 54	300×10^6
+ 55	100×10^6
LST02 = H((0)) + 56	40×10^6

It would probably be worthwhile to conduct analytic and experimental studies to redistribute the range intervals to reduce machine running time.

1. MARK locations used

HD: Flag: 0 = no uncompleted double
1 = doubling not completed

ND: If HD = 0, is 0. Otherwise number of doubles to be completed − 1.

J: Number of Runge-Kutta steps completed + 1. $J \leq m + 1$, where m = order of the highest difference retained in the Adams-Moulton integration.

ABTB: MARK subroutine which inspects HBANK1 and HBANK2 to determine need for additional halving or doubling.

2. Contents of HBANK

HBANK2 address = number of halves
HBANK1 address = number of doubles
HBANK h_0: initial step for Runge-Kutta

3. Flow Chart for the Step-size Control

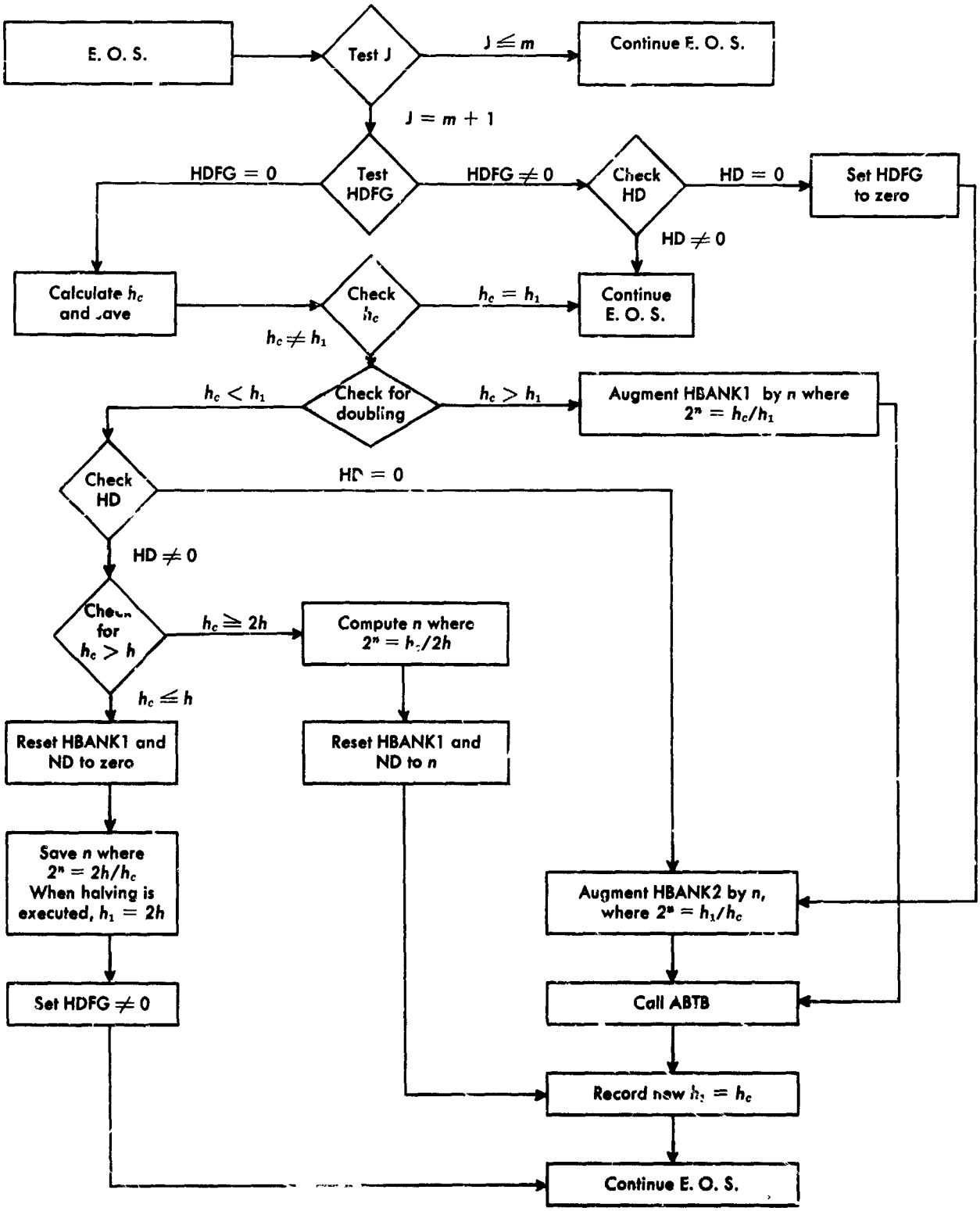

VI. DESCRIPTION OF THE OUTPUT FOR THE SPACE TRAJECTORIES PROGRAM WITH INTERPRETATION OF THE MNEMONIC CODES

A. Output Philosophy

The output of the Space Trajectories Program displays for each trajectory the fundamental astronomical constants used in the calculation, the injection conditions which serve as a starting point for the trajectory, and desired output groups which are requested principally as a function of time. The selection of the groups and the print times is phase-dependent as described in Section IVE-2. The start of the phase in which powered flight is used is heralded by the powered-flight header.

To facilitate identification of the output quantities, a lettered mnemonic code precedes the floating-point representation of the quantity printed; each output group consists of an array of pairs and falls into one of the classifications: geocentric, geocentric conic, heliocentric, heliocentric conic, spacecraft and powered flight, target, and target conic. Each output group is further identified by a header which gives the reference body for the group and the class of output, and which further identifies the group in addition to the mnemonic codes.

As a further class of output, each tracking station has for identification a unique name which appears in its output group; all station output is of the same format except for the station name which therefore functions as an identifying header.

B. Explanation of Output and Mnemonic Codes

A sample output of the Space Trajectories Program is given in Exhibit A, followed by explanations of related output groups and interpretation of the mnemonic codes.

Exhibit A. Sample of space trajectories output

CASE 1 SPACE TRAJECTORIES 1

LUNAR TRAJECTORY FOR DISPLAY OF OUTPUT

GME	.39860320 06	J	.16234500-02	H	-.57499999-05	D	.78749999-05	RE	.63781650 04	REM	.63781650 04
G	.66709998-19	A	.88745998 29	B	.88763998 29	C	.88800998 29	OME	.41780741-02	AU	.14959900 09
GMM	.49607589 04	GMS	.13271544 12	GMV	.32476950 06	GMA	.42977799 05	GMB	.00000000 00	GMJ	.12671060 09

INJECTION CONDITIONS MOON JULIAN DATE 2437605.46008102 NOV. 1,1961 23 02 31.000

GEOCENTRIC RAD .66111676 04 LAT-.13312895 02 LON .35185650 03 VR .10531770 02 PTR .53912348 01 AZR .12183937 03
EARTH-FIXED GMC .10000000 02 SGC .23500000 02 TO .82951000 05 GHA .26615809 02 GHO .40040394 02

0 DAYS 0 HRS. 0 MIN. 0.000 SEC. JULIAN DATE 2437605.46008102 NOV. 1,1961 23 02 31.000

GEOCENTRIC — EQUATORIAL COORDINATES

X	.61020315 04	Y	.20384328 04	Z	-.15223453 04	DX	-.32657006 01	DY	.87950401 01	DZ	-.56105608 01
R	.66111673 04	DEC	-.13312894 02	RA	.18472312 02	V	.10931419 02	PTH	.51935801 01	AZ	.12053672 03
R	.66111671 04	LAT	-.13312894 02	LON	.35185650 03	VE	.10531768 02	PTE	.53912356 01	AZE	.12183937 03
XS	-.11487518 09	YS	-.86241661 08	ZS	-.37395627 08	DXS	.19345540 02	DYS	-.21062717 02	DZS	-.91319481 01
XM	-.33705844 06	YM	.20458179 06	ZM	.90244289 05	DXM	-.53328919 00	DYM	-.76933039 00	DZM	-.24058118 00
XT	-.33705844 06	YT	.20458179 06	ZT	.90244289 05	DXT	-.53328919 00	DYT	-.76933039 00	DZT	-.24058118 00
RS	.14843302 09	VS	.30021333 02	RM	.40448255 06	VM	.96651224 00	RT	.40448255 06	VT	.96651224 00
GED	-.13400356 02	ALT	.23410565 03	LOS	.19028130 03	RAS	.21689711 03	RAM	.14874382 03	LOM	.12212801 03
DUT	.34000000 02	DT	.50000000 02	DR	.98952285 00	SHA	.36332697 04	DES	-.14592105 02	DEM	.12891791 02

GEOCENTRIC — CONIC ORBITAL B.T AND B.R — EQUATORIAL COORDINATES

EPOCH OF PERICENTER PASSAGE JULIAN DATE 2437605.45880927 NOV. 1,1961 23 00 41.122

SMA	.36606209 06	ECC	.98208910 00	INC	.33053889 02	LAN	.17714929 03	APF	.19449016 03	RCA	.65565008 04
VH	.99195071-01	C3	-.10888951 01	C1	.71972740 05	SLR	.12995569 05	APO	.72556767 06	TFP	.10987826 03
TA	.10482147 02	EA	.99919346 00	MA	.17946206-01	DAO	-.78438361 01	RAO	.93712649 01	MTA	.18000000 03
WX	.27126051-01	WY	.54475266 00	WZ	.83815793 00	PX	.97742251 00	PY	.16130761 00	PZ	-.13647353 00
QX	-.20954557 00	QY	.82293641 00	QZ	-.52807789 00	RX	-.18851423 00	RY	.37401758 00	RZ	-.90806012 00
S'O	.97742251 00	SYO	.16130761 00	SZO	-.13647353 00	TX	.95433517-01	TY	-.91328567 00	TZ	-.39598201 00
QX	.20954558 00	BY	-.82293645 00	BZ	.52807791 00	MX	-.38387022 00	MY	.77985642 00	MZ	-.49443663 00
B.T	.38794487 05	B.R	-.57027818 05	B	.68972345 05	PER	.36735872 05	CMO	.69215423-02	NOO	-.46179063-02

2 DAYS 17 HRS. 49 MIN. 3.027 SEC. JULIAN DATE 2437608.20247716 NOV. 4,1961 16 51 34.028

GEOCENTRIC — EQUATORIAL COORDINATES

X	-.39863348 06	Y	-.29945887 04	Z	.20618383 05	DX	-.19910060 01	DY	.60147274 00	DZ	.61111473 00
R	.39917757 06	DEC	.29607674 01	RA	.18043040 03	V	.21677951 01	PTH	.68384241 02	AZ	.30947590 03
R	.39917755 06	LAT	.29607674 01	LON	.24384899 03	VE	.29758704 02	PTE	.38832075 01	AZE	.27097978 03
XS	-.11016135 09	YS	-.91132499 08	ZS	-.39516117 08	DXS	.20435530 02	DYS	-.20210708 02	DZS	-.87627225 01
XM	-.40001575 06	YM	-.20879216 04	ZM	.21155252 05	DXM	.19506438-01	DYM	-.92545351 00	DZM	-.32619497 00
XT	-.40001575 06	YT	-.20879216 04	ZT	.21155252 05	DXT	.19506438-01	DYT	-.92545351 00	DZT	-.32619497 00
RS	.14833131 09	VS	.30047777 02	RM	.40058021 06	VM	.98145191 00	RT	.40058021 06	VT	.98145191 00
GED	.29809082 01	ALT	.39279941 06	LOS	.28301831 03	RAS	.21959972 03	RAM	.18029905 03	LOM	.24371764 03
DUT	.34000000 02	DT	.59999999 02	DR	.20153453 01	SHA	-.27174378 06	DES	-.15450419 02	DEM	.30272849 01

LUNAR TRAJECTORY FOR DISPLAY OF OUTPUT

GEOCENTRIC						CONIC		ORBITAL B.T AND B.R				EQUATORIAL COORDINATES	
EPOCH OF PERICENTER PASSAGE					JULIAN DATE 2437606.26008714						NOV. 2,1961		18 14 31.530
SMA	-.14750990 06	ECC	.16517328 01	INC	.14043133 03	LAN	.18401888 03	APF	.26201373 03	RCA	.96137042 05		
VH	.16438410 01	C3	.27022131 01	C1	.31877235 06	SLR	.25492974 06	APO	.00000000 00	TFP	.16782250 06		
TA	.10263726 03	EA	.82934364 02	MA	.10715475 03	DAO	.18148300 02	RAO	.16064909 03	MTA	.12725941 03		
WX	-.44644500-01	WY	.63543611 00	WZ	-.77086173 00	PX	.19209591 00	PY	-.75177096 00	PZ	-.63082445 00		
QX	-.98036015 00	QY	-.17624225 00	QZ	-.88502251-01	RX	-.14580064 00	RY	.45424170 00	RZ	-.87886664 00		
SXO	-.89657073 00	SYO	.31486914 00	SZO	.31147761 00	TX	.41821413 00	TY	.83337980 00	TZ	.36135171 00		
BX	-.44064475 00	BY	-.70503785 00	BZ	-.55565624 00	MX	.27038722-01	MY	.77211700 00	MZ	.63490490 00		
B.T	-.18361269 06	B.R	.45054496 05	B	.19391920 06	PER	.00000000 00	CMD	.55164090-04	NOD	.43146510-04		

HELIOCENTRIC												ECLIPTIC COORDINATES	
X	.10976271 09	Y	.99336496 08	Z	.19986000 05	DX	-.22426536 02	DY	.22823516 02	DZ	.32056320 00		
R	.14803916 09	LAT	.77352060-02	LON	.42145452 02	V	.31999456 02	PTH	-.23517084 01	AZ	.89425214 02		
XE	.11016135 09	YE	.99331033 08	ZE	-.12200000 03	DXE	-.20435530 02	DYE	.22028572 02	DZE	-.83124636-03		
XT	.10976133 09	YT	.99337542 08	ZT	.20117500 05	DXT	-.20416024 02	DYT	.21049736 02	DZT	.68064510-01		
LTE	-.47124811-04	LOE	.42040567 02	LTT	.77861176-02	LOT	.42146111 02	RST	.14803884 09	VST	.29824223 02		
EPS	.13699183 03	ESP	.10537696 00	SEP	.42902996 02	EPM	.14373027 03	EMP	.36122655 02	MEP	.14704286 00		
MPS	.79277553 02	MSP	.98911702-02	SMP	.10072178 03	SEM	.43050066 02	EMS	.13684409 03	ESM	.10607100 00		
EPT	.14373027 03	ETP	.36122655 02	TEP	.14704286 00	TPS	.79277553 02	TSP	.98911702-02	STP	.10072178 03		
SET	.43050066 02	STE	.13684409 03	EST	.10607100 00								

SPACECRAFT ATTITUDE AND POWERED FLIGHT						SELENOCENTRIC				EQUATORIAL COORDINATES	
CX	.23309914 00	CY	.49189188 00	CZ	.83887249 00	CR	-.33032792 00	CPH	.77472363 00	CTH	.53915358 00
CW	.35443289 00	CV	.39685103 00	CGM	-.84669147 00	CPE	.78863795 02	CPS	.13440009 03	CPM	.70711318 02
CPC	.11261770 03	CPT	.70711318 02			PHI	.21371750 03	PSI	.32737112 02	THA	.32737112 02
F	.00000000 00	M	.00000000 00	AC	.00000000 00	INA	.00000000 00	IAS	.00000000 00		

SELENOCENTRIC										EQUATORIAL COORDINATES	
X	.13822747 04	Y	-.90666703 03	Z	-.53686891 03	DX	-.20105124 01	DY	.15269262 01	DZ	.93730970 00
R	.17380900 04	DEC	-.17992012 02	RA	.32673817 03	V	.26929934 01	PTH	-.85574033 02	AZ	.56891172 02
R	.17380897 04	LAT	-.43402778 01	LON	.32124455 03	VR	.26926489 01	PTR	-.85669645 02	AZR	.77664858 02
LTS	.15159357 01	LNS	.22060488 03	LTE	-.38043675 01	LNE	.35745796 03				
ALT	.89981078-01	SHA	.17077466 04	ALP	.20321495 02	DR	-.26849626 01	DP	.68507379-02	ASD	.89416961 02
HGE	.22300817 03	SVL	-.18324544 00	HNG	.79277496 02	SIA	.54313308 02				

SELENOCENTRIC						CONIC		ORBITAL B.T AND B.R				EQUATORIAL COORDINATES	
EPOCH OF PERICENTER PASSAGE					JULIAN DATE 2437608.20775949						NOV. 4,1961		16 59 10.421
SMA	-.30383508 04	ECC	.10043716 01	INC	.37186323 02	LAN	.35208359 03	APF	.13790257 03	RCA	.13282400 02		
VH	.12700263 01	C3	.16129668 01	C1	.36120943 03	SLR	.26622866 02	APO	.00000000 00	TFP	-.45639272 03		
TA	-.16863648 03	EA	-.58361501 02	MA	-.10930402 02	DAI	.21200303 02	RAI	.14133522 03	MTA	.17465230 03		
WX	-.83244152-01	WY	-.59864965 00	WZ	.79667421 00	PX	-.66137613 00	PY	.63119017 00	PZ	.40519207 00		
QX	-.74542095 00	QY	-.49317148 00	QZ	-.44847548 00	RX	-.13273064 00	RY	.39774799 00	RZ	-.90784312 00		
SXO	.58902467 00	SYO	-.67440617 00	SZO	-.44522611 00	DAO	-.26437806 02	RAO	.31113388 03	TF	.65944282 02		
SXI	-.72797026 00	SYI	.58247959 00	SZI	.36163081 00	TX	.67263801 00	TY	.70888228 00	TZ	.21223581 00		
BX	.68053634 00	BY	.54985127 00	BZ	.48428696 00	MX	.79667437 00	MY	-.73559021-11	MZ	.83244170-01		
B.T	.27028028 03	B.R	-.88531979 02	B	.28441052 03	PER	.10435501 02						

JPL TECHNICAL REPORT NO. 32-223

CASE (N) SPACE TRAJECTORIES (Page K)

(Identification as input to cells 100–109)

GME $\mu_\oplus$	J J	H H	D D	RE a	REM $a_\oplus$
G G	A A	B B	C C	OME ω	AU $A_\odot$
GMM $\mu_\leftmoon$	GMS $\mu_\odot$	GMV μ_φ	GMA μ_σ	GMB μ_B	GMJ $\mu_\jmath$

$\mu_\oplus$ gravitational coefficient for the Earth in km³/sec²

J coefficient of the second harmonic in Earth's oblateness

H coefficient of the third harmonic in Earth's oblateness

D coefficient of the fourth harmonic in Earth's oblateness

a Earth radius to be used in the Earth's oblate potential, km

$a_\oplus$ Earth radius to convert lunar ephemeris to km

G universal gravitational constant for lunar oblateness, km³/sec²-kg

A, B, C moments of inertia for the Moon to be used in the lunar oblate potential; units are kg-km²

ω rotation rate of the Earth in deg/sec

$A_\odot$ Astronomical Unit to convert planetary ephemerides to km

$\mu_\leftmoon$ gravitational coefficient for the Moon in km³/sec²

$\mu_\odot$ gravitational coefficient for the Sun in km³/sec²

μ_φ gravitational coefficient for Venus in km³/sec²

μ_σ gravitational coefficient for Mars in km³/sec²

μ_B gravitational coefficient for Barycenter in km³/sec²

$\mu_\jmath$ gravitational coefficient for Jupiter in km³/sec²

INJECTION CONDITIONS (EQUINOX) (TARGET) (JULIAN DATE) (CALENDAR DATE)

(Central Body)	*X0 X_0	Y0 Y_0	Z0 Z_0	DX0 $\dot{X}_0$	DY0 $\dot{Y}_0$	DZ0 $\dot{Z}_0$
(Type)	GMC γ_c	SGC σ_c	TO t_0	GHA $\Upsilon(T_0)$	GHO $\Upsilon(T_M)$	(Ref. plane)**

X_0, Y_0, Z_0 vernal equinox Cartesian position, km

$\dot{X}_0$, $\dot{Y}_0$, $\dot{Z}_0$ vernal equinox Cartesian velocity, km/sec

γ_c elevation angle of reference vector for powered flight, deg

σ_c azimuth angle of reference vector, deg

t_0 seconds past midnight of injection time, sec

$\Upsilon(T_0)$ Greenwich hour angle of vernal equinox at injection epoch, deg

$\Upsilon(T_M)$ Greenwich hour angle of vernal equinox at previous midnight, deg

*If type is spherical inertial, then the line appears as:

RAD R DEC Φ RA Θ V V PTI Γ AZI Σ

If Earth-fixed or selenographic, the line appears as:

RAD r LAT ϕ LON θ VR v PTR γ AZR σ

If energy-asymptote, the line is modified to read:

AZL Σ_L RAD R PTH Γ C3 c_3 DAO Φ_S RAO Θ_S

R radius, km

Φ declination, deg

Θ right ascension, deg

V velocity, km/sec

Γ path angle, deg

Σ azimuth angle, deg

r radius, km

ϕ latitude, deg

θ longitude, deg

v velocity relative to rotating coordinate system, km/sec

γ path angle relative to rotating coordinate system, deg

σ azimuth angle relative to rotating coordinate system, deg

Σ_L azimuth at launch site, deg

R radius, km

Γ path angle, deg

c_3 "energy" or *vis viva* integral, km²/sec²

Φ_S declination of ascending asymptote, deg

Θ_S right ascension of ascending asymptote, deg

**If ecliptic coordinates are input, then ECLIPTIC is printed; otherwise space is left blank.

POWERED-FLIGHT PARAMETERS THRUST F FLOW $\dot{m}$ MASS m_0 BURN t_B

F thrust, lb force

$\dot{m}$ mass flow rate, lb mass/sec

m_0 initial mass, lb

t_B burning interval, sec

The powered-flight header appears only at the start of the powered-flight phase

Format for time at print epoch:

(SEXAGESIMAL INTERVAL PAST INJECTION) (EQUINOX) (JULIAN DATE) (CALENDAR DATE)

GEOCENTRIC GROUP

GEOCENTRIC (COORDINATE PLANE)

X X	Y Y	Z Z	DX $\dot{X}$	DY $\dot{Y}$	DZ $\dot{Z}$
R R	DEC Φ	RA Θ	V V	PTH Γ	AZ Σ
R r	LAT ϕ	LON θ	VE v	PTE γ	AZE σ
XS X_S	YS Y_S	ZS Z_S	DXS $\dot{X}_S$	DYS $\dot{Y}_S$	DZS $\dot{Z}_S$
XM X_M	YM Y_M	ZM Z_M	DXM $\dot{X}_M$	DYM $\dot{Y}_M$	DZM $\dot{Z}_M$
XT X_T	YT Y_T	ZT Z_T	DXT $\dot{X}_T$	DYT $\dot{Y}_T$	DZT $\dot{Z}_T$
RS R_S	VS V_S	RM R_M	VM V_M	RT R_T	VT V_T
GED ϕ'	ALT h_E	LOS θ_S	RAS Θ_S	RAM Θ_M	LOM θ_M
DUT ΔT	DT h	DR $\dot{R}$	SHA d	DES Φ_S	DEM Φ_M

X, Y, Z vernal equinox Cartesian position, km

$\dot{X}$, $\dot{Y}$, $\dot{Z}$ vernal equinox Cartesian velocity, km/sec

R radius, km

Φ declination, deg

Θ right ascension, deg

V inertial speed, km/sec

Γ path angle, deg

Σ azimuth angle, deg

r radius, km

ϕ geocentric latitude, deg

θ longitude, deg

v Earth-fixed speed, km/sec

γ Earth-fixed path angle, deg

σ Earth-fixed azimuth angle, deg

X_T, Y_T, Z_T the geocentric position of the target body, km

$\dot{X}_T$, $\dot{Y}_T$, $\dot{Z}_T$ the geocentric velocity of the target body, km/sec

R_S Earth-Sun distance, km

V_S the geocentric speed of the Sun, km/sec

R_M Earth-Moon distance, km

V_M speed of Moon, km/sec

R_T Earth-Target distance, km

V_T speed of Target body, km/sec

ϕ' geodetic latitude

h_E altitude above the Earth's surface, km

θ_S longitude of Sun, deg

Θ_S right ascension of Sun, deg

Θ_M right ascension of Moon, deg

θ_M longitude of Moon, deg

X_S, Y_S, Z_S the geocentric position of the Sun, km

$\dot{X}_S$, $\dot{Y}_S$, $\dot{Z}_S$ the geocentric velocity of the Sun, km/sec

X_M, Y_M, Z_M the geocentric position of the Moon, km

$\dot{X}_M$, $\dot{Y}_M$, $\dot{Z}_M$ the geocentric velocity of the Moon, km/sec

ΔT Ephemeris Time minus Universal Time, sec

h Adams-Moulton step size, sec

$\dot{R}$ radial speed, km/sec

d Sun shadow parameter, km

$$d = \frac{-|\mathbf{R}_{\oplus P} \times \mathbf{R}_{\oplus \odot}|}{R_{\oplus \odot}} \operatorname{sgn}(\mathbf{R}_{\oplus P} \cdot \mathbf{R}_{\oplus \odot})$$

Φ_S declination of the Sun, deg

Φ_M declination of the Moon, deg

TRACKING STATIONS

(STATION NAME)											
POL	p_i	LKA	λ_i	HA	α_i	DEC	δ_i	ELE	γ_i	AZI	σ_i
XIP	X_{ip}	YIP	Y_{ip}	DHA	$\dot{\alpha}_i$	DDE	$\dot{\delta}_i$	DEL	$\dot{\gamma}_i$	DAZ	$\dot{\sigma}_i$
RDI	r_i	PHI	ϕ_i	ZIP	Z_{ip}	RGE	r_{ip}	DRG	$\dot{r}_{ip}$	DDR	$\ddot{r}_{ip}$
				THI	θ_i	FBI	f_{B_i}	FCI	f_{c_i}	FRQ	f_i

α_i local hour angle of probe, deg

δ_i local declination of probe, deg

γ_i elevation angle of probe, deg

σ_i north azimuth of probe, deg

p_i polarization angle, deg

λ_i look angle, deg

$\dot{\alpha}_i$ hour-angle rate, deg/hr

$\dot{\delta}_i$ declination rate, deg/hr

$\dot{\gamma}_i$ elevation rate, deg/hr

$\dot{\sigma}_i$ azimuth rate, deg/hr

X_{ip}, Y_{ip}, Z_{ip} Cartesian coordinates of the probe centered at the station and axes parallel to those of the true equator and equinox of date, km

r_{ip} slant range of probe, km

$\dot{r}_{ip}$ slant-range rate, km/sec

$\ddot{r}_{ip}$ rate of the slant-range rate, km/sec^2

r_i radius of the station, km

φ_i north geocentric latitude of the station, deg

θ_i east longitude of the station, deg

f_{B_i} additive constant for doppler, cps

f_{c_i} multiplicative constant for doppler, cps/km/sec

f_i doppler: $f_i = f_{B_i} - f_{c_i} \dot{r}_{ip}$, cps

OSCULATING CONICS

(CENTRAL BODY) CONIC (TYPE OF B·T AND B·R) (COORDINATE PLANE)

EPOCH OF PERICENTER PASSAGE (JULIAN DATE) (CALENDAR DATE)

SMA	a	ECC	ϵ	INC	i	LAN	Ω	APF	ω	RCA	q
VH	V_H	C3	c_3	C1	c_1	SLR	p	APO	q_2	TFP	Δt
TA	v	EA	E	MA	M	DAI[a]	Φ_I	RAI[a]	Θ_I	MTA	v_{max}
WX	W_x	WY	W_y	WZ	W_z	PX	P_x	PY	P_y	PZ	P_z
QX	Q_x	QY	Q_y	QZ	Q_z	RX	R_x	RY	R_y	RZ	R_z
SXI[a]	S_{xI}	SYI[a]	S_{yI}	SZI[a]	S_{zI}	TX	T_x	TY	T_y	TZ	T_z
BX	B'_x	BY	B'_y	BZ	B'_z	MX	M_x	MY	M_y	MZ	M_z
B.T	$\mathbf{B}\cdot\mathbf{T}$	B.R	$\mathbf{B}\cdot\mathbf{R}$	B	b	PER	P	OMD[b]	$\dot{\omega}$	NOD[b]	$\dot{\Omega}$

a semimajor or semitransverse axis; $a < 0$ for hyperbola, km

ϵ eccentricity, rad

i inclination, deg

Ω longitude or right ascension of ascending node, deg

ω argument of pericenter, deg

q closest approach distance, km

V_H hyperbolic excess speed (velocity at apogee for ellipse), km/sec

c_3 twice the total energy per unit mass or *vis viva* integral, km²/sec²

c_1 angular momentum, km²/sec

p semilatus rectum, km

q_2 apocenter distance, km

Δt time from pericenter passage, sec

v true anomaly, deg

E eccentric anomaly, deg

M mean anomaly, deg

Φ_I declination or latitude of incoming asymptote, deg

Θ_I right ascension or longitude of incoming asymptote, deg

v_{max} maximum true anomaly, deg

W_x W_y W_z — X-, Y-, Z-component of $\mathbf{W} = \mathbf{P} \times \mathbf{Q}$

P_x P_y P_z — X-, Y-, Z-component of $\mathbf{P}$

Q_x Q_y Q_z — X-, Y-, Z-component of $\mathbf{Q}$

R_x R_y R_z — X-, Y-, Z-component of $\mathbf{R}$

S_{xI} S_{yI} S_{zI} — X-, Y-, Z-component of $\mathbf{S}_I$, incoming asymptote

T_x T_y T_z — X-, Y-, Z-component of $\mathbf{T} = \mathbf{R} \times \mathbf{S}$

B'_x B'_y B'_z — X-, Y-, Z-component of unit vector $\mathbf{B}'$, $\mathbf{B}' = \dfrac{\mathbf{B}}{b}$

M_x M_y M_z — X-, Y-, Z-component of M, $\mathbf{M} = \mathbf{W} \times \dfrac{\mathbf{R}_0}{R_0}$

$\mathbf{B}\cdot\mathbf{T}$ T-component of $\mathbf{B}$, km

$\mathbf{B}\cdot\mathbf{R}$ R-component of $\mathbf{B}$, km

b magnitude of $\mathbf{B}$, km

P period, days if heliocentric, otherwise min; if $\epsilon \geqq 1$, P is replaced by

$$\Delta T_f = \frac{|a|^{3/2}}{\sqrt{\mu}} \sinh^{-1}\left(\frac{\epsilon^2 - 1}{2\epsilon}\right),$$

the linearized time-of-flight correction, target conic only, sec

$\dot{\omega}$ rate of change of argument of perigee, deg/day

$\dot{\Omega}$ rate of change of right ascension of the ascending node, deg/day

[a]Values are printed in the heliocentric and target-centered conics. In addition, the target-centered conic prints an extra line marked SXO SYO SZO DAO RAO TF where O is for outgoing asymptote. This line is printed just above the line marked SXI SYI .... The geocentric conic prints SXO SYO SZO in place of SXI SYI SZI in line six and prints DAO and RAO in place of DAI and RAI in line three. *TF*, the time of flight, is in hr for Moon or Earth target, in days otherwise.

[b]$\dot{\omega}$ and $\dot{\Omega}$ are printed only in geocentric conic.

HELIOCENTRIC GROUP

HELIOCENTRIC (COORDINATE PLANE)

X	X	Y	Y	Z	Z	DX	$\dot{X}$	DY	$\dot{Y}$	DZ	$\dot{Z}$
R	R	LAT	β	LON	λ	V	V	PTH	Γ	AZ	Σ
XE	X_E	YE	Y_E	ZE	Z_E	DXE	$\dot{X}_E$	DYE	$\dot{Y}_E$	DZE	$\dot{Z}_E$
XT	X_T	YT	Y_T	ZT	Z_T	DXT	$\dot{X}_T$	DYT	$\dot{Y}_T$	DZT	$\dot{Z}_T$
LTE	$\beta_\oplus$	LOE	$\lambda_\oplus$	LTT	β_T	LOT	λ_T	RST	$\dot{R}_{ST}$	VST	V_{ST}
EPS	$\angle(\mathbf{R}_{EP}, \mathbf{R}_{SP})$	ESP	$\angle(\mathbf{R}_{ES}, \mathbf{R}_{PS})$	SEP	$\angle(\mathbf{R}_{SE}, \mathbf{R}_{PE})$	EPM	$\angle(\mathbf{R}_{EP}, \mathbf{R}_{MP})$	EMP	$\angle(\mathbf{R}_{EM}, \mathbf{R}_{PM})$	MEP	$\angle(\mathbf{R}_{ME}, \mathbf{R}_{PE})$
MPS	$\angle(\mathbf{R}_{MP}, \mathbf{R}_{SP})$	MSP	$\angle(\mathbf{R}_{MS}, \mathbf{R}_{PS})$	SMP	$\angle(\mathbf{R}_{SM}, \mathbf{R}_{PM})$	SEM	$\angle(\mathbf{R}_{SE}, \mathbf{R}_{ME})$	EMS	$\angle(\mathbf{R}_{EM}, \mathbf{R}_{SM})$	ESM	$\angle(\mathbf{R}_{ES}, \mathbf{R}_{MS})$
EPT	$\angle(\mathbf{R}_{EP}, \mathbf{R}_{TP})$	ETP	$\angle(\mathbf{R}_{ET}, \mathbf{R}_{PT})$	TEP	$\angle(\mathbf{R}_{TE}, \mathbf{R}_{PE})$	TPS	$\angle(\mathbf{R}_{TP}, \mathbf{R}_{SP})$	TSP	$\angle(\mathbf{R}_{TS}, \mathbf{R}_{PS})$	STP	$\angle(\mathbf{R}_{ST}, \mathbf{R}_{PT})$
SET	$\angle(\mathbf{R}_{SP}, \mathbf{R}_{TE})$	STE	$\angle(\mathbf{R}_{ST}, \mathbf{R}_{ET})$	EST	$\angle(\mathbf{R}_{ES}, \mathbf{R}_{TS})$						

X, Y, Z } vernal equinox Cartesian position, km

$\dot{X}$, $\dot{Y}$, $\dot{Z}$ } vernal equinox Cartesian velocity, km/sec

R Sun-Probe radius, km

β celestial latitude (or Φ, the declination if equatorial), deg

λ celestial longitude (or Θ, the right ascension if equatorial), deg

V speed, km/sec

Γ path angle, deg

Σ azimuth angle, deg

X_E, Y_E, Z_E } heliocentric position of the Earth, km

$\dot{X}_E$, $\dot{Y}_E$, $\dot{Z}_E$ } heliocentric velocity of the Earth, km/sec

X_T, Y_T, Z_T } heliocentric position of the target, km

$\dot{X}_T$, $\dot{Y}_T$, $\dot{Z}_T$ } heliocentric velocity of the target, km/sec

$\beta_\oplus$ celestial latitude (or declination) of the Earth, deg

$\lambda_\oplus$ celestial longitude (or right ascension) of the Earth, deg

β_T celestial latitude (or declination) of the target, deg

λ_T celestial longitude (or right ascension) of the target, deg

R_{ST} distance of the target from the Sun, km

V_{ST} speed of the target with respect to the Sun, km/sec

$\angle(\mathbf{R}_{EP}, \mathbf{R}_{SP})$ Earth-Probe-Sun angle, deg

$\angle(\mathbf{R}_{ES}, \mathbf{R}_{PS})$ Earth-Sun-Probe angle, deg

$\angle(\mathbf{R}_{SE}, \mathbf{R}_{PE})$ Sun-Earth-Probe angle, deg

$\angle(\mathbf{R}_{EP}, \mathbf{R}_{MP})$ Earth-Probe-Moon angle, deg

$\angle(\mathbf{R}_{EM}, \mathbf{R}_{PM})$ Earth-Moon-Probe angle, deg

$\angle(\mathbf{R}_{ME}, \mathbf{R}_{PE})$ Moon-Earth-Probe angle, deg

$\angle(\mathbf{R}_{MP}, \mathbf{R}_{SP})$ Moon-Probe-Sun angle, deg

$\angle(\mathbf{R}_{MS}, \mathbf{R}_{PS})$ Moon-Sun-Probe angle, deg

$\angle(\mathbf{R}_{SM}, \mathbf{R}_{PM})$ Sun-Moon-Probe angle, deg

$\angle(\mathbf{R}_{SE}, \mathbf{R}_{ME})$ Sun-Earth-Moon angle, deg

$\angle(\mathbf{R}_{EM}, \mathbf{R}_{SM})$ Earth-Moon-Sun angle, deg

$\angle(\mathbf{R}_{ES}, \mathbf{R}_{MS})$ Earth-Sun-Moon angle, deg

$\angle(\mathbf{R}_{EP}, \mathbf{R}_{TP})$ Earth-Probe-Target angle, deg

$\angle(\mathbf{R}_{ET}, \mathbf{R}_{PT})$ Earth-Target-Probe angle, deg

$\angle(\mathbf{R}_{TE}, \mathbf{R}_{PE})$ Target-Earth-Probe angle, deg

$\angle(\mathbf{R}_{TP}, \mathbf{R}_{SP})$ Target-Probe-Sun angle, deg

$\angle(\mathbf{R}_{TS}, \mathbf{R}_{PS})$ Target-Sun-Probe angle, deg

$\angle(\mathbf{R}_{ST}, \mathbf{R}_{PT})$ Sun-Target-Probe angle, deg

$\angle(\mathbf{R}_{SE}, \mathbf{R}_{TE})$ Sun-Earth-Target angle, deg

$\angle(\mathbf{R}_{ST}, \mathbf{R}_{ET})$ Sun-Target-Earth angle, deg

$\angle(\mathbf{R}_{ES}, \mathbf{R}_{TS})$ Earth-Sun-Target angle, deg

SPACECRAFT GROUP

SPACECRAFT ATTITUDE AND POWERED FLIGHT (CENTRAL BODY) (COORDINATE PLANE)

CX	C_x	CY	C_y	CZ	C_z	CR	$\mathbf{C}\cdot\mathbf{R}'$	CPH	$\mathbf{C}\cdot\Phi'$	CTH	$\mathbf{C}\cdot\Theta'$
CW	$\cdot\mathbf{W}$	CV	$\mathbf{C}\cdot\mathbf{V}'$	CGM	$\mathbf{C}\cdot(\mathbf{W}\times\mathbf{V}')$	CPE	$\angle(\mathbf{C}, -\mathbf{R}_{EP})$	CPS	$\angle(\mathbf{C}, -\mathbf{R}_{SP})$	CPM	$\angle(\mathbf{C}, -\mathbf{R}_{MP})$
CPC	$\angle(\mathbf{C}, \mathbf{C}_{CAN})$	CPT	$\angle(\mathbf{C}, -\mathbf{R}_{TP})$			PHI	ϕ	PSI	ψ	THA	θ
F	F	M	m	AC	a	INA	$\int a$	IAS	$\int a^2$		

C_x X-component of $\mathbf{C}$
C_y Y-component of $\mathbf{C}$
C_z Z-component of $\mathbf{C}$
} $\mathbf{C}$ is given by the input quantities γ_C, σ_C

$\mathbf{C}\cdot\mathbf{R}'$ $\cos\angle(\mathbf{C}, \mathbf{R}')$
$\mathbf{C}\cdot\Phi'$ $\cos\angle(\mathbf{C}, \Phi')$
$\mathbf{C}\cdot\Theta'$ $\cos\angle(\mathbf{C}, \Theta')$
} $\mathbf{R}' = \dfrac{\mathbf{R}}{R}$

$\angle(\mathbf{C}, -\mathbf{R}_{EP})$ Axis-Probe-Earth angle, deg
$\angle(\mathbf{C}, -\mathbf{R}_{SP})$ Axis-Probe-Sun angle, deg
$\angle(\mathbf{C}, -\mathbf{R}_{MP})$ Axis-Probe-Moon angle, deg

$\angle(\mathbf{C}, \mathbf{C}_{CAN})$ Axis-Probe-Canopus angle, deg
$\angle(\mathbf{C}, -\mathbf{R}_{TP})$ Axis-Probe-Target angle, deg

$$\begin{cases} \cos\phi = \mathbf{S}_1\cdot\mathbf{C} \\ \sin\phi = (\mathbf{S}\times\mathbf{S}_1)\cdot\mathbf{C} \end{cases} \qquad 0 \le \phi < 360°$$

$$\psi = \sin^{-1}\mathbf{S}\cdot\mathbf{C} \qquad -90° \le \psi \le 90°$$

$$\theta = |\psi|$$

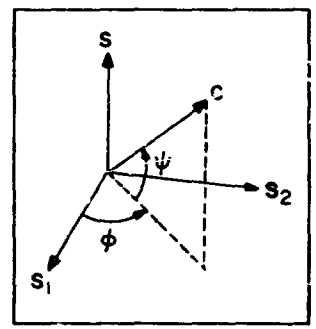

Sketch 6. Spacecraft coordinates

$$\cos\Phi\,\Phi' + \sin\Phi\,\mathbf{R}' = (0, 0, 1)$$

where

$$\sin\Phi = \frac{Z}{R} \qquad \Theta' = \Phi'\times\mathbf{R}'$$

F thrust, lb
m mass or weight, lb
a acceleration, km/sec^2
$\int a$ integral of a, km/sec
$\int a^2$ integral of a^2, km^2/sec^3

$$a = \frac{F}{m}$$

$$m = m_0 - \dot{m}(T - T_1)$$

$$\int a = \frac{F}{\dot{m}}\ln\frac{m_0}{m}$$

$$\int a^2 = \frac{F^2}{\dot{m}}\left[\frac{1}{m} - \frac{1}{m_0}\right]$$

$\mathbf{C}\cdot\mathbf{W}$ $\cos\angle(\mathbf{C}, \mathbf{W})$
$\mathbf{C}\cdot\mathbf{V}'$ $\cos\angle(\mathbf{C}, \mathbf{V}')$
$\mathbf{C}\cdot(\mathbf{W}\times\mathbf{V}')$ $\cos\angle(\mathbf{C}, (\mathbf{W}\times\mathbf{V}'))$
} $\mathbf{W} = \dfrac{\mathbf{R}\times\mathbf{V}}{|\mathbf{R}\times\mathbf{V}|}$
} $\mathbf{V}' = \dfrac{\mathbf{V}}{V}$

$$\mathbf{S}_1 = \frac{\mathbf{R}_{P\odot}}{R_{P\odot}}$$

$$\mathbf{S}_2 = \frac{\mathbf{R}_{P\oplus}}{R_{P\oplus}}$$

$$\mathbf{S} = \frac{\mathbf{S}_1\times\mathbf{S}_2}{|\mathbf{S}_1\times\mathbf{S}_2|}$$

TARGET GROUP

(TARGET) CENTRIC (COORDINATE PLANE)

X	X	Y	Y	Z	Z	ÝX	$\dot{X}$	DY	$\dot{Y}$	DZ	$\dot{Z}$
R	R	DEC	Φ	RA	Θ	V	V	PTH	Γ	AZ	Σ
R	r	LAT	ϕ	LON	θ	VR	v	PTR	γ	AZR	σ
LTS	$\beta_{\text{☾}\odot}$	LNS	$\lambda_{\text{☾}\odot}$	LTE	$\beta_{\text{☾}\oplus}$	LNE	$\lambda_{\text{☾}\oplus}$				
ALT	h_T	SHA	d	ALP	α	DR	$\dot{R}$	DP	$\dot{\psi}$	ASD	δ
HGE	Θ_{SE}	SVL	Φ_{ST}	HNG	Θ_{ST}	SIA	δ_E				

X, Y, Z } target-centered vernal equinox position, km

$\dot{X}, \dot{Y}, \dot{Z}$ } target-centered vernal equinox velocity, km/sec

R radius from target center, km

Φ declination (or celestial latitude), deg

Θ right ascension (or celestial longitude), deg

V speed relative to the target, km/sec

Γ target-body path angle, deg

Σ target-body azimuth angle, deg

r radius from target center, km

ϕ target-centered latitude, deg

θ target-centered longitude, deg

v speed relative to the rotating target, km/sec

γ rotating target-body path angle, deg

σ rotating target-body azimuth angle, deg

} (for Moon only)

$\beta_{\mathbb{C}\odot}$ selenographic latitude of the Sun, deg

$\lambda_{\mathbb{C}\odot}$ selenographic longitude of the Sun, deg

$\beta_{\mathbb{C}\oplus}$ selenographic latitude of the Earth, deg

$\lambda_{\mathbb{C}\oplus}$ selenographic longitude of the Earth, deg

} (for Moon only)

h_T altitude above the target body's surface, km

d Sun's shadow parameter, km

$$d = \frac{-|\mathbf{R}_{TI} \times \mathbf{R}_{T\odot}|}{R_{T\odot}} \operatorname{sgn}(\mathbf{R}_{TP} \cdot \mathbf{R}_{T\odot})$$

α illuminated crescent orientation viewing angle, deg

$\dot{R}$ radial rate, km/sec

$\dot{\psi}$ transverse angular velocity, deg/sec

δ angular semidiameter, deg

Θ_{SE} right ascension of Earth in spacecraft coordinate system, deg

Φ_{ST} declination of target in spacecraft coordinate system, deg

Θ_{ST} right ascension of target in spacecraft coordinate system, deg

δ_E $\angle(\mathbf{R}_{TP}, \mathbf{R}_{EP}) - \delta$, deg

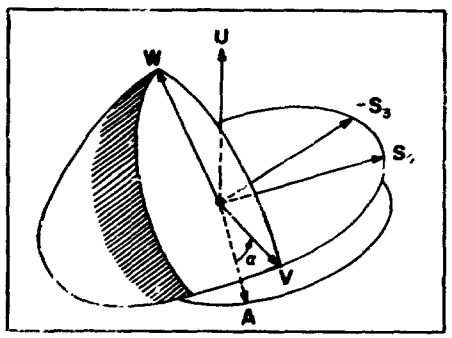

Sketch 7. Illuminated crescent orientation viewing angle

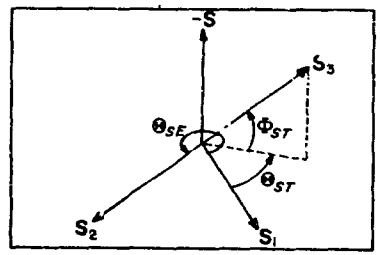

Sketch 8. Hinge and swivel angles

$$-\mathbf{S}_3 = \frac{\mathbf{R}_{TP}}{R_{TP}} \qquad \mathbf{U} = (0, 0, 1)$$

$$\mathbf{S}_4 = \frac{\mathbf{R}_{T\odot}}{R_{T\odot}} \qquad \mathbf{V} = \mathbf{W} \times \mathbf{S}_3$$

$$\mathbf{A} = \frac{\mathbf{U} \times \mathbf{S}_3}{|\mathbf{U} \times \mathbf{S}_3|}$$

$$\mathbf{W} = \frac{\mathbf{S}_3 \times \mathbf{S}_4}{|\mathbf{S}_3 \times \mathbf{S}_4|} \qquad \cos\alpha = \mathbf{A} \cdot \mathbf{V}$$

Earth hinge angle
$$\begin{cases} \cos\Theta_{SE} = \mathbf{S}_2 \cdot \mathbf{S}_1 \\ \sin\Theta_{SE} = \mathbf{S}_2 \cdot (\mathbf{S}_1 \times \mathbf{S}) \end{cases} \qquad 0 \leq \Theta_{SE} < 360°$$

Target swivel angle
$$\sin\Phi_{ST} = -\mathbf{S}_3 \cdot \mathbf{S} \qquad -90° \leq \Phi_{ST} \leq 90°$$

Target hinge angle
$$\begin{cases} \cos\Theta_{ST} = \mathbf{S}_3 \cdot \mathbf{S}_1 \\ \sin\Theta_{ST} = \mathbf{S}_3 \cdot (\mathbf{S}_1 \times \mathbf{S}) \end{cases} \qquad 0 \leq \Theta_{ST} < 360°$$

$$\mathbf{S}_1 = \frac{\mathbf{R}_{P\odot}}{R_{P\odot}} \qquad \mathbf{S} = \frac{\mathbf{S}_1 \times \mathbf{S}_2}{|\mathbf{S}_1 \times \mathbf{S}_2|}$$

$$\mathbf{S}_2 = \frac{\mathbf{R}_{P\oplus}}{R_{P\oplus}} \qquad \mathbf{S}_3 = \frac{\mathbf{R}_{PT}}{R_{PT}}$$

APPENDIX

Description of Major Subroutines

INDEX

INDEX (Cont'd)

1. Input-Output Routines

ECLIP

The ecliptic plane is characterized by its inclination to the equator, ϵ, the obliquity of the ecliptic, and its ascending node on the equator, the vernal equinox.

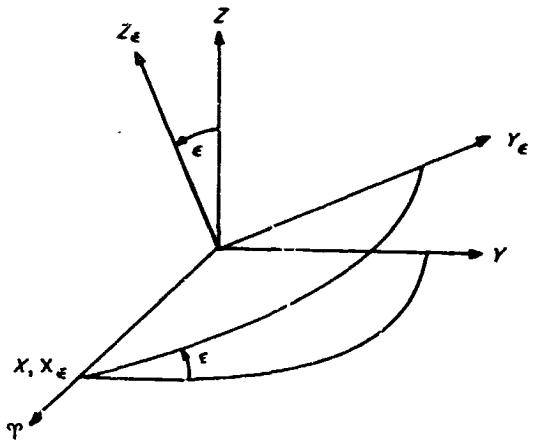

Sketch A-1. Relation between ecliptic and equatorial planes

In Sketch A-1, X, Y, Z is the equatorial frame; X_ϵ, Y_ϵ, Z_ϵ the ecliptic. Υ is the vernal equinox. The coordinates are related by

$$\begin{pmatrix} X_\epsilon \\ Y_\epsilon \\ Z_\epsilon \end{pmatrix} = \begin{pmatrix} 1 & 0 & 0 \\ 0 & \cos\epsilon & \sin\epsilon \\ 0 & -\sin\epsilon & \cos\epsilon \end{pmatrix} \begin{pmatrix} X \\ Y \\ Z \end{pmatrix}$$

The calling sequence is given by

CALL ECLIP
(OP) X,,Y

X − 3, X − 2, X − 1 contain the input vector; Y − 3, Y − 2, Y − 1 contain the output vector; X = Y is permitted. OP = PZE assumes equatorial input to be rotated to ecliptic; OP = MZE regards input as ecliptic and rotates to equatorial.

Normally X, Y, Z is regarded as the true equator and equinox of date and ϵ the true obliquity; however, for some applications it is necessary to rotate between the mean equator and equinox of 1950.0 and the ecliptic of 1950.0; for the latter purpose $\bar{\epsilon}_{1950.0}$, the mean obliquity of 1950.0, is used. To provide for this flexibility, ECLIP assumes that the desired obliquity has been placed in the COMMON location ET.

The subroutine uses nine cells of erasable storage starting at COMMON.

GHA

For purposes of calculating $\Upsilon(T)$, the Greenwich hour angle of the vernal equinox at epoch T, the following mean value is assumed:

$$\Upsilon_M(T) \equiv 100°07554260 + 0°9856473460d + (2°9015)\,10^{-13}d^2 + \omega t \pmod{360°}$$
$$0 \leqq \Upsilon_M(T) < 360°$$

where T is the epoch under consideration in U.T.; d is integer days past 0^h January 1, 1950; t is seconds past 0^h of the epoch T. ω, the Earth's rotation rate, is assumed to be a function of time:

$$\omega = \frac{0.00417807417}{1 + (5.21)\,10^{-13}d} \text{ deg/sec}$$

Given $\delta\alpha$, the nutation in right ascension, the true value of the hour angle is computed:

$$\Upsilon(T) = \Upsilon_M(T) + \delta\alpha$$

The calling sequence consists of

CALL GHA,

where it is assumed that the U.T. epoch appears in double-precision seconds past 0^h January 1, 1950, in the COMMON cells T, T + 1, and that $\delta\alpha$ has been computed and appears in NUTRA. $\Upsilon(T)$ is stored in the COMMON location GHA(T), while ω is placed in OMEGA and ω in rad/sec is stored in LOMEGA.

The subroutine uses seven cells of erasable storage starting at COMMON.

GEDLAT

To obtain an accurate numerical expression for the small difference between the geodetic latitude ϕ' and the geocentric latitude ϕ, a Fourier series expansion is resorted to. The geometry appears in Sketch A-2:

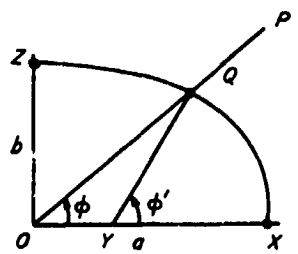

Sketch A-2. Geodetic and geocentric latitudes

Consider a point P above the Earth and extend a line to the center of the Earth O. If a spheroidal Earth is assumed, then let OZ be the spin axis of the Earth and the plane ZOX contain the line OP with Q the intersection of OP with the surface; OX lies in the equatorial plane. Then the angle ϕ, the geocentric latitude, is the angle between the lines OQ and OX. If the normal YQ to the surface is constructed at Q to intersect OX at Y, then ϕ', the geodetic latitude, is the angle between the lines YQ and YX. The ellipse of cross section is characterized by a, the semimajor axis, and b, the semiminor axis. It is convenient to introduce $\varepsilon^2 = 1 - b^2/a^2$ to describe $\phi - \phi'$ by a Fourier series.

As the defining relation, $\tan \phi = (1 - \varepsilon^2) \tan \phi'$ is adopted which leads to the series in $2\phi'$ for $\phi - \phi'$:

$$\phi - \phi' = \sum_{j=1}^{\infty} a_j \sin 2j\phi'$$

where

$$a_j = \frac{(-1)^j}{j}\left(\frac{\varepsilon^2}{2-\varepsilon^2}\right)^j$$

Alternatively, $\phi' - \phi$ may be expanded as a Fourier series in 2ϕ:

$$\phi' - \phi = \sum_{j=1}^{\infty} b_j \sin 2j\phi$$

where the b_j are obtained by replacing $1 - \varepsilon^2$ by $1/(1 - \varepsilon^2)$ in the expression for the a_j. Incidentally, $b_j = (-1)^j a_j$ is obtained by performing the substitution.

Using the Clarke spheroid of 1866 with $a = 6378.2064$ km, $b = 6356.5838$ km, and the derived value $\varepsilon^2 = 0.006768657997$, the following numerical formula results:

$$\phi' - \phi = b_1 \sin 2\phi + b_2 \sin 4\phi + b_3 \sin 6\phi$$

where

$$b_1 = 0°.19456624$$
$$b_2 = 0°.00033036$$
$$b_3 = 0°.00000075$$

An auxiliary problem is the determination of the altitude of P above the spheroid. An approximate solution is obtained by regarding $\overline{QP} = h$ as the desired altitude. If $R = \overline{OP}$ is given, then if $\rho = \overline{OQ}$ is calculated, h would be given by $h = R - \rho$.

The arc of the ellipse may be described by the parameter ψ, where $x = a \cos \psi$, $y = b \sin \psi$ for $Q(x, y)$. Then the expression for ρ is

$$\rho = a\sqrt{1 - \varepsilon^2 \sin^2 \psi}$$

Actually, the formula programmed for ρ differs in that ϕ was used for ψ:

$$\rho' = a\sqrt{1 - \varepsilon^2 \sin^2 \phi}$$

The numerical difference between the two formulas may be assessed by expanding ρ and ρ' in power series in ε^2 and using the relation

$$\sin^2 \phi = \frac{(1-\varepsilon^2)\sin^2 \psi}{1 - \varepsilon^2 \sin^2 \psi}:$$

$$\frac{\rho}{a} = 1 - \frac{1}{2}\varepsilon^2 \sin^2 \psi - \frac{1}{8}\varepsilon^4 \sin^4 \psi - \frac{1}{16}\varepsilon^6 \sin^6 \psi + O(\varepsilon^8)$$

$$\frac{\rho'}{a} = 1 - \frac{1}{2}\varepsilon^2 \sin^2 \psi + \varepsilon^4\left\{-\frac{1}{2}\sin^2 \psi (\sin^2 \psi - 1) - \frac{1}{8}\sin^4 \psi\right\} + \varepsilon^6\left\{-\frac{3}{4}\sin^4 \psi (\sin^2 \psi - 1) - \frac{1}{16}\sin^6 \psi\right\} + O(\varepsilon^8)$$

so

$$\rho' - \rho = a\left\{\frac{1}{8}\varepsilon^4 \sin^2 2\psi + \frac{3}{16}\varepsilon^6 \sin^2 \psi \sin^2 2\psi + O(\varepsilon^8)\right\}$$

Thus the maximum difference, occurring near $\psi = 45°$, should be about $a\varepsilon^4/8 \approx 0.06$ km.

The calling sequence is given by

(AC) = ϕ

CALL GEDLAT

and upon return

(AC) = ϕ', (MQ) = ρ'

The subroutine uses 10 words of erasable storage starting at COMMON.

JEKYL

JEKYL is the subroutine which is used to generate orbital elements to be used either as input to the subroutines CLASS and SPECL or for printed output. The equations used are similar in most respects to those described in the discussion of CONIC (Section 4, Appendix) and are listed here for comparison.

$p = \dfrac{R^2 V^2 - (R\dot{R})^2}{\mu}$, the semilatus rectum,

where

$$R\dot{R} = \mathbf{R}\cdot\mathbf{V},$$

$c_1 = \sqrt{R^2V^2 - (R\dot{R})^2}$, the angular momentum

$$\frac{1}{a} = \frac{2\mu - RV^2}{R\mu}$$

$c_3 = -\frac{\mu}{a}$, the "energy" or *vis viva* integral

At this point a test is made with the help of the I.D. input to determine whether or not a is an acceptable parameter. a^* is defined by

$$a^* = \begin{cases} 10^{10} \text{ km for the planets} \\ 10^{9} \text{ km for the Sun} \\ 10^{12} \text{ km for the Moon} \end{cases}$$

The motion is considered parabolic and c_3 is set to zero whenever $|a| > a^*$.

$$1 - \varepsilon^2 = \frac{p}{a}$$

$\varepsilon = \sqrt{1 - (1 - \varepsilon^2)}$, the eccentricity

$$\begin{cases} \cos v = \dfrac{p - R}{\varepsilon R} \\ \sin v = \dfrac{\dot{R}}{\varepsilon}\sqrt{\dfrac{p}{\mu}} \end{cases}$$, true anomaly

$q = \frac{p}{1+\varepsilon}$, closest approach distance

$\mathbf{W} = \frac{\mathbf{R}\times\mathbf{V}}{c_1}$, unit angular momentum vector

$$\mathbf{U}_1 = \frac{\mathbf{R}}{R}$$

$$\mathbf{V}_1 = \frac{R}{c_1}\mathbf{V} - \frac{\dot{R}}{c_1}\mathbf{R}$$

$$\mathbf{P} = \cos v\,\mathbf{U}_1 - \sin v\,\mathbf{V}_1$$

$$\mathbf{Q} = \sin v\,\mathbf{U}_1 + \cos v\,\mathbf{V}_1$$

If $c_3 \neq 0$, $T - T_p$ is computed from Kepler's equation according to the sign of a:

If $a > 0$:

$$\begin{cases} \cos E = \dfrac{R}{p}(\cos v + \varepsilon) \\ \sin E = \dfrac{R}{p}\sqrt{1-\varepsilon^2}\sin v \end{cases}$$

$M = E - \varepsilon\sin E$ if $1 - \varepsilon > 0.1$ or if $1 - \varepsilon \leqq 0.1$ and $|\sin E| > 0.1$

$M = (1-\varepsilon)\sin E + \left(\frac{\sin^3 E}{6} + \frac{3\sin^5 E}{40}\right)$ if $1 - \varepsilon \leqq 0.1$ and $\cos E > 0$, $|\sin E| \leqq 0.1$

$M = n(T - T_p)$ where $n = \sqrt{\mu}\,a^{-3/2}$

If $a < 0$:

$$\sinh F = \frac{R\dot{R}}{\varepsilon\sqrt{\mu|a|}}$$

$M = \varepsilon\sinh F - F$ if $\varepsilon - 1 > 0.1$ or if $\varepsilon - 1 \leqq 0.1$ and $|\sinh F| > 0.1$

$M = (\varepsilon - 1)\sinh F - \left(\frac{3\sinh^5 F}{40} - \frac{\sinh^3 F}{6}\right)$ if $\varepsilon - 1 \leqq 0.1$ and $|\sinh F| \leqq 0.1$

$M = n(T - T_p)$ where $n = \sqrt{\mu}\,|a|^{-3/2}$

If $c_3 = 0$, the formula for the parabola is used:

$$M = \sqrt{\mu}(T - T_p) = qD + \frac{1}{6}D^3$$

where $D = R\dot{R}/\sqrt{\mu} = \sqrt{2q}\tan v/2$

JEKYL may be called by the sequence

```
CALL  JEKYL
PZE   0,,A
PZE   B,,C
PZE   D,,0
PZE   E,,F
PZE   G
(ERROR RETURN)
```

The locations A, A + 1 contain for input μ and an I.D. number:

0 = planets

1 = Moon

2 = Sun

The cells B, B + 1, B + 2 contain the input position vector **R**, and the locations C, C + 1, C + 2 contain the input velocity vector **V**; the vectors **P**, **Q**, and **W** are output to the locations D, ..., D + 8. The single-precision epoch T is input to location E, while the single-precision epoch of closest approach T_p is output to location F. Finally, the locations G, ..., G + 2 are used to output the quantities $\Delta T = T - T_p$, c_1, and c_3.

Additional quantities are stored at the COMMON locations

ECCEN	ε
1MINE	$1 - \varepsilon$
AVAL	a
PVAL	p
NORB	n
NU	v
JECAN	E (or F)
MENAN	M

The subroutine uses 15 words of erasable storage starting at COMMON.

SPECL

The subroutine SPECL is used to calculate the auxiliary impact parameters $\mathbf{B}\cdot\mathbf{T}$ and $\mathbf{B}\cdot\mathbf{R}$ along with reference unit vectors **R**, **S**, **T** and also **B** itself. Two cases arise according to the value of ε:

(1) $\varepsilon \geqq 1$, the hyperbolic case with $a < 0$

$$\mathbf{S} = \begin{cases} \frac{1}{\varepsilon}\mathbf{P} + \frac{\sqrt{\varepsilon^2 - 1}}{\varepsilon}\mathbf{Q} \\ \quad \text{for the incoming asymptote} \\ \frac{-1}{\varepsilon}\mathbf{P} + \frac{\sqrt{\varepsilon^2 - 1}}{\varepsilon}\mathbf{Q} \\ \quad \text{for the outgoing asymptote} \end{cases}$$

$$\mathbf{B} = \begin{cases} \frac{|a|(\varepsilon^2 - 1)}{\varepsilon}\mathbf{P} - \frac{|a|\sqrt{\varepsilon^2 - 1}}{\varepsilon}\mathbf{Q} \\ \quad \text{for the incoming asymptote} \\ \frac{|a|(\varepsilon^2 - 1)}{\varepsilon}\mathbf{P} + \frac{|a|\sqrt{\varepsilon^2 - 1}}{\varepsilon}\mathbf{Q} \\ \quad \text{for the outgoing asymptote} \end{cases}$$

(2) $\varepsilon < 1$, the elliptic case with $a > 0$

$$\left.\begin{aligned} \mathbf{S} &= \mathbf{P} \\ \mathbf{B} &= a\sqrt{|\varepsilon^2 - 1|}\,\mathbf{Q} \end{aligned}\right\} \text{for both the incoming and outgoing asymptote options}$$

The remaining two reference vectors **T** and **R** are given in either the hyperbolic or elliptic case by

$$\mathbf{T} = \left(\frac{S_y}{\sqrt{S_x^2 + S_y^2}}, \frac{-S_x}{\sqrt{S_x^2 + S_y^2}}, 0\right)$$

$$\mathbf{R} = \mathbf{S} \times \mathbf{T}$$

SPECL is called according to the sequence

(AC) $= a, a < 0$ for hyperbola

(MQ) $= \varepsilon$

CALL SPECL

PZE A, , n

PZE B

(ERROR RETURN)

The locations A, . . . , A + 8 contain the vectors **P**, **Q**, **W**; $n = 0$ is a flag for output to be referenced to an incoming asymptote while $n = 1$ references the output to an outgoing asymptote. The output is placed in the table B, . . . , B + 14 where the assignment is in sequence $\mathbf{B}\cdot\mathbf{T}$, $\mathbf{B}\cdot\mathbf{R}$, **S**, **B**, **T**, **R**.

The error return will only be used in the case that $|a|$ is so large that a^2 exceeds the machine capacity, an event which may happen only for wild trajectories resulting from an input error.

The subroutine uses four words of erasable storage beginning at COMMON.

CLASS

CLASS was written as a subroutine to calculate additional orbital elements from those provided by JEKYL.

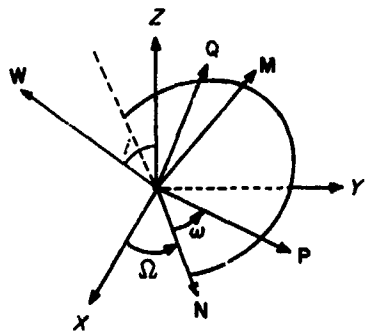

Sketch A-3. Description of the Euler angles for the orbital plane

The formulas that may be deduced from Sketch A-3 are as follows:

$i = \cos^{-1} W_z$, where $0 \leqq i \leqq 180°$ for the inclination

$$\begin{cases} \sin\Omega = \frac{W_x}{\sin i} \\ \cos\Omega = \frac{-W_y}{\sin i}, \end{cases} \quad \text{where } 0 \leqq \Omega < 360° \text{ for the right ascension of the ascending node}$$

$$\begin{cases} \sin\omega = \dfrac{P_z}{\sin i} \\ \cos\omega = \dfrac{Q_z}{\sin i} \end{cases}, \quad \text{where } 0 \leqq \omega \leqq 360^\circ \text{ for the argument of the pericenter}$$

The formulas for Ω may be derived by constructing the unit vector **N** at the ascending node:

$$\mathbf{N} = \frac{\mathbf{U} \times \mathbf{W}}{|\mathbf{U} \times \mathbf{W}|}$$

where $\mathbf{U} = (0, 0, 1)$ and $\sin i = |\mathbf{U} \times \mathbf{W}|$. **N** is then projected onto the X and Y axes to give the formulas for the cosine and the sine.

Next, the auxiliary unit vector $\mathbf{M} = \mathbf{W} \times \mathbf{N}$ is constructed so that ω is given by

$$\begin{cases} \sin\omega = \mathbf{P}\cdot\mathbf{M} = \mathbf{P}\cdot(\mathbf{W}\times\mathbf{N}) = -\mathbf{N}\cdot(\mathbf{W}\times\mathbf{P}) = -\mathbf{N}\cdot\mathbf{Q} \\ \cos\omega = \mathbf{P}\cdot\mathbf{N} \end{cases}$$

The conic parameters are given by the standard formulas for $c_1 \neq 0$:

$q = \dfrac{p}{1+\varepsilon}$, the closest approach distance

$V_p = \dfrac{\mu(1+\varepsilon)}{c_1}$, the velocity at closest approach

$V_a = \dfrac{\mu(1-\varepsilon)}{c_1}$, velocity at farthest departure ($c_3 < 0$)

$V_h = \sqrt{c_3}$, hyperbolic excess velocity ($c_3 > 0$)

$q_2 = a(1+\varepsilon)$, farthest departure distance ($c_3 < 0$)

$P = \dfrac{2\pi}{n}$, the period

For an Earth satellite, the quantities $\dot\omega$ and $\dot\Omega$ are also computed:

$$\dot\omega = \frac{nJa_\oplus^2}{p^2}\left(2 - \frac{5}{2}\sin^2 i\right)$$

$$\dot\Omega = \frac{-nJa_\oplus^2}{p^2}\cos i$$

where J is the coefficient of the second harmonic in the Earth's oblateness and $a_\oplus$ is the value of the Earth radius in km. The subroutine assumes that n has been given in rad/sec and p in km so that $\dot\omega$ and $\dot\Omega$ may be converted to deg/day for output.

The subroutine is called according to the sequence

CALL	CLASS
PZE	A, , B
PZE	C
(ERROR RETURN)	
(ERROR RETURN FOR PARABOLA)	

Input locations A, . . . , A + 8 contain the vectors **P**, **Q**, **W**, while the table composed of c_1, c_3, μ, ε, $1-\varepsilon$, a, p, and n is used as input from the cells B, . . . , B + 7. The output is stored in the cells C, . . . , C + 9 forming the table

i
Ω
ω
q
V_p
V_a (or V_h if $c_3 > 0$)
q_2 (or zero if $c_3 > 0$)
P (or zero if $c_3 > 0$)
$\dot\omega$
$\dot\Omega$

In the event $c_3 = 0$ at entry, the parabola error return is given.

The subroutine uses four cells of erasable storage starting at COMMON.

EARTH, SPACE

At the epoch T a "space-fixed" Cartesian coordinate system is defined, centered at the Earth with the $X-Y$ plane the equator, the X axis the direction of the vernal equinox, and the Z axis the spin axis of the Earth. The "Earth-fixed" frame is obtained from the space-fixed by rotating about the Z axis by an angle $\Upsilon(T)$, the Greenwich hour angle of the vernal equinox, to bring the x axis in coincidence with the Greenwich meridian (Sketch A-4).

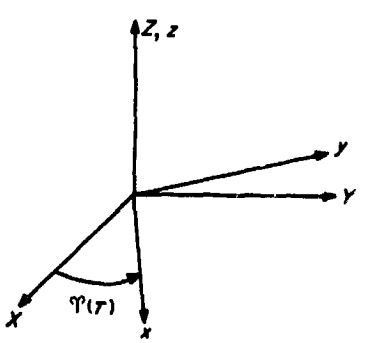

Sketch A-4. Earth-fixed equatorial coordinate system

The coordinates are then related by

$$\begin{pmatrix} x \\ y \end{pmatrix} = \begin{pmatrix} \cos \Upsilon (T) & \sin \Upsilon (T) \\ -\sin \Upsilon (T) & \cos \Upsilon (T) \end{pmatrix} \begin{pmatrix} X \\ Y \end{pmatrix}$$

$$z = Z,$$

and

$$\begin{pmatrix} \dot{x} \\ \dot{y} \end{pmatrix} = \begin{pmatrix} \cos \Upsilon (T) & \sin \Upsilon (T) \\ -\sin \Upsilon (T) & \cos \Upsilon (T) \end{pmatrix} \begin{pmatrix} \dot{X} \\ \dot{Y} \end{pmatrix} + \omega \begin{pmatrix} -\sin \Upsilon (T) & \cos \Upsilon (T) \\ -\cos \Upsilon (T) & -\sin \Upsilon (T) \end{pmatrix} \begin{pmatrix} \dot{X} \\ \dot{Y} \end{pmatrix}$$

$$\dot{z} = \dot{Z},$$

where ω is the rotation rate of the Earth.

The coordinates may be inverted to give

$$\begin{pmatrix} X \\ Y \end{pmatrix} = \begin{pmatrix} \cos \Upsilon (T) & -\sin \Upsilon (T) \\ \sin \Upsilon (T) & \cos \Upsilon (T) \end{pmatrix} \begin{pmatrix} x \\ y \end{pmatrix}$$

$$Z = z$$

and

$$\begin{pmatrix} \dot{X} \\ \dot{Y} \end{pmatrix} = \begin{pmatrix} \cos \Upsilon (T) & -\sin \Upsilon (T) \\ \sin \Upsilon (T) & \cos \Upsilon (T) \end{pmatrix} \begin{pmatrix} \dot{x} \\ \dot{y} \end{pmatrix} + \omega \begin{pmatrix} -\sin \Upsilon (T) & -\cos \Upsilon (T) \\ \cos \Upsilon (T) & -\sin \Upsilon (T) \end{pmatrix} \begin{pmatrix} x \\ y \end{pmatrix}$$

$$\dot{Z} = \dot{z}$$

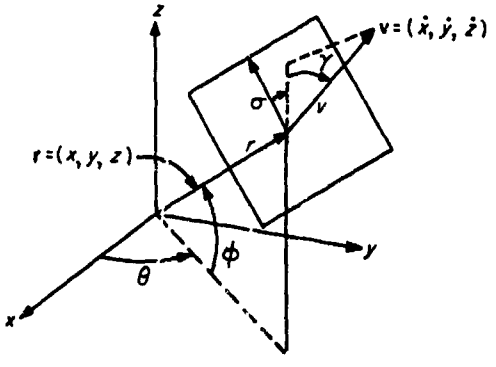

Sketch A-5. An Earth-fixed spherical set of coordinate system

In Sketch A-5, r is the radius, ϕ the north latitude, and θ the east longitude of the Earth-fixed position vector. It is convenient to translate the Earth-fixed velocity vector v to the end of the position vector and project it on the local horizontal, a plane perpendicular to r. v is the magnitude, γ the path angle or the elevation angle above the local horizontal, and σ the azimuth from north of the velocity vector. The transformation between spherical and Cartesian coordinates, and the inverse, are described in the discussions of subroutines RVIN and RVOUT, respectively, which follow.

EARTH is the subroutine which makes the transformation from Earth-fixed spherical to Earth-fixed Cartesian via RVIN and then rotates to space-fixed Cartesian. SPACE manages the inverse transformation by first rotating from space-fixed Cartesian to Earth-fixed Cartesian and obtaining the spherical set with the aid of RVOUT. Both EARTH and SPACE assume that the subroutine GHA has been called and that the COMMON locations GHA(T) and LOMEGA contain, respectively, $\Upsilon(T)$ in deg and ω in rad/sec.

The calling sequence for EARTH is

```
CALL    EARTH
PZE     A
PZE     B,,C
```

A, . . . , A + 5 contain the spherical set r, ϕ, θ, v, γ, σ. X, Y, Z are placed in the cells B, B + 1, B + 2; $\dot{X}$, $\dot{Y}$, $\dot{Z}$ are placed in the cells C, C + 1, C + 2.

The calling sequence for SPACE is

```
CALL    SPACE
PZE     A,,B
PZE     C,,D
```

A, A + 1, A + 2 contain X, Y, Z; B, B + 1, B + 2 contain $\dot{X}$, $\dot{Y}$, $\dot{Z}$.

The Earth-fixed spherical set r, ϕ, θ, v, γ, σ is deposited in the cells C, . . . , C + 5, while the Earth-fixed Cartesian set x, y, z, $\dot{x}$, $\dot{y}$, $\dot{z}$ is placed in the locations D, . . . , D + 5.

The subroutines use four words of erasable storage starting at COMMON.

RVIN, RVOUT

Transformations between Cartesian position and velocity **R** and **V** and the spherical set (R, Φ, Θ, V, Γ, Σ) are provided for by RVOUT, while the inverse transformation from spherical to Cartesian is obtained with RVIN.

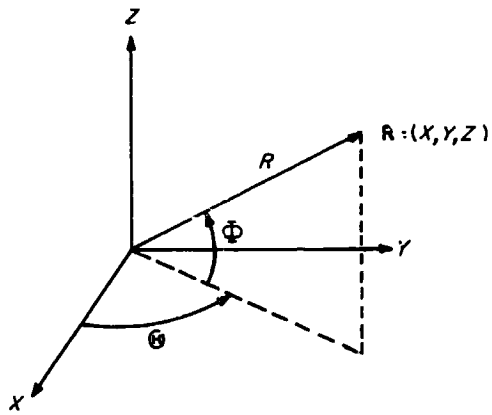

Sketch A-6. Inertial spherical position coordinates

Projecting **R** on the $X - Y$ plane, Θ is the angle from the X axis to the projection measured counterclockwise. Φ is the elevation of **R** above the $X - Y$ plane (Sketch A-6). The formulas are

$$\mathbf{R} = \begin{pmatrix} X \\ Y \\ Z \end{pmatrix} = \begin{pmatrix} R\cos\Phi\cos\Theta \\ R\cos\Phi\sin\Theta \\ R\sin\Phi \end{pmatrix}$$

and inversely,

$$R = \sqrt{X^2 + Y^2 + Z^2}$$

$$\Phi = \sin^{-1}\frac{Z}{R}, \quad -90° \leqq \Phi \leqq 90°$$

$$\Theta = \arg(X, Y), \quad 0 \leqq \Theta < 360°$$

$$\arg(x, y) = \begin{cases} \tan^{-1}\dfrac{y}{x} & \text{if } x > 0 \\ \tan^{-1}\dfrac{y}{x} + 180° & \text{if } x \leqq -0 \end{cases}$$

To describe the spherical coordinates for the velocity vector **V**, it is convenient to construct a new reference frame obtained by first rotating about the Z axis by an amount Θ so that the new X axis lies along the projection of **R** on the $X - Y$ plane; a subsequent rotation about the intermediate Y axis by the angle Φ completes the coordinate change. The resultant X' axis lies along **R**, the Z' axis lies in the plane formed by the Z axis and **R**, and the Y' axis completes the right-handed system and thus remains in the $X - Y$ plane (Sketch A-7).

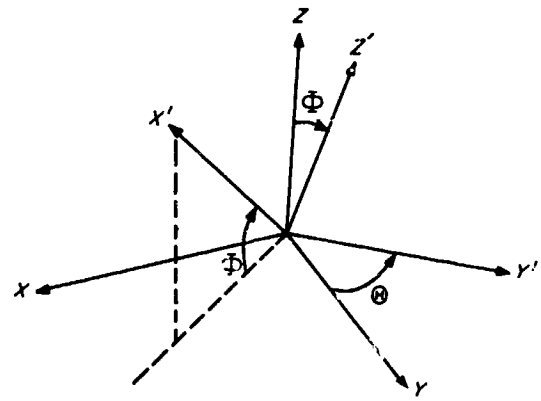

Sketch A-7. Rotation to the local plane

Evidently

$$\begin{pmatrix} X \\ Y \\ Z \end{pmatrix} = \begin{pmatrix} \cos\Phi\cos\Theta & -\sin\Theta & -\sin\Phi\cos\Theta \\ \cos\Phi\sin\Theta & \cos\Theta & -\sin\Phi\sin\Theta \\ \sin\Phi & 0 & \cos\Phi \end{pmatrix} \begin{pmatrix} X' \\ Y' \\ Z' \end{pmatrix}$$

Representing the velocity vector **V** in the X', Y', Z' system, the path angle Γ is the elevation of **V** above the $Y' - Z'$ plane, positive in the radial outward or X' direction; the azimuth Σ is the angle measured clockwise from the Z' axis to the projection of **V** on the $Y' - Z'$ plane. The geometry appears in Sketch A-8.

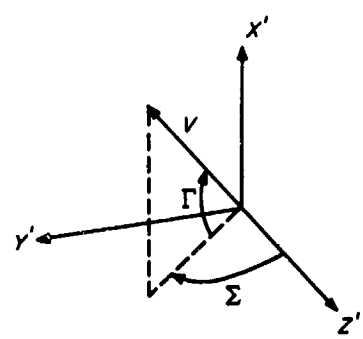

Sketch A-8. Inertial velocity vector in the local horizontal plane

Regarding the X', Y', Z' frame as nonrotating, **V** may be expressed as

$$\mathbf{V} = \begin{pmatrix} \dot{X}' \\ \dot{Y}' \\ \dot{Z}' \end{pmatrix} = \begin{pmatrix} V\sin\Gamma \\ V\cos\Gamma\sin\Sigma \\ V\cos\Gamma\cos\Sigma \end{pmatrix}$$

and rotate to the original frame to obtain $\dot{X}$, $\dot{Y}$, $\dot{Z}$.

Inversion may be obtained as follows:

$$V = \sqrt{\dot{X}^2 + \dot{Y}^2 + \dot{Z}^2}$$

$$\Gamma = \sin^{-1} \frac{\dot{X}'}{V}, \quad -90° \leqq \Gamma \leqq 90°$$

$$\Sigma = \arg (\dot{Z}', \dot{Y}'), \quad 0 \leqq \Sigma < 360°$$

Of course **V** expressed in the X', Y', Z' system is given by

$$\begin{pmatrix} \dot{X}' \\ \dot{Y}' \\ \dot{Z}' \end{pmatrix} = \begin{pmatrix} \cos\Phi\cos\Theta & \cos\Phi\sin\Theta & \sin\Phi \\ -\sin\Theta & \cos\Theta & 0 \\ -\sin\Phi\cos\Theta & -\sin\Phi\sin\Theta & \cos\Phi \end{pmatrix} \begin{pmatrix} \dot{X} \\ \dot{Y} \\ \dot{Z} \end{pmatrix}$$

The calling sequence for RVIN is

```
CALL RVIN
PZE „A
PZE „B
PZE „C
```

A, . . . , A + 5 contain the spherical coordinates R, Φ, Θ, V, Γ, Σ; X, Y, Z are placed in the locations B, B + 1, B + 2, while the Cartesian velocity components $\dot{X}$, $\dot{Y}$, $\dot{Z}$ are stored in the cells C, C + 1, C + 2.

For RVOUT, the calling sequence is

```
CALL RVOUT
PZE 1„A
PZE 1„B
PZE 1„C
```

X, Y, Z are contained in the cells A, A + 1, A + 2, while the locations B, B + 1, B + 2 contain $\dot{X}$, $\dot{Y}$, $\dot{Z}$. The spherical set R, Φ, Θ, V, Γ, Σ is placed in the cells C, . . . , C + 5 as output.

The subroutines use four words of erasable storage starting at COMMON.

LOOP

Let **R** = (X, Y, Z) and **V** = ($\dot{X}$, $\dot{Y}$, $\dot{Z}$) be the Earth-centered "space-fixed" Cartesian coordinates of the probe referenced to the true equator and equinox of date. For a given station with Earth-fixed spherical coordinates (r_i, ϕ_i, θ_i), it is desired to compute a number of topocentric quantities as given below. The basic coordinate systems are shown in Sketch A-9.

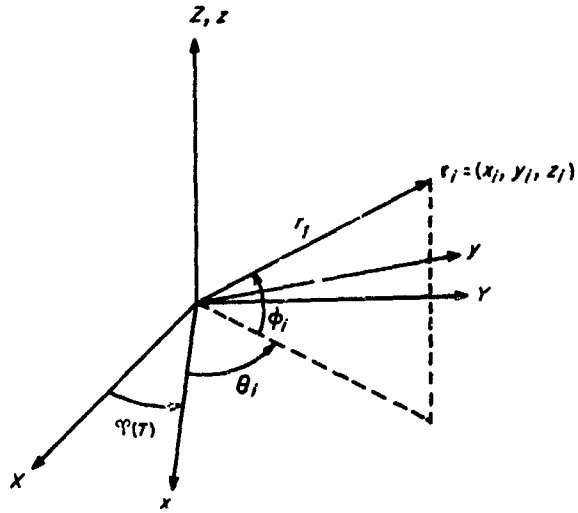

Sketch A-9. Earth-fixed station coordinates

$\Upsilon(T)$ is the Greenwich hour angle of vernal equinox at epoch T or alternatively, the right ascension of the Greenwich meridian. It is assumed that GHA has computed $\Upsilon(T)$ and the correct value appears in the COMMON location GHA(T). r_i is the distance of the station from the center of the Earth, ϕ_i is the geocentric north latitude, and θ_i is the east longitude.

The Earth-fixed Cartesian coordinates of the station are

$$x_i = r_i \cos\phi_i \cos\theta_i$$

$$y_i = r_i \cos\phi_i \sin\theta_i$$

$$z_i = r_i \sin\phi_i$$

Those for the probe are

$$x = X\cos\Upsilon(T) + Y\sin\Upsilon(T)$$

$$y = -X\sin\Upsilon(T) + Y\cos\Upsilon(T)$$

$$z = Z$$

$$\dot{x} = \dot{X}\cos\Upsilon(T) + \dot{Y}\sin\Upsilon(T) + \omega y$$

$$\dot{y} = -\dot{X}\sin\Upsilon(T) + \dot{Y}\cos\Upsilon(T) - \omega x$$

$$\dot{z} = \dot{Z}$$

$$\dot{\mathbf{r}} = (\dot{x}, \dot{y}, \dot{z})$$

where ω is the rotation rate of the Earth.

Thus the topocentric Cartesian coordinates of the probe are

$$\mathbf{r}_{i_p} = (x - x_i, y - y_i, z - z_i)$$

$$\dot{\mathbf{r}}_{i_p} = (\dot{x}, \dot{y}, \dot{z}) = \dot{\mathbf{r}}$$

The slant range r_{ip} is then given by $|\mathbf{r}_{ip}|$, while the slant-range rate $\dot{r}_{ip}$ may be obtained from the formula

$$2r_{ip}\dot{r}_{ip} = \frac{d(r_{ip}^2)}{dt} = \frac{d(\mathbf{r}_{ip}\cdot\mathbf{r}_{ip})}{dt} = 2\mathbf{r}_{ip}\cdot\dot{\mathbf{r}}_{ip}$$

Provisions have been made to compute $\ddot{r}_{ip}$, the slant-range acceleration, when the Earth is the central body. The pertinent formulas may be developed as follows:

$$\begin{pmatrix}\dot{x}\\ \dot{y}\end{pmatrix} = \begin{pmatrix}\cos\Upsilon(T) & \sin\Upsilon(T)\\ -\sin\Upsilon(T) & \cos\Upsilon(T)\end{pmatrix}\begin{pmatrix}\dot{X}\\ \dot{Y}\end{pmatrix} + \omega\begin{pmatrix}-\sin\Upsilon(T) & \cos\Upsilon(T)\\ -\cos\Upsilon(T) & -\sin\Upsilon(T)\end{pmatrix}\begin{pmatrix}X\\ Y\end{pmatrix}$$

$$\dot{z} = \dot{Z}$$

$$\begin{pmatrix}\ddot{x}\\ \ddot{y}\end{pmatrix} = \begin{pmatrix}\cos\Upsilon(T) & \sin\Upsilon(T)\\ -\sin\Upsilon(T) & \cos\Upsilon(T)\end{pmatrix} \times \left\{\begin{pmatrix}\ddot{X}\\ \ddot{Y}\end{pmatrix} + 2\omega\begin{pmatrix}\dot{Y}\\ -\dot{X}\end{pmatrix} - \omega^2\begin{pmatrix}X\\ Y\end{pmatrix}\right\}$$

$$\ddot{z} = \ddot{Z}$$

From

$$r_{ip}\dot{r}_{ip} = \mathbf{r}_{ip}\cdot\dot{\mathbf{r}}_{ip} = \mathbf{r}_{ip}\cdot\dot{\mathbf{r}}$$

obtain

$$r_{ip}\ddot{r}_{ip} + \dot{r}_{ip}^2 = \mathbf{r}_{ip}\cdot\ddot{\mathbf{r}} + \dot{\mathbf{r}}_{ip}\cdot\dot{\mathbf{r}}_{ip}$$

or

$$\ddot{r}_{ip} = \frac{1}{r_{ip}}\left\{\mathbf{r}_{ip}\cdot\ddot{\mathbf{r}} + v^2 - \dot{r}_{ip}^2\right\}$$

where $v = |\dot{\mathbf{r}}|$, $\ddot{\mathbf{r}} = (\ddot{x}, \ddot{y}, \ddot{z})$

Contributions to $\ddot{\mathbf{R}}$ are obtained from COMMON locations where they have been deposited by DOT and are only valid for the Earth as a central body.

The topocentric hour-angle declination system is described in Sketches A-10 and A-11.

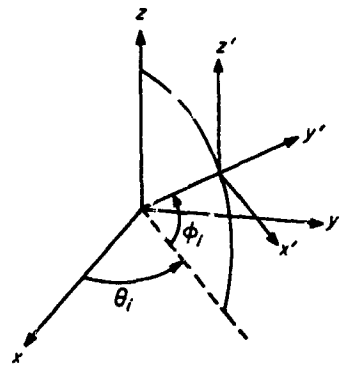

Sketch A-10. Rotation to the station meridian

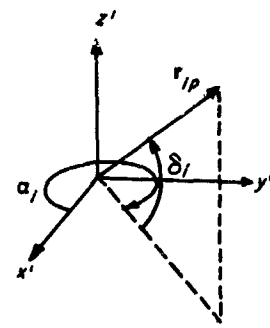

Sketch A-11. Local hour-angle declination coordinate system

The $x-y$ plane has been translated to the station and rotated through the angle θ_i so that x' lies along the meridian; the z' axis remains parallel to the z axis. The declination δ_i is given by

$$\delta_i = \sin^{-1}\frac{z_{ip}}{r_{ip}}, \quad -90° \leqq \delta_i \leqq 90°$$

and the hour angle may be computed from

$$\alpha_i \equiv \theta_i - \arg(x_{ip}, y_{ip}) \pmod{360°}, \quad 0 \leqq \alpha_i < 360°$$

where

$$\arg(x,y) = \begin{cases}\tan^{-1}\dfrac{y}{x} & \text{if } x > 0, \quad -90° \leqq \tan^{-1}u \leqq 90°\\ \tan^{-1}\dfrac{y}{x} + 180° & \text{otherwise}\end{cases}$$

From the above formulas, the angular rates follow:

$$\dot{\delta}_i = \frac{\dot{z} - \dot{r}_{ip}\sin\delta_i}{r_{ip}\cos\delta_i}$$

$$\dot{\alpha}_i = \frac{\dot{x}y_{ip} - \dot{y}x_{ip}}{x^2_{ip} + y^2_{ip}}$$

To construct the azimuth-elevation topocentric coordinate system, rotate the x' and z' axes about the y' axis so that the resultant $x''-y''$ plane is perpendicular to $\mathbf{r}_i$ and the z'' axis points to the zenith; the $x''-z''$ plane is still the meridian plane as illustrated in Sketches A-12 and A-13.

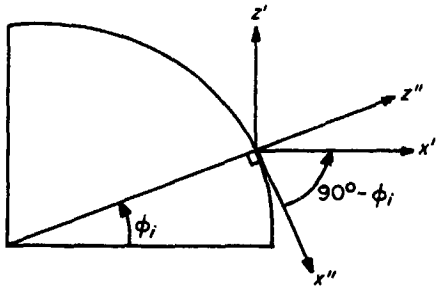

Sketch A-12. Rotation to station latitude

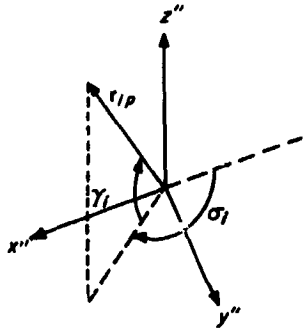

Sketch A-13. Azimuth elevation coordinate system

The elevation angle γ_i may be obtained immediately by

$$\sin\gamma_i = \frac{\mathbf{r}_i \cdot \mathbf{r}_{ip}}{r_i\, r_{ip}}, \quad -90° \leqq \gamma_i \leqq 90°$$

The component of $\mathbf{r}_{ip}$ which lies in the $x''-y''$ plane is $r_{ip}\cos\gamma_i$ so that the azimuth σ_i is given by

$$\begin{cases} \cos\sigma_i = \dfrac{-x''_{ip}}{r_{ip}\cos\gamma_i} \\ \sin\sigma_i = \dfrac{y''_{ip}}{r_{ip}\cos\gamma_i} \end{cases}$$

By performing the rotations to transform the coordinate systems, $\mathbf{r}_{ip}$ may be determined in the $x''-y''-z''$ reference:

$$x''_{ip} = x_{ip}\sin\phi_i\cos\theta_i + y_{ip}\sin\varphi_i\sin\theta_i - z_{ip}\cos\phi_i$$

$$y''_{ip} = -x_{ip}\sin\theta_i + y_{ip}\cos\theta_i$$

$$z''_{ip} = x_{ip}\cos\phi_i\cos\theta_i + y_{ip}\cos\phi_i\sin\theta_i + z_{ip}\sin\phi_i$$

The program uses an inverse function defined for $0 \leqq \cos^{-1} u \leqq 180°$ so that

$$\sigma_i = \begin{cases} \cos^{-1}\left(\dfrac{-x''_{ip}}{r_{ip}\cos\gamma_i}\right) & \text{if } \sin\sigma_i \geqq 0 \\ 360° - \cos^{-1}\left(\dfrac{-x''_{ip}}{r_{ip}\cos\gamma_i}\right) & \text{otherwise} \end{cases}$$

Thus $0 \leqq \sigma_i \leqq 360°$.

The angular rates are calculated from the formulas

$$\dot\gamma_i = \frac{\mathbf{r}_i \cdot \dot{\mathbf{r}} - r_i\,\dot r_{ip}\sin\gamma_i}{r_i\, r_{ip}\cos\gamma_i}$$

$$\dot\sigma_i = \frac{\dot x''_{ip} + \cos\sigma_i\,(\dot r_{ip}\cos\gamma_i - r_{ip}\dot\gamma_i\sin\gamma_i)}{r_{ip}\cos\gamma_i\sin\sigma_i}$$

where $\dot x''_{ip} = \dot x\sin\phi_i\cos\theta_i + \dot y\sin\phi_i\sin\theta_i - \dot z\cos\phi_i$.

The look angle λ_i is the angle between the spacecraft attitude vector $\mathbf{C}$ and the slant-range vector where $\mathbf{C}$ is specified by the calling sequence and is a unit vector expressed in the true equator and equinox of date. It is convenient to construct $\mathbf{R}_{ip}$ in a topocentric system parallel to the X, Y, Z axes:

$$X_i = x_i\cos\Upsilon(T) - y_i\sin\Upsilon(T)$$

$$Y_i = x_i\sin\Upsilon(T) + y_i\cos\Upsilon(T)$$

$$Z_i = z_i$$

$$\mathbf{R}_{ip} = (X - X_i, Y - Y_i, Z - Z_i)$$

Then λ_i is obtained from

$$\lambda_i = \cos^{-1}\left(\frac{\mathbf{R}_{ip}\cdot\mathbf{C}}{R_{ip}}\right), \quad 0 \leqq \lambda_i \leqq 180°$$

The polarization angle p_i is defined as

$$p_i = \cos^{-1}\left\{\frac{\mathbf{R}\times\mathbf{R}_{ip}}{|\mathbf{R}\times\mathbf{R}_{ip}|}\cdot\frac{\mathbf{C}\times\mathbf{R}_{ip}}{|\mathbf{C}\times\mathbf{R}_{ip}|}\right\}, \quad 0 \leqq p_i \leqq 180°$$

An expression for the measured received frequency, including a scaled doppler shift, appears as

$$f = f_{Bi} - f_{ci}\,\dot r_{ip}$$

where f_{Bi} represents a bias frequency in the receiver and f_{ci} includes the velocity of light and may be adjusted to represent either two-way or normal doppler.

The calling sequence is

```
CALL   LOOP
PZE    X,,Y
OP     B,,C
```

X, X + 1, X + 2 contain **R**; Y, Y + 1, Y + 2 contain **V**.

B contains the binary control word which selects the appropriate stations from among the available 15. The small subroutine CW1 transforms the octal input to the required binary format which permits LOOP to scan the stations from bit 35 to bit 21.

C, C + 1, C + 2 contain the unit vector **C**.

If OP = PZE, LOOP will compute the quantities for each station in turn and will print out whenever $\gamma_i \geqq -10°$. If OP = MZE, γ_i and $\dot{\gamma}_i$, for each station up to a maximum of five, will be stored in a buffer to be used by MARK as dependent variables for the view-period computation.

The parameters describing the stations are stored in the following sequence:

STABCD	+0		4 BCD words for station 1 name
	1		
	2		
	3		
	.		
	.		
	.		
	70		4 BCD words for station 15 name
	71		
	72		
	73		
STACRD	+0	ϕ_1	coordinates for station 1
	1	θ_1	
	2	r_1	
	3	f_{B_1}	frequency parameters for station 1
	4	f_{C_1}	
	.		
	.		
	.		
	106	ϕ_{15}	coordinates for station 15
	107	θ_{15}	
	110	r_{15}	
	111	$f_{B_{15}}$	frequency parameters for station 15
	112	$f_{C_{15}}$	

To describe the view periods for the stations, three other parameters are used:

STACRD	−3	γ_B
	−2	$\dot{\gamma}_B$
	−1	γ_0

The elevation condition is met for rise or set with respect to the station whenever $|\gamma_i - \gamma_0| \leqq \gamma_B$; at this time the station quantities are printed and further testing is suppressed for one integration step. The elevation-rate condition is met for extreme elevation whenever $|\dot{\gamma}_i| \leqq \dot{\gamma}_B$ and $\gamma_i \geqq \gamma_0$. Upon success, the station quantities are printed and the test is suppressed for one integration step.

The subroutine uses 100 words of erasable storage starting at COMMON.

2. Basic Coordinate Transformations

ROTEQ

The general precession of the Earth's equator and the consequent retrograde motion of the equinox on the ecliptic may be represented by the rotation matrix:

$$\begin{pmatrix} X' \\ Y' \\ Z' \end{pmatrix} = \begin{pmatrix} a_{11} & a_{12} & a_{13} \\ a_{21} & a_{22} & a_{23} \\ a_{31} & a_{32} & a_{33} \end{pmatrix} \begin{pmatrix} X \\ Y \\ Z \end{pmatrix}$$

where X, Y, and Z are expressed in the mean equator and equinox of 1950.0 and X', Y', Z' are the coordinates in the mean equator and equinox of date. The geometry of the precession has been represented by the three small parameters ζ_0, z, and θ in Sketch A-14:

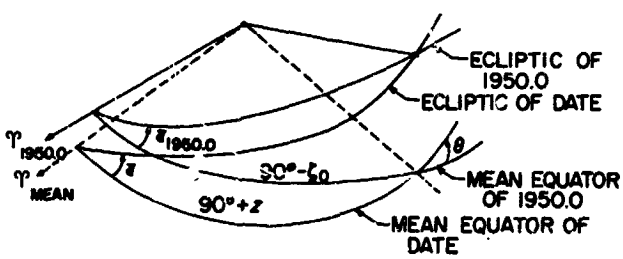

Sketch A-14. Relationship between fundamental reference equators

$\Upsilon_{1950.0}$ is the mean equinox of 1950.0; $\bar{\epsilon}_{1950.0}$ is the mean obliquity of 1950.0; Υ_{mean} is the mean equinox of date; $\bar{\epsilon}$ is the mean obliquity of date. Measured in the mean equator of 1950.0 from the mean equinox of 1950.0, $90° - \zeta_0$ is the right ascension of the ascending node of the mean equator of date on the mean equator of 1950.0. $90° + z$ is the right ascension of the node measured in the mean equator of date from the mean equinox of date. θ is the inclination of the mean equator of date to the mean equator of 1950.0.

In terms of ζ_0, z, and θ, (a_{ij}) is given by

$$a_{11} = -\sin\zeta_0 \sin z + \cos\zeta_0 \cos z \cos\theta$$
$$a_{12} = -\cos\zeta_0 \sin z - \sin\zeta_0 \cos z \cos\theta$$
$$a_{13} = -\cos z \sin\theta$$

$$a_{21} = \sin\zeta_0 \cos z + \cos\zeta_0 \sin z \cos\theta$$
$$a_{22} = \cos\zeta_0 \cos z - \sin\zeta_0 \sin z \cos\theta$$
$$a_{23} = -\sin z \sin\theta$$

$$a_{31} = \cos\zeta_0 \sin\theta$$
$$a_{32} = -\sin\zeta_0 \sin\theta$$
$$a_{33} = \cos\theta$$

$$\zeta_0 = 2304''.997T + 0''.302T^2 + 0''.0179T^3$$
$$z = 2304''.997T + 1''.093T^2 + 0''.0192T^3$$
$$\theta = 2004''.298T - 0''.426T^2 - 0''.0416T^3$$

with T the number of Julian centuries of 36,525 days past the epoch 1950.0.

The actual computational form of (a_{ij}) is obtained by expanding the a_{ij} in power series in ζ_0, z, θ and replacing the arguments by the above time series. The results are

$$a_{11} = 1 - 0.00029697T^2 - 0.00000013T^3$$
$$a_{12} = -a_{21} = -0.02234988T - 0.00000676T^2 + 0.00000221T^3$$
$$a_{13} = -a_{31} = -0.00971711T + 0.00000207T^2 + 0.00000096T^3$$
$$a_{22} = 1 - 0.00024976T^2 - 0.00000015T^3$$
$$a_{23} = a_{32} = -0.00010859T^2 - 0.00000003T^3$$
$$a_{33} = 1 - 0.00004721T^2 + 0.00000002T^3$$

The calling sequence has the form

(AC) = days past 0^h January 1, 1950, E.T.

CALL ROTEQ

(OP) X,,Y

X−3, X−2, X−1 contain the input vector; Y−3, Y−2, Y−1 contain the output vector; X = Y is permitted.

OP = PZE regards X as 1950.0 and rotates to date in Y; OP = MZE regards X as of date and rotates to 1950.0 in Y.

The matrix (a_{ij}) is saved in the COMMON locations AA, . . . , AA + 8 and recomputed only when the time has changed by 1/64 day.

The subroutine uses three cells of erasable storage starting at COMMON.

NUTATE

To describe the nutation of the Earth about its precessing mean equator, it is convenient to construct the nutation matrix N which relates the Cartesian coordinates expressed in the true equator and equinox to those in the mean equator and equinox (Sketch A-15).

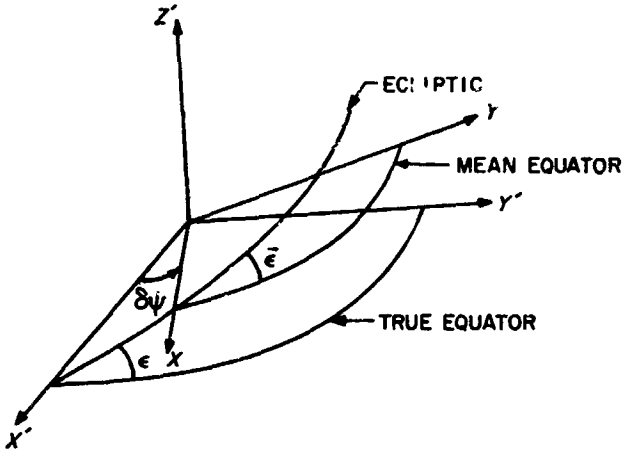

Sketch A-15. Relationship between true equator and mean equator of date

$\delta\psi$ is the nutation in longitude measured from the true vernal equinox at the X' axis to the mean vernal equinox at the X axis. $\bar{\epsilon}$ is the mean obliquity, while $\epsilon = \bar{\epsilon} + \delta\epsilon$ is the true obliquity where $\delta\epsilon$ is the nutation in obliquity. Numerical expressions for the above quantities appear in the discussion of subroutine MNA following.

If N is defined in the sense

$$\begin{pmatrix} X' \\ Y' \\ Z' \end{pmatrix} = N \begin{pmatrix} X \\ Y \\ Z \end{pmatrix}$$

where the primed system is the true equator and equinox and the unprimed is the mean equator and equinox, then the N_{ij} are given by

$$N_{11} = \cos\delta\psi$$
$$N_{12} = -\sin\delta\psi\cos\bar{\epsilon}$$
$$N_{13} = -\sin\delta\psi\cos\bar{\epsilon}$$

$$N_{21} = \sin\delta\psi\cos\epsilon$$
$$N_{22} = \cos\delta\psi\cos\epsilon\cos\bar{\epsilon} + \sin\epsilon\sin\bar{\epsilon}$$

$$N_{23} = \cos\delta\psi\cos\epsilon\sin\bar{\epsilon} - \sin\epsilon\cos\bar{\epsilon}$$

$$N_{31} = \sin\delta\psi\sin\epsilon$$

$$N_{32} = \cos\delta\psi\sin\epsilon\cos\bar{\epsilon} - \cos\epsilon\sin\bar{\epsilon}$$

$$N_{33} = \cos\delta\psi\sin\epsilon\sin\bar{\epsilon} + \cos\epsilon\cos\bar{\epsilon}$$

Since $|\delta\psi| < 10^{-4}$ and $|\delta\epsilon| < 10^{-4}$, the N_{ij} are expanded to first order in $\delta\psi$ and $\delta\epsilon$ to obtain a form which is better behaved for numerical calculation:

$$N = \begin{pmatrix} 1 & -\delta\psi\cos\bar{\epsilon} & -\delta\psi\sin\bar{\epsilon} \\ \delta\psi\cos\bar{\epsilon} & 1 & -\delta\epsilon \\ \delta\psi\sin\bar{\epsilon} & \delta\epsilon & 1 \end{pmatrix}$$

NUTATE is used as a utility routine to generate the matrix product NA, where A is obtained by calling ROTEQ; the resultant NA is used to rotate from the equator and equinox of 1950.0 to the true equator and equinox of date and is saved in the COMMON cells (NA), ..., (NA) + 8. As N is a slowly varying matrix, it is saved and recomputed only if the time has changed by at least 0.1 day. The generation of N is effected by calling MNA which also internally stores N.

MNA, MNA1

It is the principal function of MNA to provide the rotation matrix MNA which allows vectors in the 1950.0 system to be expressed relative to the Moon's true equator and conversely.

For this purpose it is assumed that the matrix A has been formed by ROTEQ and appears in the COMMON locations AA, ..., AA + 8. The form of the matrix N (see preceding discussion of NUTATE) depends upon the nutations $\delta\psi$ and $\delta\epsilon$. In the discussion of XYZDD to follow, M is identified as (b_{ij}).

The numerical expressions for the necessary quantities appear below:

$\delta\epsilon = \Delta\epsilon + d\epsilon$, where $\Delta\epsilon$ denotes the long-period and $d\epsilon$ the short-period terms for the nutation in obliquity. In a similar manner the nutation in longitude $\delta\psi$ is given with long-period and short-period terms $\Delta\psi$ and $d\psi$.

$$\begin{aligned}\Delta\epsilon = {} & 25^{\circ}5844 \times 10^{-4}\cos\Omega - 0^{\circ}2511 \times 10^{-4}\cos 2\Omega \\ & + 1^{\circ}5336 \times 10^{-4}\cos 2L + 0^{\circ}0666 \times 10^{-4}\cos(3L - \Gamma) \\ & - 0^{\circ}0258 \times 10^{-4}\cos(L + \Gamma) \\ & - 0^{\circ}0183 \times 10^{-4}\cos(2L - \Omega) \\ & - 0^{\circ}0067 \times 10^{-4}\cos(2\Gamma' - \Omega)\end{aligned}$$

$$\begin{aligned}d\epsilon = {} & 0^{\circ}2456 \times 10^{-4}\cos 2\mathcal{C} + 0^{\circ}0598 \times 10^{-4}\cos(2\mathcal{C} - \Omega) \\ & + 0^{\circ}0369 \times 10^{-4}\cos(3\mathcal{C} - \Gamma') \\ & - 0^{\circ}0139 \times 10^{-4}\cos(\mathcal{C} + \Gamma') \\ & - 0^{\circ}0086 \times 10^{-4}\cos(\mathcal{C} - \Gamma' + \Omega) \\ & + 0^{\circ}0083 \times 10^{-4}\cos(\mathcal{C} - \Gamma' - \Omega) \\ & + 0^{\circ}0061 \times 10^{-4}\cos(3\mathcal{C} + \Gamma' - 2L) \\ & + 0^{\circ}0064 \times 10^{-4}\cos(3\mathcal{C} - \Gamma' - \Omega)\end{aligned}$$

$$\begin{aligned}\Delta\psi = {} & -(47^{\circ}8927 + 0^{\circ}0482\,T) \times 10^{-4}\sin\Omega \\ & + 0^{\circ}5800 \times 10^{-4}\sin 2\Omega - 3^{\circ}5361 \times 10^{-4}\sin 2L \\ & - 0^{\circ}1378 \times 10^{-4}\sin(3L - \Gamma) \\ & + 0^{\circ}0594 \times 10^{-4}\sin(L + \Gamma) \\ & + 0^{\circ}0344 \times 10^{-4}\sin(2L - \Omega) \\ & + 0^{\circ}0125 \times 10^{-4}\sin(2\Gamma' - \Omega) \\ & + 0^{\circ}3500 \times 10^{-4}\sin(L - \Gamma) \\ & + 0^{\circ}0125 \times 10^{-4}\sin(2L - 2\Gamma')\end{aligned}$$

$$\begin{aligned}d\psi = {} & -0^{\circ}5658 \times 10^{-4}\sin 2\mathcal{C} \\ & - 0^{\circ}0950 \times 10^{-4}\sin(2\mathcal{C} - \Omega) \\ & - 0^{\circ}0725 \times 10^{-4}\sin(3\mathcal{C} - \Gamma') \\ & + 0^{\circ}0317 \times 10^{-4}\sin(\mathcal{C} + \Gamma') \\ & + 0^{\circ}0161 \times 10^{-4}\sin(\mathcal{C} - \Gamma' + \Omega) \\ & + 0^{\circ}0158 \times 10^{-4}\sin(\mathcal{C} - \Gamma' - \Omega) \\ & - 0^{\circ}0144 \times 10^{-4}\sin(3\mathcal{C} + \Gamma' - 2L) \\ & - 0^{\circ}0122 \times 10^{-4}\sin(3\mathcal{C} - \Gamma' - \Omega) \\ & + 0^{\circ}1875 \times 10^{-4}\sin(\mathcal{C} - \Gamma') \\ & + 0^{\circ}0078 \times 10^{-4}\sin(2\mathcal{C} - 2\Gamma') \\ & + 0^{\circ}0414 \times 10^{-4}\sin(\mathcal{C} + \Gamma' - 2L) \\ & + 0^{\circ}0167 \times 10^{-4}\sin(2\mathcal{C} - 2L) \\ & - 0^{\circ}0089 \times 10^{-4}\sin(4\mathcal{C} - 2L)\end{aligned}$$

$$\Omega = 12^{\circ}1127902 - 0^{\circ}0529539222\,d + 20^{\circ}795 \times 10^{-4}\,T + 20^{\circ}81 \times 10^{-4}\,T^2 + 0^{\circ}02 \times 10^{-4}\,T^3$$

$$\mathcal{C} = 64^{\circ}37545167 + 13^{\circ}1763965268\,d - 11^{\circ}31575 \times 10^{-4}\,T - 11^{\circ}3015 \times 10^{-4}\,T^2 + 0^{\circ}019 \times 10^{-4}\,T^3$$

$$\Gamma' = 208^{\circ}8439877 + 0^{\circ}1114040803\,d - 0^{\circ}010334\,T - 0^{\circ}010343\,T^2 - 0^{\circ}12 \times 10^{-4}\,T^3$$

$$L = 280^{\circ}08121009 + 0^{\circ}9856473354\,d + 3^{\circ}03 \times 10^{-4}\,T + 3^{\circ}03 \times 10^{-1}\,T^2$$

$$\Gamma = 282^{\circ}08053028 + 0^{\circ}470684 \times 10^{-1}\,d + 4^{\circ}5525 \times 10^{-4}\,T + 4^{\circ}575 \times 10^{-4}\,T^2 + 0^{\circ}03 \times 10^{-4}\,T^3$$

T is the number of Julian centuries of 36,525 days past the epoch 0^h January 1, 1950, E.T., while d is the number of days past the same epoch. The program uses d in double precision. The mean obliquity is calculated from

$$\bar{\epsilon} = 23°.4457587 - 0°.01309404\,T - 0°.0088 \times 10^{-4}\,T^2 + 0°.0050 \times 10^{-4}\,T^3$$

The quantity $\delta\alpha = \delta\psi \cos \bar{\epsilon}$ is computed and stored in the COMMON cell NUTRA for the GHA routine to use as the nutation in right ascension for calculation of the true value of the Greenwich hour angle of the vernal equinox.

The librations are given by

$$\sigma \sin I = -0°.0302777 \sin g + 0°.0102777 \sin (g + 2\omega) - 0°.00305555 \sin (2g + 2\omega)$$

$$\tau = -0°.003333 \sin g + 0°.0163888 \sin g' + 0°.005 \sin 2\omega$$

$$\rho = -0°.0297222 \cos g + 0°.0102777 \cos (g + 2\omega) - 0°.00305555 \cos (2g + 2\omega)$$

$$I = 1°.535$$

The following expressions have been programmed for g, g', and ω:

$$g = 215°.54013 + 13°.064992\,d$$

$$g' = 358°.009067 + 0°.9856005\,d$$

$$\omega = 196°.745637 + 0°.1643586\,d$$

Evidently $g = \mathbb{C} - \Gamma^{\gamma}$, the mean anomaly of the Moon; $g' = L - \Gamma$, the mean anomaly of the Sun; and $\omega = \Gamma^{\gamma} - \Omega$, the argument of the perigee of the Moon. All quantities relate to mean motions of the Sun and the Moon.

$$\cos i = \cos (\Omega + \sigma + \delta\psi) \sin \epsilon \sin (I + \rho) + \cos \epsilon \cos (I + \rho), \quad 0 < i < 90°$$

$$\sin \Omega' = -\sin (\Omega + \sigma + \delta\psi) \sin (I + \rho) \csc i, \quad -90° < \Omega' < 90°$$

$$\sin \Delta = -\sin (\Omega + \sigma + \delta\psi) \sin \epsilon \csc i$$

$$\cos \Delta = -\sin (\Omega + \sigma + \delta\psi) \sin \Omega' \cos \epsilon - \cos (\Omega + \sigma + \delta\psi) \cos \Omega', \quad 0 \leqq \Delta < 360°$$

$$\Lambda = \Delta + (\mathbb{C} + \tau) - (\Omega + \sigma)$$

$$\epsilon = \bar{\epsilon} + \delta\epsilon$$

The calling sequence to MNA is

(AC) = fractional day past 0^h of epoch T in E.T.

(MQ) = integer days past 0^h January 1, 1950 of the epoch T

```
CALL MNA
PZE 1,,A
PZE 1,,B
```

The cells A, A + 1, A + 2 contain the 1950.0 position vector $\mathbf{R} = (X, Y, Z)$, while the output vector $\mathbf{r} = (x, y, z)$ in the Moon-fixed coordinate system is placed in the locations B, B + 1, B + 2. The coordinate transformation is given by

$$\begin{pmatrix} x \\ y \\ z \end{pmatrix} = MNA \begin{pmatrix} X \\ Y \\ Z \end{pmatrix}$$

The inverse transformation

$$\begin{pmatrix} X \\ Y \\ Z \end{pmatrix} = (MNA)' \begin{pmatrix} x \\ y \\ z \end{pmatrix}$$

is indicated by

```
CALL MNA
PZE 1,,A
PZE 0,,B
```

A, A + 1, A + 2 contain $\mathbf{r}$ and the output $\mathbf{R}$ is placed in B, B + 1, B + 2.

If MNA1 is called instead of MNA, the matrices are not recomputed unless time has changed by 0.01 day.

The subroutines use four cells of erasable storage starting at COMMON.

MNAMD, MNAMD1

As it is necessary to form the Moon-fixed velocity, the subroutine MNAMD has been provided to accomplish this task. As in the preceding discussion of MNA, the formulas for transforming positions are

$$\begin{pmatrix} x \\ y \\ z \end{pmatrix} = MNA \begin{pmatrix} X \\ Y \\ Z \end{pmatrix}$$

for the transformation from 1950.0 position to Moon-fixed position and inversely,

$$\begin{pmatrix} X \\ Y \\ Z \end{pmatrix} = (MNA)' \begin{pmatrix} x \\ y \\ z \end{pmatrix}$$

for the position transformation in the other direction.

To obtain velocity transformations, the above formulas are differentiated and the approximation is made that

$$\dot{N} = \dot{A} = 0$$

Thus

$$\begin{pmatrix} \dot{x} \\ \dot{y} \\ \dot{z} \end{pmatrix} = MNA \begin{pmatrix} \dot{X} \\ \dot{Y} \\ \dot{Z} \end{pmatrix} + \dot{M}NA \begin{pmatrix} X \\ Y \\ Z \end{pmatrix}$$

and for the inverse transformation

$$\begin{pmatrix} \dot{X} \\ \dot{Y} \\ \dot{Z} \end{pmatrix} = (MNA)' \begin{pmatrix} \dot{x} \\ \dot{y} \\ \dot{z} \end{pmatrix} + (\dot{M}NA)' \begin{pmatrix} x \\ y \\ z \end{pmatrix}$$

In computing $\dot{M}$ the rates for the slowly varying angles Ω' and i are taken to be zero.

$$\dot{M} = (\dot{M}_{ij})$$

where

$$\dot{M}_{11} = (-\sin\Lambda\cos\Omega' - \cos\Lambda\sin\Omega'\cos i)\,\dot{\Lambda}$$
$$\dot{M}_{12} = (-\sin\Lambda\sin\Omega' + \cos\Lambda\cos\Omega'\cos i)\,\dot{\Lambda}$$
$$\dot{M}_{13} = (\cos\Lambda\sin i)\,\dot{\Lambda}$$
$$\dot{M}_{21} = (-\cos\Lambda\cos\Omega' + \sin\Lambda\sin\Omega'\cos i)\,\dot{\Lambda}$$
$$\dot{M}_{22} = (-\cos\Lambda\sin\Omega' - \sin\Lambda\cos\Omega'\cos i)\,\dot{\Lambda}$$
$$\dot{M}_{23} = (-\sin\Lambda\sin i)\,\dot{\Lambda}$$
$$\dot{M}_{31} = 0$$
$$\dot{M}_{32} = 0$$
$$\dot{M}_{33} = 0$$

From the formula

$$\Lambda = \Delta + (\mathfrak{C} + \tau) - (\Omega + \sigma)$$

obtain

$$\dot{\Lambda} = \dot{\Delta} + \dot{\mathfrak{C}} + \dot{\tau} - \dot{\Omega} - \dot{\sigma}$$

The adopted numerical expressions for the rates are

$$\dot{\Delta} = \frac{-\cos(\Omega + \sigma + \delta\psi)\sin\epsilon\,(\dot{\Omega} + \dot{\sigma})}{\sin i\cos\Delta}$$

$$\dot{\mathfrak{C}} = 0.266170762 \times 10^{-5} - 0.12499171 \times 10^{-13}\,T \text{ rad/sec}$$

$$\dot{\Omega} = -0.1069698435 \times 10^{-7} + 0.23015329 \times 10^{-13}\,T \text{ rad/sec}$$

$$\dot{\tau} = -0.1535272946 \times 10^{-9}\cos g + 0.569494067 \times 10^{-10}\cos g' + 0.579473484 \times 10^{-11}\cos 2\omega \text{ rad/sec}$$

$$\dot{\sigma} = -0.520642191 \times 10^{-7}\cos g + 0.1811774451 \times 10^{-7}\cos(g + 2\omega) - 0.1064057858 \times 10^{-7}\cos(2\omega + 2g) \text{ rad/sec}$$

The calling sequence to MNAMD has the form

(AC) = fractional day past 0^h of epoch T under consideration

(MQ) = integer days past 0^h January 1, 1950, E.T. to T in E.T.

```
CALL MNAMD
PZE 1,,A
PZE 1,,B
PZE 1,,C
```

The 1950.0 position vector $\mathbf{R} = (X, Y, Z)$ is input to cells A, A + 1, A + 2, while the 1950.0 velocity vector $\mathbf{V} = (\dot{X}, \dot{Y}, \dot{Z})$ occupies locations B, B + 1, B + 2. The output vector $\mathbf{v} = (\dot{x}, \dot{y}, \dot{z})$ is placed in C, C + 1, C + 2.

If the inverse transformation is desired, the calling sequence is modified to read

```
CALL MNAMD
PZE 1,,A
PZE 1,,B
PZE 0,,C
```

The Moon-fixed position vector $\mathbf{r} = (x, y, z)$ occupies cells A, A + 1, A + 2 as the Moon-fixed velocity vector $\mathbf{v} = (\dot{x}, \dot{y}, \dot{z})$ uses B, B + 1, B + 2 for input. The 1950.0 velocity vector $\mathbf{V} = (\dot{X}, \dot{Y}, \dot{Z})$ is the output and is placed in locations C, C + 1, C + 2.

The alternate entry MNAMD1 differs from the entry MNAMD in that the matrices M and $\dot{M}$ are recomputed only if time has changed by 0.01 day.

The subroutines use four words of erasable storage starting at COMMON.

3. Ephemeris

INTR, INTR1

The subroutine INTR assumes a high-density ephemeris tape on A8 with 20-day records of 596 words in the following format:

T_0	integer days past 0^h January 1, 1950, E.T. (floating point)
$X_☾(T_j)$, $\delta^2X_☾(T_j)$, $\delta^4X_☾(T_j)$ $Y_☾(T_j)$, $\delta^2Y_☾(T_j)$, $\delta^4Y_☾(T_j)$ $Z_☾(T_j)$, $\delta^2Z_☾(T_j)$, $\delta^4Z_☾(T_j)$ $X_☉(T_j)$, $\delta^2X_☉(T_j)$, $\delta^4X_☉(T_j)$ $Y_☉(T_j)$, $\delta^2Y_☉(T_j)$, $\delta^4Y_☉(T_j)$ $Z_☉(T_j)$, $\delta^2Z_☉(T_j)$, $\delta^4Z_☉(T_j)$	geocentric block $j = 0,\ldots,20$ time interval is 1 day 378 words
$X_♀(T_j)$, $\delta^2X_♀(T_j)$, $\delta^4X_♀(T_j)$ $Y_♀(T_j)$, $\delta^2Y_♀(T_j)$, $\delta^4Y_♀(T_j)$ $Z_♀(T_j)$, $\delta^2Z_♀(T_j)$, $\delta^4Z_♀(T_j)$ $X_♂(T_j)$, $\delta^2X_♂(T_j)$, $\delta^4X_♂(T_j)$ $Y_♂(T_j)$, $\delta^2Y_♂(T_j)$, $\delta^4Y_♂(T_j)$ $Z_♂(T_j)$, $\delta^2Z_♂(T_j)$, $\delta^4Z_♂(T_j)$ (Nine words per time point representing what was the Earth-Moon barycenter used in an older version) $X_♃(T_j)$, $\delta^2X_♃(T_j)$, $\delta^4X_♃(T_j)$ $Y_♃(T_j)$, $\delta^2Y_♃(T_j)$, $\delta^4Y_♃(T_j)$ $Z_♃(T_j)$, $\delta^2Z_♃(T_j)$, $\delta^4Z_♃(T_j)$	heliocentric block $j = 0, 4, 8, 12, 16, 20$ time interval is 4 days 216 words

The last word of the record is the check sum for the previous 595 words.

From record to record the time must be incremented by 20 days. In addition, the time on the first record T_F and the time on the last record T_L are subroutine parameters which give the base point of the ephemeris and also a check for time out of the range of the ephemeris. The symbolic locations are TFIRST and TLAST for T_F and T_L respectively.

The lunar coordinates are assumed to use the Earth radius as a unit of length, while all other coordinates are expressed in terms of the Astronomical Unit. As the program runs in km, conversion factors are provided at SCALE1 for the Earth radius and SCALE2 for the Astronomical Unit. The rectangular coordinates are assumed to be expressed in the mean equator and equinox of the epoch 1950.0 E.T., the beginning of the Besselian year.

As the argument of the tables is E.T. (Ephemeris Time) and the program uses U.T. (Universal Time) the subroutine E.T. is used to form the double-precision ephemeris time in sec E.T. = U.T. + ΔT, where the constant ΔT appears at GRAV−2 and thus may be input via INP1 in the symbolic mode.

Beginning at GRAV, a list of gravitational coefficients for the bodies appears in the units km³/sec². As a function of the central body, certain sets of these coefficients are provided for the subroutine BODY in the COMMON list KB0, . . . , KB6. The following illustrates the transfers:

Central body	Effective noncentral bodies
Earth	Moon, Sun; Jupiter if $R_{\oplus♃} \geqq 10^6$ km
Moon	Earth, Sun
Sun	Earth, Moon, Venus, Mars, Jupiter
Venus	Earth, Moon, Sun, Mars, Jupiter
Mars	Earth, Moon, Venus, Sun, Jupiter
Jupiter	Earth, Moon, Venus, Mars, Sun

The entry INTR takes as argument the double-precision seconds past 0^h January 1, 1950, U.T., stored in T, T + 1, makes the conversion to E.T., and interpolates as a function of the central body on the required coordinates for the bodies listed above. There are two conditions under which actual interpolation takes place:

1. Central body has changed
2. Time has changed

If neither (1) nor (2) is satisfied, then INTR gives an immediate return.

In contrast with INTR, the entry INTR1 always interpolates; in addition, this entry obtains the positions of all the bodies in terms of the central body instead of the selective list used with BODY. The positions appear in the COMMON bank XN. Additionally, INTR1 numerically differentiates the positions to obtain the velocities which are deposited in the bank XN. in COMMON.

Positioning of the ephemeris tape on A8 is accomplished by the following scheme:

1. If $T < T_F$ or $T \geqq T_L$, an error point is given and ABORT is called.
2. If $T \geqq T_N + 20$, where T_N is the time on the record currently in core, the tape is searched in a forward direction until the correct record is found. If the tape has not been previously read, a dummy T_N causes a forward search.
3. If $T_N \leqq T < T_N + 20$, interpolation proceeds.
4. If $T < T_N$, the correct number m of backspaces is calculated.
   a. If $m \leqq 15$, the tape is backspaced m times and proceeds to do a forward search.

b. If $m > 15$, the tape is backspaced 1 file and a forward search is undertaken.

After the correct record has been found, it is read into core and both check-summed and redundancy-tested. Reading of the desired record is attempted a maximum of 10 times, after which an error comment is printed and ABORT is called. In the forward search the above two tests are not made.

The following Everett's formula is used for the interpolation:

$$y(t) = \left\{u y_0 + t y_1\right\} + \left\{\frac{u(u^2-1)}{3!}\delta^2 y_0 + \frac{t(t^2-1)}{3!}\delta^2 y_1\right\} + \left\{\frac{u(u^2-1)(u^2-4)}{5!}\delta^4 y_0 + \frac{t(t^2-1)(t^2-4)}{5!}\delta^4 y_1\right\}$$

where

$y_0 = y(T_j)$

$y_1 = y(T_j + h)$

h = ephemeris interval

$t = \dfrac{T - T_j}{h}$

$u = 1 - t$

$T_j \leqq T < T + h$

To obtain a formula for the velocity, the above Everett's form is differentiated and scaled:

$$\dot{y}(T) = \frac{1}{h}\frac{dy(t)}{dt} = \frac{1}{h}\left\{-y_0 + y_1\right\} + \frac{1}{h}\left\{-\frac{3u^2-1}{3!}\delta^2 y_0 + \frac{3t^2-1}{3!}\delta^2 y_1\right\} + \frac{1}{h}\left\{-\frac{5u^4-15u^2+4}{5!}\delta^4 y_0 + \frac{5t^4-15t+4}{5!}\delta^4 y_1\right\}$$

The ephemeris tape currently used has the following modified differences for the Moon:

$$\delta_m^2 y = \delta^2 y - 0.01312\,\delta^6 y + 0.0043\,\delta^8 y$$

$$\delta_m^4 y = \delta^4 y - 0.27827\,\delta^6 y + 0.0685\,\delta^8 y$$

Thus δ_m^2 and δ_m^4 are used in the Everett's formula instead of δ^2 and δ^4 to provide for the influence of the higher differences.

The following constants are used:

E.R. = 6378.165
A.U. = 0.149599×10^9
} km

$\mu_\oplus = 0.3986032 \times 10^6$
$\mu_\mathbb{C} = 0.4900759 \times 10^4$
$\mu_\odot = 0.132715445 \times 10^{12}$
$\mu_\mathbb{Q} = 0.3247695 \times 10^6$
$\mu_\sigma = 0.4297780 \times 10^5$
$\mu_\mathbb{U} = 0.1267106 \times 10^9$
} km^3/sec^2

The subroutine uses 20 cells of erasable storage starting at COMMON.

4. Encke Method Calculations

ENCKE, ORTHO

The subroutine ENCKE has been provided to perform the calculation of the Encke contribution to the acceleration

$$\frac{\mu}{R_0^3}\left(\mathbf{R}F(Q) - \boldsymbol{\rho}\right)$$

where $\mathbf{R} = \mathbf{R}_0 + \boldsymbol{\rho}$. The solution $\mathbf{R}_0$ for the position in the two-body orbit is provided by KEPLER, and is saved from step to step so that a new $\mathbf{R}_0$ is calculated only when the time has changed; thus KEPLER is called normally once per integration step while using the Adams-Moulton predictor-corrector.

$F(Q) = 1 - (1 + 2Q)^{-3/2}$ is calculated from the series expansion

$$F(Q) = Q\sum_{j=0}^{6} a_j Q^j$$

where

$a_0 = 3$
$a_1 = -7.5$
$a_2 = 17.5$
$a_3 = -39.375$
$a_4 = 86.625$
$a_5 = -187.6875$
$a_6 = 402.1875$

and

$$Q = \frac{\boldsymbol{\rho}\cdot\left(\mathbf{R}_0 + \frac{\boldsymbol{\rho}}{2}\right)}{R_0^2}$$

The expansion gives accurate results for $|Q| \leqq 0.03$; if the limit is exceeded, an error print will be given and the trajectory will be terminated. Normally, Q grows slowly enough so that rectification may be performed at the end

of the integration step; however, for wild trajectories the error procedure has been observed to occur.

ENCKE deposits the true positior $\mathbf{R}$ in the COMMON cells QX, QX + 1, QX + 2 and the acceleration term $\mu/R_0^3\,(\mathbf{R}\,F(Q)-\boldsymbol{\rho})$ in the cells CX.., CX.. + 1, CX.. + 2.

At the osculation epoch T_0 the subroutine ORTHO provides the Encke scheme with initial conditions:

$$\boldsymbol{\rho}\,(T_0) = \mathbf{R}(T_0) - \mathbf{R}_0(T_0)$$
$$\dot{\boldsymbol{\rho}}\,(T_0) = \mathbf{V}(T_0) - \mathbf{V}_0(T_0)$$

$\boldsymbol{\rho}\,(T_0)$ is placed in the COMMON cells CX, CX + 1, CX + 2, while $\dot{\boldsymbol{\rho}}\,(T_0)$ is placed in storage locations CX.. CX. + 1, CX. + 2.

CONIC

The subroutine CONIC supplies the Encke machinery with the necessary orbital elements given an epoch T_0 and the Cartesian position and velocity vectors $\mathbf{R}_0$ and $\mathbf{V}_0$. Under certain circumstances described below the derived elements are nonosculating.

The computation starts with the formation of the angular momentum c_1 given by

$$c_1\,\mathbf{W} = \mathbf{R}_0 \times \mathbf{V}_0$$

If $c_1 > (0.99\epsilon)R_0V_0$, where $\epsilon = 0.5 \times 10^{-3}$, the orbit is considered nonrectilinear and the subroutine proceeds in the normal case. However, for $c_1 \leqq (0.99\epsilon)R_0V_0$, $\mathbf{V}_0$ is replaced by $\mathbf{V}_0^*$ given by

$$\mathbf{V}_0^* = V_0\left[\sqrt{1-\epsilon^2}\,\operatorname{sgn}(\mathbf{R}_0\cdot\mathbf{V}_0)\,\frac{\mathbf{R}_0}{R_0} + \epsilon\mathbf{M}\right]$$

where

$$\mathbf{M} = \begin{cases} \dfrac{1}{\sqrt{X_0^2+Y_0^2}}(Y_0, -X_0, 0) & \text{if } X_0^2 + Y_0^2 \neq 0, \\ (1,0,0) \quad \text{otherwise} \end{cases}$$

and the routine cycles back to recompute the angular momentum. Observe that $c_1^* = \epsilon R_0 V_0$ so that $\mathbf{V}_0^*$ is acceptable; of course, $V_0^* = V_0$ and $c_3^* = c_3$.

Next come the elements

$$p = \frac{c_1^2}{\mu}\text{, the semilatus rectum}$$

$$c_3 = V_0^2 - \frac{2\mu}{R_0}\text{, the "energy" or } \textit{vis viva} \text{ integral}$$

$$1 - e^2 = -\frac{c_1^2 c_3}{\mu^2}$$

At this point the eccentricity e is computed and tested:

$$e = \begin{cases} \sqrt{1-(1-e^2)} & \text{if radicand} > 0, \\ 0 \quad \text{otherwise} \end{cases}$$

If the computed e is smaller than 0.01, then a circular orbit is assumed and the remaining elements are made consistent with the assumption of $e = 0$. There follows in quick succession

$$q = \frac{p}{1+e}\text{, the closest approach distance}$$

$$\lambda = \frac{1-e^2}{(1+e)^2}\text{, the pericenter parameter}$$

$$g = \frac{c_1}{2q^2}\text{, the mean motion for the pericenter method}$$

$$a = \frac{\mu}{|c_3|}\text{, the semimajor or transverse axis}$$

$$n = \frac{\sqrt{|c_3|}}{a}\text{, the mean motion}$$

$$b = a\sqrt{|1-e^2|}\text{, the semiminor or conjugate axis}$$

and finally,

$$1 - e = \frac{1-e^2}{1+e}$$

It remains to calculate $\mathbf{P}$ and $\mathbf{Q}$ along with $\Delta T = T_0 - T_p$ and to make the two sets agree sufficiently so that the Encke starting values will not be too large.

If $e = 0$,

$$\mathbf{P} = \frac{\mathbf{R}_0}{R_0} \text{ and } \mathbf{Q} = \frac{\mathbf{W}\times\mathbf{R}_0}{|\mathbf{W}\times\mathbf{R}_0|} \text{ with } \Delta T = 0$$

Otherwise, the vectors are constructed:

$$e\,R_0^2\,\mathbf{P} = (e\,R_0\cos v_0)\,\mathbf{R}_0 - (e\,R_0\sin v_0)\,\mathbf{W}\times\mathbf{R}_0$$
$$e\,R_0^2\,\mathbf{Q} = (e\,R_0\sin v_0)\,\mathbf{R}_0 + (e\,R_0\cos v_0)\,\mathbf{W}\times\mathbf{R}_0$$

Divide by R_0, and normalize the resultant vectors to obtain $\mathbf{P}$ and $\mathbf{Q}$. The expressions involving the true anomaly at epoch are calculated from

$$e\,R_0\cos v_0 = p - R_0$$

$$e\,R_0\sin v_0 = \frac{c_1}{\mu}\,\mathbf{R}_0\cdot\mathbf{V}_0$$

To obtain ΔT, the applicability of the pericenter method for $|\lambda| < 0.45$ is tested. w_0 is formed according to

$$w_0 = \begin{cases} \dfrac{\sin v_0}{1+\cos v_0} & \text{if } \cos v_0 \geqq 0 \\ \dfrac{1-\cos v_0}{\sin v_0} & \text{otherwise} \end{cases}$$

and tested. If $|w_0| \leqq w_{max}$, then

$$g\Delta T = \sum_{j=0}^{6} a_j(\lambda)\, w_0^{2j}$$

where the coefficients $a_j(\lambda)$ along with w_{max} are given in the discussion of the subroutine PERI.

Whenever $|w_0| > w_{max}$, the eccentric anomaly and Kepler's equation are resorted to. The scheme is divided into two cases according to the value of ε:

(1) $\varepsilon < 1$, elliptic case

The following expressions are constructed for the eccentric anomaly:

$$\varepsilon \cos E_0 = 1 - \frac{R_0}{a}$$

$$\varepsilon \sin E_0 = \frac{\mathbf{R}_0 \cdot \mathbf{V}_0}{a\sqrt{|c_3|}}$$

from which E_0 is determined.

If $|\varepsilon \sin E_0| \leqq |\varepsilon \cos E_0|$, then the auxiliary variable E^* is constructed:

$$E^* = \sin^{-1} \frac{\mathbf{R}_0 \cdot \mathbf{V}_0}{a\varepsilon\sqrt{|c_3|}}, \quad -\frac{\pi}{2} < E^* < \frac{\pi}{2}$$

Then E_0 is given by

$$E_0 = \begin{cases} E^* & \text{if } 1 - \dfrac{R_0}{a} > 0 \\ \pi\, \mathrm{sgn}\,(E^*) - E^* & \text{otherwise} \end{cases}$$

On the other hand, if $|\varepsilon \sin E_0| > |\varepsilon \cos E_0|$, then

$$E^* = \cos^{-1} \frac{1}{\varepsilon}\left(1 - \frac{R_0}{a}\right), \quad 0 < E^* < \pi,$$

with

$$E_0 = \mathrm{sgn}\,(\mathbf{R}_0 \cdot \mathbf{V})\, E^*$$

Finally, ΔT is calculated from

$$n\Delta T = E_0 - \varepsilon \sin E_0 = E_0 - \frac{\mathbf{R}_0 \cdot \mathbf{V}_0}{a\sqrt{|c_3|}}$$

(2) $\varepsilon > 1$, hyperbolic case

The eccentric anomaly F_0 is found from the relation

$$\varepsilon \sinh F_0 = \frac{\mathbf{R}_0 \cdot \mathbf{V}_0}{a\sqrt{c_3}} = \varepsilon\alpha$$

$$F_0 = \mathrm{sgn}\,(\mathbf{R}_0 \cdot \mathbf{V}_0) \ln\left(|\alpha| + \sqrt{1 + \alpha^2}\right)$$

Then ΔT is obtained from Kepler's equation:

$$n\Delta T = \varepsilon \sinh F_0 - F_0 = \frac{\mathbf{R}_0 \cdot \mathbf{V}_0}{a\sqrt{c_3}} - F_0$$

QUADKP

The subroutine QUADKP was written to provide an iterative solution to Kepler's equation for the elliptic and hyperbolic cases using a second-order gradient method. However, only the machinery for the latter case has been utilized in the main program for the Encke solution.

Let Kepler's equation be represented in the hyperbolic case by

$$f(F) = \varepsilon \sinh F - F - M, \quad M = n\,(T - T_p)$$

Then for the approximate solution F_j the Taylor series expansion through second-order terms may be used to obtain a new estimate F_{j+1} of the root $f(F) = 0$.

$$0 = f(F_j + \delta F_j) = f(F) \approx f(F_j) + \delta F_j f'(F_j) + \frac{\delta F_j^2}{2} f''(F_j)$$

Solving directly for the roots of the quadratic,

$$\delta F_j = F_{j+1} - F_j = \frac{2f(F_j)}{-f'(F_j) - \sqrt{f'^2(F_j) - 2f(F_j)f''(F_j)}}$$

where the minus sign is taken before the radical to insure that $\delta F_j \to 0$ as $f(F_j) \to 0$; for a wild guess, however, the radicand may become negative, in which case the radical is replaced by zero. With a good initial approximation the latter case arises only infrequently.

A similar result may be obtained for the elliptic case, namely

$$f(E) = E - \varepsilon \sin E - M$$

Convergence in either the hyperbolic or elliptic case is evidently given by

$$F_{j+1} - F = O\left((F_j - F)^3\right)$$

The program is made complex by the attention necessarily paid to obtaining a good initial approximation for starting the higher order iteration scheme and the behavior of Kepler's equation when ε is near 1 and M is small.

The initial approximation is obtained as a function of ε and M:

(1) $\varepsilon > 1.1, \quad F_{-1} = \dfrac{M}{\varepsilon - 1}$

$$F_0 = \begin{cases} \operatorname{sgn}(M) \min\left\{1, \ln \dfrac{2|M|}{\varepsilon}\right\} & \text{if } |F_{-1}| > 1 \\ F_{-1} - \dfrac{\dfrac{F_{-1}^3}{3!} + \dfrac{F_{-1}^5}{5!}}{\dfrac{\varepsilon - 1}{\varepsilon} + \dfrac{F_{-1}^2}{2!} + \dfrac{F_{-1}^4}{4!}} & \text{if } |F_{-1}| \leqq 1 \end{cases}$$

(1 iteration by Newton's method)

(2) $1 \leqq \varepsilon \leqq 1.1$

$$F_0 = \begin{cases} \operatorname{sgn}(M) \min\left\{1, \ln \dfrac{2|M|}{\varepsilon}\right\} & \text{if } |M| > 1 \\ (6M)^{1/3} & \text{otherwise} \end{cases}$$

(3) $0.9 < \varepsilon \leqq 1$

$$E_0 = (6M)^{1/3}$$

(4) $0 < \varepsilon \leqq 0.9, \quad E_{-1} = \dfrac{M}{1 - \varepsilon}$

$$E_0 = \begin{cases} 2.5 \times \operatorname{sgn}(M) & \text{if } |E_{-1}| > 3 \\ E_{-1} - \dfrac{\dfrac{E_{-1}^3}{3!} - \dfrac{E_{-1}^5}{5!}}{\dfrac{1 - \varepsilon}{\varepsilon} + \dfrac{E_{-1}^2}{2!} - \dfrac{E_{-1}^4}{4!}} & \text{if } |E_{-1}| \leqq 3 \end{cases}$$

(1 iteration by Newton's method)

(5) $\varepsilon = 0$

$$E_0 = M = E$$

In the iteration scheme, a modification occurs in the numerical evaluation of f, f', and f'' for the hyperbolic case.

(1) For $|F_j| < 1.98$

$$\varepsilon \sinh F_j - F_j = (\sinh F_j - F_j) + (\varepsilon - 1) \sinh F_j$$

$$\sinh F_j - F_j = \frac{F_j^3}{3!} \sum_{i=0}^{5} \frac{(3!)^{i+1}}{(2i+3)!} \left(\frac{F_j^2}{3!}\right)^i$$

$$\sinh F_j = F_j + (\sinh F_j - F_j)$$

(2) For $|F_j| < 2.28$

$$\cosh F_j - 1 = \frac{F_j^2}{2!} \sum_{i=0}^{6} \frac{(2!)^{i+1}}{(2i+2)!} \left(\frac{F_j^2}{2!}\right)^i$$

$$\varepsilon - \cosh F_j = (\varepsilon - 1) - (\cosh F_j - 1)$$

The power series developments are employed since the quantity $1 - \varepsilon$ is regarded as an independent orbital element and ε is made consistent with this choice. For small values of F_j, underflow is avoided by choosing fewer terms in the expansions.

Additionally, if $M = 0$, F is set to zero and no iteration is performed. The calling sequence has the form

```
(AC)  = M
(MQ)  = 1 - ε
CALL  QUADKP
DEC   ε
PZE   A
(ERROR RETURN)
```

For the elliptic case, it is assumed that M has been normalized so that $|M| \leqq \pi$.

The location A contains a positive number for the elliptic case and a negative number for the hyperbolic case to choose the correct form of Kepler's equation for the rectilinear orbit.

As a convergence criterion, $\epsilon = 5 \times 10^{-8}$ has been chosen to apply such that the normal return is given with (AC) $= F$ or E whenever $|f(F_j)| < \epsilon |M|$ and $F = F_j$ for the hyperbolic case, or $|f(E_j)| < \epsilon |M|$ and $E = E_j$ for the elliptic case. However, if the process fails to converge to within ϵ in $N = 50$ iterations, the following comment is printed:

QUADRATIC METHOD FAILED

M ε F_j (or E_j) $f(F_j)$ [or $f(E_j)$]

and the error return is given with (AC) $= F_j$ or E_j. Generally, convergence is obtained in five or fewer iterations. After the first time QUADKP has been called in a phase, subsequent initial approximations are obtained by using the solution at the previous time point.

The subroutine uses eleven words of erasable storage starting at COMMON.

KEPLER, PERI, SPEED

KEPLER is the subroutine which provides the solution to the two-body problem at the epoch T. The necessary elements are assumed to have been provided at the osculation epoch by ORTHO and CONIC. Different methods of solution are chosen according to the following criteria:

1. The pericenter method is used whenever
   a. $|\lambda| < 0.45$ and
   b. $|w_0| \leqq g\,\Delta T_{\max}$
2. QUADKP is used for $e > 1$ and if item 1 is not satisfied.
3. If the conditions in item 1 are not met and if $e < 1$, then the methods described below for the ellipse are used.

As the orbital elements furnished by CONIC are nonosculating if true osculating elements give nearly rectilinear results, the case for $e = 1$ and $c_3 \neq 0$ need not be treated.

Pericenter Method

The first problem to be solved in the pericenter method is the determination of w from the formula

$$w_0 = g\,(T - T_p) = \int_0^w \frac{1 + u^2}{(1 + \lambda u^2)^2}\,du$$

where $g = c_1/2q^2$. The quadrature is approximated by the expansion

$$w \sum_{j=0}^{6} c_j w^{2j}$$

where the coefficients are a function of λ:

$$a_0 = 1$$

$$a_j = (-1)^j \frac{1}{2j+1}\left[(j+1)\,\lambda^j - j\lambda^{j-1}\right]$$

$$w_{\max} = \max\left\{\left(\frac{\epsilon}{a_7}\right)^{1/14}, \quad \left(\frac{\epsilon}{3a_7}\right)^{1/12}\right\},$$

where $\epsilon = 0.5 \times 10^{-8}$.

$$g\,\Delta T_{\max} = w_{\max} \sum_{j=0}^{6} a_j\, w_{\max}^{2j}$$

w_1, the initial approximation, is given by

$$w_1 = \begin{cases} (3w_0)^{1/3} & \text{if } |w_0| > 3 \\ 1/2\, w_0 & \text{if } 1 < |w_0| \leqq 3 \\ w_0 & \text{if } 0 \leqq |w_0| \leqq 1 \end{cases}$$

Iteration proceeds by Newton's method:

$$w_{j+1} = w_j - \frac{f(w_j)}{f'(w_j)}$$

where

$$f(w) = w \sum_{j=0}^{6} a_j w^{2j} - w_0$$

and

$$f'(w) = \frac{1 + w^2}{(1 + \lambda w^2)^2}$$

Convergence is usually obtained in a maximum of four iterations for cases which have arisen in practice, assuming a criterion of $|f(w_j)| < 5 \times 10^{-8}\,|w_0|$.

When convergence has been obtained the coordinates may be calculated from the formulas

$$\mathbf{R} = \frac{1 - w^2}{1 + \lambda w^2}\,q\mathbf{P} + \frac{2w}{1 + \lambda w^2}\,q\mathbf{Q}$$

$$\mathbf{V} = -\frac{(1 + \lambda)\,w\,c_1}{q\,(1 + w^2)}\,\mathbf{P} + \frac{(1 - \lambda w^2)\,c_1}{q\,(1 + w^2)}\,\mathbf{Q}$$

Hyperbolic Case

If method 2 is to be used, the subroutine QUADKP is called and returns with the solution to Kepler's equation. The coordinates are then calculated from the expressions

$$\mathbf{R} = a\,(e - \cosh F)\,\mathbf{P} + a\sqrt{e^2 - 1}\,\sinh F\,\mathbf{Q}$$

$$\mathbf{V} = -\frac{a\sqrt{c_3}\,\sinh F}{R}\,\mathbf{P} + \frac{a\sqrt{c_3}\,\sqrt{e^2 - 1}\,\cosh F}{R}\,\mathbf{Q}$$

Elliptic Case

Begin by defining the auxiliary quantity M^* by

$$M^* \equiv M = n(T - T_p) \pmod{2\pi} \quad -\pi < M^* \leqq \pi$$

and

$$b_7 = -\left\{\operatorname{sgn}(M^*)\right\}\frac{\epsilon}{2}$$

Then for $|M^*| \leqq \pi/6 - \epsilon/2$, take

$$E_2 = M$$

$$E_1 = M - b_7$$

$$E_0 = M + b_7$$

and for $|M^*| > \pi/6 - \epsilon/2$ the approximations are

$$E_2 = M - b_7$$

$$E_1 = M - 2b_7$$

$$E_0 = M$$

Now if $|M^*| \geqq 0.25$, iteration is performed using Newton's method with E_2 as the initial approximation:

$$E_{j+1} = E_j - \frac{f(E_j)}{f'(E_j)}$$

where $f(E) = E - \varepsilon \sin E - M$. Convergence for Newton's method is evidently given by

$$E_{j+1} - E = O((E_j - E)^2)$$

where $f(E) = 0$.

Whenever $|M^*| < 0.25$ Muller's method[2] is used:

$$E_{j+1} = E_j + h_{j+1}$$

$$h_{j+1} = \lambda_{j+1} h_j$$

$$\lambda_{j+1} = -\frac{2\delta_j f(E_j)}{g_j + \{\mathrm{sgn}(g_j)\}\sqrt{|a_j|}}$$

$$a_j = g_j^2 - 4\lambda_j \delta_j f(E_j) \times [\lambda_j f(E_{j-2}) - \delta_j f(E_{j-1}) + f(E_j)]$$

$$g_j = \lambda_j^2 f(E_{j-2}) - \delta_j^2 f(E_{j-1}) + (\lambda_j + \delta_j) f(E_j)$$

$$\delta_j = 1 + \lambda_j$$

Initially, of course,

$$\lambda_2 = \frac{E_2 - E_1}{E_1 - E_0} = -\frac{1}{2}$$

The convergence rate is given by

$$E_{j+1} - E = O(\varepsilon_M^3)$$

where $\varepsilon_M = \max\{|E_j - E|, |E_{j-1} - E|, |E_{j-2} - E|\}$ and $f(E) = 0$. The method owes much of its usefulness to the obtaining of E_{j+1} by interpolation, which makes it relatively insensitive to $f'(E) \approx 0$.

For both the Newton and Muller methods, convergence is defined by

$$|f(E_j)| \leqq \epsilon |M|$$

where $\epsilon = 5 \times 10^{-8}$ or until E_{j+1} and E_j agree to 25 bits. In practice, for the values of M and e encountered, three or four iterations are usually sufficient for convergence.

Whenever $0.5 < e < 1$, the following series expansions are resorted to:

(1) For $|E_j| < 1.98$

$$E_j - \varepsilon \sin E_j = (E_j - \sin E_j) + (1 - \varepsilon) \sin E_j$$

$$E_j - \sin E_j = \frac{E_j^3}{3!} \sum_{i=0}^{8} \frac{(3!)^{i+1}}{(2i+3)!} \left(-\frac{E_j^2}{3!}\right)^i$$

(2) For $|E_j| < 2.28$

$$1 - \cos E_j = \frac{E_j^2}{2!} \sum_{i=0}^{6} \frac{(2!)^{i+1}}{(2i+2)!} \left(-\frac{E_j^2}{2!}\right)^i$$

$$\cos E_j - \varepsilon = (1 - \varepsilon) - (1 - \cos E_j)$$

Here ε is made consistent with the choice of $1 - \varepsilon$ as an independent orbital element.

The coordinates are obtained after convergence by use of the formulas

$$\mathbf{R} = a(\cos E - \varepsilon)\mathbf{P} + a\sqrt{1 - e^2}\sin E\,\mathbf{Q}$$

$$\mathbf{V} = -\frac{a\sqrt{|c_3|}\sin E}{R}\mathbf{P} + \frac{a\sqrt{|c_3|}\sqrt{1 - e^2}\cos E}{R}\mathbf{Q}$$

As usually only the position is required for the two-body orbit in the Encke scheme, KEPLER is additionally used to calculate $\mathbf{R}$. Whenever $\mathbf{V}$ is needed, the subroutine SPEED is called upon, which makes use of the previous solution E, F, or w. $\mathbf{R}$ is placed in the COMMON cells QX0, QX0 + 1, QX0 + 2 by KEPLER, while SPEED places $\mathbf{V}$ in the cells QX0., QX0. + 1, QX0. + 2 and also calculates the true velocity $\mathbf{V} + \dot{\boldsymbol{\rho}}$ which is placed in the cells QX., QX. + 1, QX. + 2.

After the first use of KEPLER in a phase, further time points use as initial approximation the solution at the preceding time point.

5. Perturbations

HARMN, HARMN1

The oblate potential of the Earth is assumed to contain the second, third, and fourth spherical harmonics:

$$U_\oplus = \frac{\mu_\oplus}{R}\left\{\frac{Ja_\oplus^2}{3R^2}(1 - 3\sin^2\phi) + \frac{Ha_\oplus^3}{5R^3}(3 - 5\sin^2\phi)\sin\phi + \frac{Da_\oplus^4}{35R^4}(3 - 30\sin^2\phi + 35\sin^4\phi)\right\}$$

where $\mu_\oplus$ is the gravitational coefficient of the Earth and $a_\oplus$ is the equatorial radius of the Earth.

$\mathbf{R} = (X, Y, Z)$ is the position vector from the Earth's center of mass expressed in the mean equator and equi-

[2]David E. Muller, "A Method for Solving Algebraic Equations Using an Automatic Computer," *Mathematical Tables and Other Aids to Computation*, 1956, pp. 208-215.

nox of 1950.0. To obtain ϕ, the geocentric latitude, $\mathbf{r} = (x, y, z)$, the position vector expressed in the true equator and equinox of date, must be obtained. NUTATE provides the necessary rotation matrix A:

$$\begin{pmatrix} x \\ y \\ z \end{pmatrix} = \begin{pmatrix} a_{11} & a_{12} & a_{13} \\ a_{21} & a_{22} & a_{23} \\ a_{31} & a_{32} & a_{33} \end{pmatrix} \begin{pmatrix} X \\ Y \\ Z \end{pmatrix}$$

Thus $\sin \phi = z/R$.

To obtain the perturbing acceleration, $\nabla U_\oplus$ is formed:

$$\nabla U_\oplus = \left(\frac{\partial U_\oplus}{\partial u_1}, \frac{\partial U_\oplus}{\partial u_2}, \frac{\partial U_\oplus}{\partial u_3} \right)$$

where $u_1 = X$, $u_2 = Y$, and $u_3 = Z$.

$$\frac{\partial U_\oplus}{\partial u_j} = -\frac{J\mu_\oplus}{R^2}\frac{a_\oplus^2}{R^2}\left\{\left(1 - \frac{5z^2}{R^2}\right)\frac{u_j}{R} + 2\frac{z}{R}a_{3j}\right\}$$

$$-\frac{H\mu_\oplus}{R^2}\frac{a_\oplus^3}{R^3}\left\{\left(3 - 7\frac{z^2}{R^2}\right)\frac{z}{R}\frac{u_j}{R} + \left(-\frac{3}{5} + \frac{3z^2}{R^2}\right)a_{3j}\right\}$$

$$-\frac{D\mu_\oplus}{R^2}\frac{a_\oplus^4}{R^4}\left\{\left(\frac{3}{7} - 6\frac{z^2}{R^2} + 9\frac{z^4}{R^4}\right)\frac{u_j}{R} + \left(\frac{12}{7} - 4\frac{z^2}{R^2}\right)\frac{z}{R}a_{3j}\right\}$$

where $j = 1, 2, 3$.

The calling sequence for the setup entry is

```
CALL    HARMN
PZE     X,,B
PZE     K,,ZT
PZE     R
```

X, X + 1, X + 2 contain the vector $\mathbf{R} = (X, Y, Z)$; B, B + 1, B + 2 will contain $-\nabla U_\oplus$, the negative of the perturbing acceleration; K contains $\mu_\oplus$, the Earth's gravity coefficient; ZT contains z, the distance above the true equator of the Earth; and R contains R, the distance to the center of the Earth.

HARMN1 is the execution entry which assumes the above storage layout. In addition, provisions have been made to omit the calculation of the various harmonics as a function of the geocentric range. The internal parameters are listed in the following:

Location	Quantity	Nominal value	Explanation
HARMN + 2	J	1.62345×10^{-3}	Coefficient for second harmonic
+ 3	H	-0.575×10^{-5}	Coefficient for third harmonic
+ 4	D	0.7875×10^{-5}	Coefficient for fourth harmonic
+ 5	$a_\oplus$	6378.165 km	Earth radius
+ 6	R_2	500,000 km	$R > R_2$ suppress second harmonic
+ 7	R_3	200,000 km	$R > R_3$, suppress third harmonic
+ 10	R_4	100,000 km	$R > R_4$, suppress fourth harmonic

As HARMN is contained in the symbol table for INP1, the above parameters may be input in the symbolic mode of INP1.

The subroutine uses 15 cells of erasable storage starting at COMMON.

XYZDD, XYZDD1

For purposes of computing the oblate potential, the Moon is assumed to have a triaxial ellipsoidal figure. The moments of inertia A, B, and C are taken about the principal axes of the ellipsoid x, y, and z originated at the Moon's center of mass.

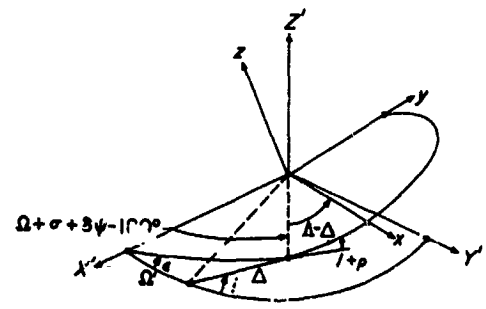

Sketch A-16. Geometry of the true equator of the Moon

In Sketch A-16, the X', Y', Z' frame is the Earth's true equator and equinox; the $x-y$ plane lies in Moon's true equator with z completing the right-hand system by lying along the Moon's spin axis. i is the inclination of the Moon's true equator to the Earth's true equator; Ω' is the right ascension of the ascending node of the Moon's true equator; Λ is the anomaly from the node to the x axis; Δ is the anomaly from the node to the ascending node of the Moon's true equator on the ecliptic; ϵ is the true obliquity of the ecliptic; $\delta\psi$ is the nutation in longitude; Ω is the mean longitude of the descending node of the Moon's mean equator on the ecliptic; $\mathbb{C}$ is the mean longitude of the Moon; I is the inclination of the Moon's mean equator to the ecliptic; σ is the libration in the node; τ is the libration in the mean longitude; and ρ is the libration in the inclination. The anomalies are related by $\Lambda - \Delta = (\mathbb{C} + \tau) - (\Omega + \sigma)$. Expressions for the above quantities appear in the discussion of subroutine MNA.

The two rectangular systems are related through Λ, Ω', and i by the rotation:

$$\begin{pmatrix} x \\ y \\ z \end{pmatrix} = \begin{pmatrix} b_{11} & b_{12} & b_{13} \\ b_{21} & b_{22} & b_{23} \\ b_{31} & b_{32} & b_{33} \end{pmatrix} \begin{pmatrix} X' \\ Y' \\ Z' \end{pmatrix}$$

where

$$b_{11} = \cos\Lambda\cos\Omega' - \sin\Lambda\sin\Omega'\cos i$$

$$b_{12} = \cos\Lambda\sin\Omega' + \sin\Lambda\cos\Omega'\cos i$$

$$b_{13} = \sin\Lambda\sin i$$

$$b_{21} = -\sin\Lambda\cos\Omega' - \cos\Lambda\sin\Omega'\cos i$$

$$b_{22} = -\sin\Lambda\sin\Omega' + \cos\Lambda\cos\Omega'\cos i$$

$$b_{23} = \cos\Lambda\sin i$$

$$b_{31} = \sin\Omega'\sin i$$

$$b_{32} = -\cos\Omega'\sin i$$

$$b_{33} = \cos i$$

Combining the above rotation with the one to rotate 1950.0 coordinates to true of-date, as described in NUTATE, derives the additional relation

$$\begin{pmatrix} x \\ y \\ z \end{pmatrix} = \begin{pmatrix} m_{11} & m_{12} & m_{13} \\ m_{21} & m_{22} & m_{23} \\ m_{31} & m_{32} & m_{33} \end{pmatrix} \begin{pmatrix} X \\ Y \\ Z \end{pmatrix}$$

where X, Y, and Z are the 1950.0 coordinates.

The following form of the potential function which accounts for a second harmonic has been adopted:

$$U_{\mathbb{C}} = \frac{G}{R}\,\frac{(A+B+C-3I)}{2R^2}$$

$$G = \frac{\mu_{\mathbb{C}}}{m_{\mathbb{C}}} = k^2, \text{ the universal gravitational constant}$$

$$I = A\left(\frac{x}{R}\right)^2 + B\left(\frac{y}{R}\right)^2 + C\left(\frac{z}{R}\right)^2$$

To obtain an expression for the perturbing acceleration

$$\nabla U_{\mathbb{C}} = \left(\frac{\partial U_{\mathbb{C}}}{\partial u_1}, \frac{\partial U_{\mathbb{C}}}{\partial u_2}, \frac{\partial U_{\mathbb{C}}}{\partial u_3}\right)$$

is formed, where $u_1 = X$, $u_2 = Y$, and $u_3 = Z$.

$$\frac{\partial U_{\mathbb{C}}}{\partial u_j} = \frac{G}{R^2}\left\{\left[-\frac{3}{2}\,\frac{A+B+C}{R^2} + \frac{15}{2}\,\frac{I}{R^2}\right]\frac{u_j}{R} - \frac{3}{R^3}\left[Am_{1j}x + Bm_{2j}y + Cm_{3j}z\right]\right\}$$

where $j = 1, 2, 3$. In current use, the values of the parameters are

$$G = 0.6671 \times 10^{-19}\ \text{km}^3/\text{kg-sec}^2$$

$$A = 0.88746 \times 10^{29}\ \text{kg-km}^2$$

$$B = 0.88764 \times 10^{29}\ \text{kg-km}^2$$

$$C = 0.88801 \times 10^{29}\ \text{kg-km}^2$$

The calling sequences are

(AC) = fractional days past 0^h of epoch

(MQ) = integer days past 0^h January 1, 1950, E.T.

CALL XYZDD (or XYZDD1 for time change check)

PZE 1,,X

PZE ,,X..

X, X + 1, X + 2 contain **R** in the 1950.0 system; X.., X.. + 1, X.. + 2 will contain the perturbing acceleration.

If the entry XYZDD1 is used, the matrix (m_{ij}) is recomputed only after time has changed by $d = 0.01$ day, where d is a program parameter. On the other hand, the entry XYZDD will give recalculation of (m_{ij}) each time. It has been determined by numerical experimentation that $d = 0.01$ day gives the perturbing acceleration to sufficient accuracy to represent faithfully the motion of a

low-altitude satellite in the field of an oblate Moon, as compared with an evaluation of $(m_{;j})$ at each integration step.

If $R > R_0 = 40{,}000$ km, then the contribution from the oblateness is set to zero. R_0 is a program parameter.

The subroutine uses six cells of erasable storage starting at COMMON.

BODY, BODY1

The subroutine BODY has been provided to perform the calculation of the n-body perturbation term

$$\mathbf{P} = -\sum_{j=1}^{n} \mu_j \left(\frac{\mathbf{R}_{jp}}{R_{jp}^3} + \frac{\mathbf{R}_j}{R_j^3} \right)$$

where $\mathbf{R}_{jp} = \mathbf{R} - \mathbf{R}_j$.

The subroutine has the execution entry

```
CALL BODY1
```

and the setup entry

```
CALL   BODY
PZE    X,,n
PZE    XN,,KJ
PZE    RJ,,RJP
PZE    X..
```

where the locations X, X + 1, X + 2, contain the vector **R**, the position of the probe with respect to the central body. The maximum number of noncentral bodies is given by n; the gravitational coefficients μ_j for the noncentral bodies are assumed to be stored in the list KJ, ..., KJ + (n − 1) with the convention that a cell containing zero means that the corresponding body is not used in the formation of **P**. The vectors $\mathbf{R}_j$, the positions of the n bodies with respect to the central body, are assumed to be stored in the bank XN, ..., XN + 3(n − 1) + 2 where the ordering is the same as for the μ_j.

The execution entry results in three types of output: −**P** is stored in the cells X.., X.. + 1, X.. + 2; the R_j for the effective bodies are stored in locations RJ, ..., RJ + (n − 1), while the R_{jp} for the same bodies are placed in the list RJP, . ., RJP + (n − 1).

The subroutine uses 14 cells of erasable storage starting at COMMON.

6. Variational Equations

VARY, SVARY

The subroutine VARY has been written to provide for the calculation of the derivatives of the first-order variational coefficients, i.e., of the partial derivatives $\partial\mathbf{R}/\partial u_j$ where $\{u_j\} = \{X_0, Y_0, Z_0, \dot{X}_0, \dot{Y}_0, \dot{Z}_0\}$ and all quantities are referred to the mean equator and equinox of 1950.0. The $\partial\ddot{\mathbf{R}}/\partial u_j$ may be expressed in the form $\partial\ddot{\mathbf{R}}/\partial u_j = (A + B)\ \partial\mathbf{R}/\partial u_j$ where the matrix A arises from the central-body term and the n-body perturbation and B approximates the effect of the Earth's oblateness to be used only in the vicinity of the Earth.

The form of A is obtained by differentiating $\ddot{\mathbf{R}}$ with respect to u_j and exchanging the order of differentiation where

$$\ddot{\mathbf{R}} = -\mu \frac{\mathbf{R}}{R^3} - \sum_{k=1}^{n} \mu_k \left\{ \frac{\mathbf{R}_{kp}}{R_{kp}^3} + \frac{\mathbf{R}_k}{R_k^3} \right\}$$

$$\frac{\partial \ddot{\mathbf{R}}}{\partial u_j} = -\sum_{k=0}^{n} \mu_k \left\{ \frac{1}{R_{kp}^3} \frac{\partial \mathbf{R}}{\partial u_j} - \frac{3}{R_{kp}^5} \left(\mathbf{R}_{kp} \cdot \frac{\partial \mathbf{R}}{\partial u_j} \right) \mathbf{R}_{kp} \right\}$$

with $\mu_0 = \mu$ and $\mathbf{R}_{0p} = \mathbf{R}$. Expanding the dot products, the computational form of A results:

$$A_{11} = -\sum_{k=0}^{n} \mu_k \left\{ \frac{1}{R_{kp}^3} - \frac{3X_{kp}^2}{R_{kp}^5} \right\}$$

$$A_{12} = A_{21} = 3\sum_{k=0}^{n} \mu_k \frac{X_{kp} Y_{kp}}{R_{kp}^5}$$

$$A_{13} = A_{31} = 3\sum_{k=0}^{n} \mu_k \frac{X_{kp} Z_{kp}}{R_{kp}^5}$$

$$A_{22} = -\sum_{k=0}^{n} \mu_k \left\{ \frac{1}{R_{kp}^3} - \frac{3Y_{kp}^2}{R_{kp}^5} \right\}$$

$$A_{23} = A_{32} = 3\sum_{k=0}^{n} \mu_k \frac{Y_{kp} Z_{kp}}{R_{kp}^5}$$

$$A_{33} = -\sum_{k=0}^{n} \mu_k \left\{ \frac{1}{R_{kp}^3} - 3\frac{Z_{kp}^2}{R_{kp}^5} \right\}$$

To obtain an approximate expression for the oblateness contribution B, choose the perturbation which retains just the second harmonic term:

$$\left(g_1\frac{X}{R},\ g_1\frac{Y}{R},\ g_2\frac{Z}{R}\right)$$

where

$$g_1 = -\frac{J a_\oplus^2 \mu_\oplus}{R^4}\left(1 - \frac{5Z^2}{R^2}\right)$$

$$g_2 = -\frac{J a_\oplus^2 \mu_\oplus}{R^4}\left(3 - \frac{5Z^2}{R^2}\right)$$

At this point a further approximation is made in that the coordinates are regarded as being expressed in the reference system, the mean equator and equinox of 1950.0.

Forming the partial derivatives

$$\frac{\partial \ddot{X}}{\partial u_j} = g_1\frac{X}{R}\left(\frac{1}{X}\frac{\partial X}{\partial u_j} - \frac{3}{R^2}\mathbf{R}\cdot\frac{\partial \mathbf{R}}{\partial u_j}\right) + \frac{\mu_\oplus X}{R^3}\frac{J a_\oplus^2}{R^4}\left\{10Z\frac{\partial Z}{\partial u_j} + 2\left(1 - \frac{10Z^2}{R^2}\right)\mathbf{R}\cdot\frac{\partial \mathbf{R}}{\partial u_j}\right\}$$

$$\frac{\partial \ddot{Y}}{\partial u_j} = g_1\frac{Y}{R}\left(\frac{1}{Y}\frac{\partial Y}{\partial u_j} - \frac{3}{R^2}\mathbf{R}\cdot\frac{\partial \mathbf{R}}{\partial u_j}\right) + \frac{\mu_\oplus Y}{R^3}\frac{J a_\oplus^2}{R^4}\left\{10Z\frac{\partial Z}{\partial u_j} + 2\left(1 - \frac{10Z^2}{R^2}\right)\mathbf{R}\cdot\frac{\partial \mathbf{R}}{\partial u_j}\right\}$$

$$\frac{\partial \ddot{Z}}{\partial u_j} = g_2\frac{Z}{R}\left(\frac{1}{Z}\frac{\partial Z}{\partial u_j} - \frac{3}{R^2}\mathbf{R}\cdot\frac{\partial \mathbf{R}}{\partial u_j}\right) + \frac{\mu_\oplus Z}{R^3}\frac{J a_\oplus^2}{R^4}\left\{10Z\frac{\partial Z}{\partial u_j} + 2\left(3 - \frac{10Z^2}{R^2}\right)\mathbf{R}\cdot\frac{\partial \mathbf{R}}{\partial u_j}\right\}$$

where $\partial \ddot{\mathbf{R}}/\partial u_j$ represents the contribution arising from the oblateness only. The final form of B is obtained by the expansion of the dot products:

$$B_{11} = g_1\frac{X}{R}\left(\frac{1}{X} - \frac{3X}{R^2}\right) + 2\mu_\oplus\frac{X^2}{R^3}\frac{J a_\oplus^2}{R^4}\left(1 - \frac{10Z^2}{R^2}\right)$$

$$B_{12} = g_1\frac{X}{R}\left(-\frac{3Y}{R^2}\right) + 2\mu_\oplus\frac{XY}{R^3}\frac{J a_\oplus^2}{R^4}\left(1 - \frac{10Z^2}{R^2}\right)$$

$$B_{13} = g_1\frac{X}{R}\left(-\frac{3Z}{R^2}\right) + 2\mu_\oplus\frac{XZ}{R^3}\frac{J a_\oplus^2}{R^4}\left(6 - \frac{10Z^2}{R^2}\right)$$

$$B_{21} = g_1\frac{Y}{R}\left(-\frac{3X}{R^2}\right) + 2\mu_\oplus\frac{XY}{R^3}\frac{J a_\oplus^2}{R^4}\left(1 - \frac{10Z^2}{R^2}\right)$$

$$B_{22} = g_1\frac{Y}{R}\left(\frac{1}{Y} - \frac{3Y}{R^2}\right) + 2\mu_\oplus\frac{Y^2}{R^3}\frac{J a_\oplus^2}{R^4}\left(1 - \frac{10Z^2}{R^2}\right)$$

$$B_{23} = g_2\frac{Y}{R}\left(-\frac{3Z}{R^2}\right) + 2\mu_\oplus\frac{YZ}{R^3}\frac{J a_\oplus^2}{R^4}\left(6 - \frac{10Z^2}{R^2}\right)$$

$$B_{31} = g_2\frac{Z}{R}\left(-\frac{3X}{R^2}\right) + 2\mu_\oplus\frac{XZ}{R^3}\frac{J a_\oplus^2}{R^4}\left(3 - \frac{10Z^2}{R^2}\right)$$

$$B_{32} = g_2\frac{Z}{R}\left(-\frac{3Y}{R^2}\right) + 2\mu_\oplus\frac{YZ}{R^3}\frac{J a_\oplus^2}{R^4}\left(3 - \frac{10Z^2}{R^2}\right)$$

$$B_{33} = g_2\frac{Z}{R}\left(\frac{1}{Z} - \frac{3Z}{R^2}\right) + 2\mu_\oplus\frac{Z^2}{R^3}\frac{J a_\oplus^2}{R^4}\left(8 - \frac{10Z^2}{R^2}\right)$$

The vector $(g_1 X/R, g_1 Y/R, g_2 Z/R)$ is assumed to be calculated externally while the parts of B which do not contain g_1 or g_2 are replaced by zero whenever $R > 3\,a_\oplus$.

The execution entry VARY is preceded by the setup entry SVARY:

CALL SVARY, A, B, C, D, E, F, G, H, I, J, K

where **R**, the position of the probe with respect to the central body, is contained in the cells A − 3, A − 2, A − 1. The block B − 3n, ..., B − 1 contains the noncentral body position vectors $\mathbf{R}_1, \ldots, \mathbf{R}_n$; R is contained in location C while the block D − n, ..., D − 1 contains the quantities $R_{1p}, \ldots, R_{np}$. μ is in location E and the cells F − n, ..., F − 1 are occupied by $\mu_1, \ldots, \mu_n$; a zero in one of the latter cells is used as a flag to skip the corresponding body in the calculation of A. The oblateness perturbation is assumed to be stored in the locations G − 3, G − 2, G − 1; an internal test is made to determine whether the Earth is the central body, since B is set to zero whenever the calculation is not centered at the Earth. To determine the maximum number of perturbing bodies, the decrement of the cell H contains n. The oblateness parameters $a_\oplus$ and J occupy the locations I and J respectively.

As output from the execution entry, the matrix $A + B$ is deposited in the storage locations K − 9, ..., K − 1. Execution of the subroutine requires 30 cells of erasable storage starting at COMMON.

7. Numerical Integration

MARK

MARK is the subroutine which obtains the numerical stepwise solution of a set of linear first-order differential equations by employing an Adams-Moulton predictor-corrector of virtually arbitrary order which utilizes backwards differences; a Runge-Kutta scheme is used to form the necessary differences of the derivatives to start the integration for the multistep method. The step size is halved or doubled upon external request by subtabulation of the derivatives in the former case and by elimination of intermediate points in the latter; hence it is not necessary to restart with Runge-Kutta to effect a step-size change. MARK has been designed to carry out the auxiliary functions of obtaining the numerical solution at specified values of the double-precision independent variable; i.e., for desired times, or doing the same job whenever a specified dependent variable attains a null value. To permit the main program to determine the desired times and to define the dependent variables, a list of control words called triggers is appended to the calling sequence; the structure of the triggers is described in the explanation of the calling sequence to follow.

To allow the main program to monitor the numerical solution, EOS, a supervisory routine provided by the main program, is called at the end of each step by MARK. Additionally, MARK must be given access to a subroutine for the evaluation of the derivatives and the calculation of all necessary dependent variables so that isolated zeros may be iterated down upon and captured.

If m is the highest-order difference retained for the Adams-Moulton method, then for starting purposes the Runge-Kutta portion of MARK must integrate ahead m steps of h, at which time the necessary backwards difference tables for the derivatives will have been completed. Assuming one variable for simplicity, the Runge-Kutta formulas are

$$y_{n+1} = y_n + \frac{1}{6}(k_1 + 2k_2 + 2k_3 + k_4)$$

$$k_1 = hf(t_n, y_n)$$

$$k_2 = hf\left(t_n + \frac{h}{2}, y_n + \frac{1}{2}k_1\right)$$

$$k_3 = hf\left(t_n + \frac{h}{2}, y_n + \frac{1}{2}k_2\right)$$

$$k_4 = hf(t_n + h, y_n + k_3)$$

where the differential equation to be solved has the form $\dot{y} = f(t, y)$. The ordinate y_n is accumulated double precision, while the k_j are evaluated and summed in single precision to be added to y_n in double-precision form. The solution at intermediate times is obtained by altering h to step forward to the desired time and resuming the integration with the old step size h upon return from the trigger execution; while homing in on a zero of a dependent variable, the step size may even become negative. The collecting of the derivatives for the difference tables is accomplished by the setting up of internal time stops at the necessary mesh points; thus the Runge-Kutta section will obtain the solution at the necessary times for the tables while carrying on the ordinary functions of MARK.

The Runge-Kutta formulas give results which agree through fourth order in h with a Taylor series expansion as may be seen from the following development:

$$k_1 = hf$$

$$k_i = h\sum_{j=0}^{3}\frac{\lambda_j^{(i)}}{j!}\left(h\frac{\partial}{\partial t} + k_{i-1}\frac{\partial}{\partial y}\right)^j f + O(h^5), \quad i = 2,3,4$$

$$\lambda_j^{(i)} = \begin{cases} 1 & \text{for } i = 4 \\ 2^{-j} & \text{for } i = 2,3 \end{cases}$$

Expanding the operator and using the notation $\partial f^k/\partial t^j\,\partial y^{k-j} = f_{t^j y^{k-j}}$, there results

$$k_2 = hf + \frac{h^2}{2!}(f_t + ff_y) + \frac{h^3}{3!}\left[\frac{3}{4}(f_{t^2} + 2ff_{ty} + f^2 f_{y^2})\right] + \frac{h^4}{4!}\left[\frac{1}{2}(f_{t^3} + 3ff_{t^2y} + 3f^2 f_{ty^2} + f^3 f_{y^3})\right] + O(h^5),$$

$$k_3 = hf + \frac{h^2}{2!}(f_t + ff_y) + \frac{h^3}{3!}\left[\frac{3}{2}f_y(f_t + ff_y) + \frac{3}{4}(f_{t^2} + 2ff_{ty} + f^2 f_{y^2})\right] + \frac{h^4}{4!}\left[3(f_t + ff_y)(f_{ty} + ff_{y^2}) + \frac{3}{2}f_y(f_{t^2} + 2ff_{ty} + f^2 f_{y^2}) + \frac{1}{2}(f_{t^3} + 3ff_{t^2y} + 3f^2 f_{ty^2} + f^3 f_{y^3})\right] + O(h^5)$$

$$k_4 = hf + \frac{h^2}{2!}[2(f_t + ff_y)]$$
$$+ \frac{h^3}{3!}[3f_y(f_t + ff_y) + 3(f_{t^2} + 2ff_{ty} + f^2 f_{y^2})]$$
$$+ \frac{h^4}{4!}[6f_y^2(f_t + ff_y) + 12(f_t + ff_y)(f_{ty} + ff_{y^2})$$
$$+ 3f_y(f_{t^2} + 2ff_{ty} + f^2 f_{y^2})$$
$$+ 4(f_{t^3} + 3ff_{t^2y} + 3f^2 f_{ty^2} + f^3 f_{y^3})] + O(h^5)$$

$$\frac{1}{6}(k_1 + 2k_2 + 2k_3 + k_4)$$
$$= hf + \frac{h^2}{2!}(f_t + ff_y)$$
$$+ \frac{h^3}{3!}[f_y(f_t + ff_y) + (f_{t^2} + 2ff_{ty} + f^2 f_{y^2})]$$
$$+ \frac{h^4}{4!}[f_y^2(f_t + ff_y) + 3(f_t + ff_y)(f_{ty} + ff_{y^2})$$
$$+ f_y(f_{t^2} + 2ff_{ty} + f^2 f_{y^2})$$
$$+ (f_{t^3} + 3ff_{t^2y} + 3f^2 f_{ty^2} + f^3 f_{y^3})] + O(h^5)$$

But y_{n+1} is given explicitly by the series

$$y_{n+1} = y_n + \sum_{j=1}^{4} \frac{h^j}{j!} y^{(j)} + O(h^5)$$

where

$$y^{(j)} = \left(\frac{d^j y}{dt^j}\right)_{t_n} = \left(\frac{\partial}{\partial t} + f\frac{\partial}{\partial y}\right)^{j-1} f$$

In particular,

$$y^{(1)} = f$$
$$y^{(2)} = f_t + ff_y$$
$$y^{(3)} = f_y(f_t + ff_y) + (f_{t^2} + 2ff_{ty} + f^2 f_{y^2})$$
$$y^{(4)} = f_y^2(f_t + ff_y) + 3(f_t + ff_y)(f_{ty} + ff_{y^2})$$
$$+ f_y(f_{t^2} + 2ff_{ty} + f^2 f_{y^2})$$
$$+ (f_{t^3} + 3ff_{t^2y} + 3f^2 f_{ty^2} + f^3 f_{y^3})$$

Thus the two series expansions agree through terms of h^4.

To show that the truncation error is, in general, at least $O(h^5)$, consider as an example the simple differential equation

$$\dot{y} = y$$

with solution

$$y_{n+1} = y_n\left[1 + h + \frac{h^2}{2!} + \frac{h^3}{3!} + \frac{h^4}{4!} + \frac{h^5}{5!}\right] + O(h^6)$$

In comparison, the Runge-Kutta formulas yield

$$k_1 = hy_n$$
$$k_2 = hy_n\left(1 + \frac{h}{2}\right)$$
$$k_3 = hy_n\left(1 + \frac{h}{2} + \frac{h^2}{4}\right)$$
$$k_4 = hy_n\left(1 + h + \frac{h^2}{2} + \frac{h^3}{4}\right)$$
$$\frac{1}{6}(k_1 + 2k_2 + 2k_3 + k_4) = y_n\left[h + \frac{h^2}{2!} + \frac{h^3}{3!} + \frac{h^4}{4!}\right]$$

Thus the two series disagree beginning with terms of h^5.

The formulas used for the Adams-Moulton integration are derived from the expression

$$y_{n,\mu} = y_n + h\frac{(1-\nabla)^\mu - 1}{-\ln(1-\nabla)}\dot{y}_n$$

If a series expansion is obtained and differences through order m are retained, then the truncation error is evidently $O(h^{m+2})$ since

$$h\nabla^{m+p}\dot{y}_n = h\{h^{m+p}D^{m+p}\dot{y}_n + O(h^{m+p+1})\}$$

The predictor formula results from $\mu = -1$:

$$y_{n+1} = y_n + h\frac{(1-\nabla)^{-1}}{-\ln(1-\nabla)}\dot{y}_n$$

The computational form is obtained by expanding into a series and retaining differences up through mth order.

$$y_{n+1} = y_n + h\left(\sum_{j=0}^{m} a_j \nabla^j\right)\dot{y}_n$$

where the first few coefficients are

$$a_0 = 1$$
$$a_1 = \frac{1}{2}$$
$$a_2 = \frac{5}{12}$$
$$a_3 = \frac{3}{8}$$
$$a_4 = \frac{251}{720}$$
$$a_5 = \frac{95}{288}$$
$$a_6 = \frac{19087}{60480}$$

As the predictor is relatively unstable for $m \geqq 5$, an option has been provided in MARK for the use of a corrector formula which may be obtained by setting $\mu = 1$ in the general expression

$$y_n = y_{n-1} + \frac{h\nabla}{-\ln(1-\nabla)}\dot{y}_n$$

For purposes of computation this becomes

$$y_n = y_{n-1} + h\left(\sum_{j=0}^{m} b_j \nabla^j\right)\dot{y}_n$$

where the low-order coefficients are

$$b_0 = 1$$

$$b_1 = -\frac{1}{2}$$

$$b_2 = -\frac{1}{12}$$

$$b_3 = -\frac{1}{24}$$

$$b_4 = -\frac{19}{720}$$

$$b_5 = -\frac{3}{160}$$

$$b_6 = -\frac{863}{60480}$$

The predictor and corrector each require separate evaluations of the derivatives; after application of the corrector and the calculation of the derivatives at the new time station t_n, the solution may be obtained at intermediate points t by choice of $\mu = (t_n - t)/h$, where $t_n - h < t < t_n$:

$$y_{n-\mu} = y_n + h\left(\sum_{j=0}^{m} c_j \nabla^j\right)\dot{y}_n$$

where the c_j are obtained by the convolution of the series

$$\frac{(1-\nabla)^{\mu} - 1}{\nabla} = \sum_{j=0}^{\infty} (-1)^{j+1}\binom{\mu}{j+1}\nabla^j$$

with the series for the corrector

$$\sum_{j=0}^{\infty} b_j \nabla^j$$

The interpolated solution may then be used either for an intermediate time stop or to help find the zero of a dependent variable.

At the return from the execution of a trigger, MARK may be signaled to change step size by powers of 2 over the nominal value; any other type of step-size change must be effected by restarting the numerical solution.

Each time a double is called for, MARK sets internal time stops to save the necessary information for doubling during the next m steps as measured from the end of the current step; of course, the necessary past information is regenerated at this time and saved to be adjoined to the future information to form a difference table of derivatives with twice the step size. At the completion of first doubling, further doubles may be executed in sequence as called for by the main program.

Halving is accomplished by the subtabulation of the derivatives according to Newton's formula:

$$\dot{y}_{n-\mu} = (1-\nabla)^{\mu}\dot{y}_n \approx \left(\sum_{j=0}^{m} (-1)^j \binom{\mu}{j} \nabla^j\right)\dot{y}_n$$

for $\mu = 1/2, 1, \ldots, m/2$.

At this point new differences of the derivatives corresponding to half the step size may be generated, and further halving may be accomplished if called for by the main program.

Step-size changes by doubling or halving are executed only at the end of an Adams-Moulton step and after all time stops and dependent variable stops occurring at times inside the current interval have been executed. While integration is being carried out by the Runge-Kutta section, the doubling and halving signals are ignored; both signals given simultaneously will result in internal confusion.

MARK has the calling sequence

```
CALL   MARK
PZE    HBANK,T,EOS
PZE    DER1,,DER2
(ERROR RETURN)
(FIRST TRIGGER)
        .
        .
        .
(LAST TRIGGER)
HTR                    End of calling sequence
```

Most of the information to be shared by the main program and MARK is organized in the following buffer:

HBANK −3	PZE	m	Adams-Moulton order
−2	PZE	NH	Number of initial halves
−1	PZE	ND	Number of initial doubles
+0	DEC	h	Initial Runge-Kutta step
+1	PZE	$N_{,,}n$	Total and effective variables
+2	DEC	T_1	Double precision
+3	DEC	T_2	Time
	BSS	n	y, solution of differential equations
	BSS	$N-n$	Expansion for more equations
	BSS	n	y, derivatives
	BSS	$N-n$	Expansion for more equations
	BSS	$(2m+5)N$	Working area for MARK

T $\neq 0$ flags time as double precision; otherwise, computation would be with single-precision interpretation. At the end of step, MARK calls the routine EOS; return is via TRA 1, 4. For the calculation of the derivatives, MARK calls a routine which may be divided into two parts: DER1 for time-dependent derivatives and DER2 for the other derivatives. If time has just changed, MARK calls the first entry, while the second entry is called if time remains the same as a previous evaluation. The return device is provided by TRA 1, 4.

A generation of a time which is smaller than the current time will cause MARK to give the error return; if the number of active dependent variables exceeds 20, the error return is likewise given. Normally, the main routine controls the integration by means of the subroutine EOS and by the triggers, but MARK does most of the detail work.

While in the Adams-Moulton mode, the main routine must determine how many times the corrector formula is to be applied; the symbolic location NI in MARK must have in its address the desired number of applications of the corrector.

Each trigger has the structure

OP A,,B

PZE C

The trigger is active whenever the sign bit of the first word is plus; otherwise, a minus sign will cause MARK to ignore the trigger. At location A is a subroutine in the main program which MARK calls whenever the condition defined by the trigger has been met. This subroutine returns via TRA 1, 4; if the trigger is not disabled by the subroutine at execution time, then the value of the variable must in general be changed, lest MARK attempt to execute the trigger again upon return of control. The tag of the first word of the trigger is used as a flag by MARK in the case of a dependent variable so that many triggers may be worked on in a single interval.

The variable defined by a trigger may be of two types—independent (time-stop) or dependent. The former case is flagged by B = 0 and C is then the location of the desired double-precision time for execution of the trigger. In the latter case, the dependent variable is defined to be the difference between the contents of B (B $\neq 0$) and the contents of C. In practice, the quantity in C is the desired value of the variable which is computed in the derivative or the end-of-step routine and stored in the location B.

At the end of each step MARK scans the list of triggers and determines the smallest time which will result in a time stop; all the active dependent variable triggers are inspected to determine those variables which have exhibited a sign change over the preceding step. A linear approximation is made to the root of each variable and the variable which apparently has a root at the earliest time in the interval is iterated upon; a new set of linear estimates of the roots for all the pertinent variables is formed at each step of the iterative solution. At convergence, the time stops and the dependent variable stops are executed in proper time sequence.

For purposes of convergence, two times are considered the same whenever agreement is obtained out to approximately the last two bits; the same test is applied to the sequence of times formed by the iteration process in finding the zero of a dependent variable. Each new time generated requires the calculation of the derivatives appropriate to the new time solution. After all the triggers in an interval have been cleaned up, the information at the end of step is restored and the derivatives are recalculated.